NAVAL POSTGRADUATE SCHOOL
Monterey, California

THESIS

A COMPARISON OF UPPER FRONT
STRENGTH AS ANALYZED BY NORAPS AND AS
OBSERVED BY ACARS-EQUIPPED AIRCRAFT

by

Edward L. Stephens II

September, 1997

Thesis Advisor: Patricia M. Pauley

19980212 090

REPORT DOCUMENTATION PAGE

Form Approved OMB No. 0704-0188

1. AGENCY USE ONLY *(Leave blank)*	2. REPORT DATE September 1997	3. REPORT TYPE AND DATES COVERED Master's Thesis

4. TITLE AND SUBTITLE A COMPARISON OF UPPER FRONT STRENGTH AS ANALYZED BY NORAPS AND AS OBSERVED BY ACARS-EQUIPPED AIRCRAFT	5. FUNDING NUMBERS
6. AUTHOR(S) Edward L. Stephens II	

7. PERFORMING ORGANIZATION NAME(S) AND ADDRESS(ES) Naval Postgraduate School Monterey CA 93943-5000	8. PERFORMING ORGANIZATION REPORT NUMBER

9. SPONSORING/MONITORING AGENCY NAME(S) AND ADDRESS(ES)	10. SPONSORING/MONITORING AGENCY REPORT NUMBER

11. SUPPLEMENTARY NOTES The views expressed in this thesis are those of the author and do not reflect the official policy or position of the Department of Defense or the U.S. Government.

12a. DISTRIBUTION/AVAILABILITY STATEMENT Approved for public release; distribution is unlimited.	12b. DISTRIBUTION CODE

13. ABSTRACT *(maximum 200 words)*

Upper fronts are associated with strong horizontal gradients of both temperature and wind speed on a scale that is not well resolved by rawinsonde observations. Even so, mesoscale data assimilation systems are capable of ingesting observations from a variety of sources and depicting such features. This study examines upper fronts that occurred over the continental U.S. during March-April 1996 with the objective of verifying the performance of the NORAPS (Navy Operational Regional Atmospheric Prediction System) data assimilation system using ACARS (ARINC Communications, Addressing, And Reporting System) aircraft observations. ACARS observations are taken every 5-8 minutes during level flight, which yields a horizontal resolution along the flight track of less than 100 km and so can resolve the approximately 200 km width scale for upper fronts. The ACARS temperature observations are not currently used in the data assimilation system and so present an independent set of observations.

Thirty distinct upper fronts (duration greater than 12 h and temperature gradient greater than $2°C/100km$) were identified and tracked from the NORAPS analyses during the period of the study. In general, the analyzed temperature gradient was weaker than that observed in the ACARS data. The latter depicted a temperature gradient of $8°C/100$ km for two cases, whereas the analyzed gradient did not exceed $6°C/100$ km. Most upper fronts (47%) attained maximum intensity when located in the base of the upper-level trough, although 33% (13%) did so just downstream (upstream) of the trough line. Most of the useable aircraft tracks were near 200-300 mb, therefore the portion of the upper front above the tropopause was examined in greater detail than the portion below the tropopause, although the latter would be expected to contain stronger temperature gradients.

14. SUBJECT TERMS Upper Front Strength, NORAPS Temperature Analyses, ACARS-Equipped Aircraft; Turbulence	15. NUMBER OF PAGES 127
	16. PRICE CODE

17. SECURITY CLASSIFICATION OF REPORT Unclassified	18. SECURITY CLASSIFICATION OF THIS PAGE Unclassified	19. SECURITY CLASSIFICATION OF ABSTRACT Unclassified	20. LIMITATION OF ABSTRACT UL

NSN 7540-01-280-5500

Standard Form 298 (Rev. 2-89)
Prescribed by ANSI Std. 239-18 298-102

A COMPARSON OF UPPER FRONT STRENGTH AS ANALYZED BY NORAPS AND AS OBSERVED BY ACARS-EQUIPPED AIRCRAFT

Edward L. Stephens II
Lieutenant, United States Naval Reserve
B.S., United States Naval Academy, 1987
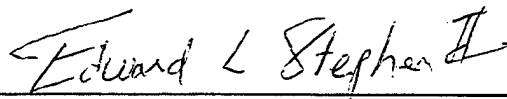M.B.A., Embry-Riddle Aeronautical University, 1994

Submitted in partial fulfillment
of the requirements for the degree of

MASTER OF SCIENCE IN METEOROLOGY AND PHYSICAL OCEANOGRAPHY

from the

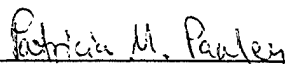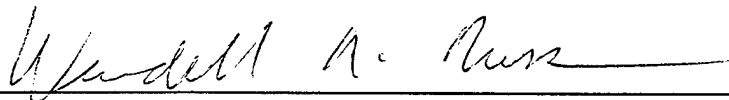## NAVAL POSTGRADUATE SCHOOL

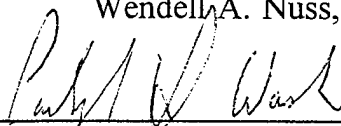**September 1997**

Author: _____

Edward L. Stephens II

Approved by: _____

Partricia M. Pauley, Thesis Advisor

_____

Wendell A. Nuss, Second Reader

_____

Carlyle H. Wash, Chairman
Department of Meteorology

iii

ABSTRACT

Upper fronts are associated with strong horizontal gradients of both temperature and wind speed on a scale that is not well resolved by rawinsonde observations. Even so, mesoscale data assimilation systems are capable of ingesting observations from a variety of sources and depicting such features. This study examines upper fronts that occurred over the continental U.S. during March-April 1996 with the objective of verifying the performance of the NORAPS (Navy Operational Regional Atmospheric Prediction System) data assimilation system using ACARS (ARINC Communications, Addressing, And Reporting System) aircraft observations. ACARS observations are taken every 5-8 minutes during level flight, which yields a horizontal resolution along the flight track of less than 100 km and so can resolve the approximately 200 km width scale for upper fronts. The ACARS temperature observations are not currently used in the data assimilation system and so present an independent set of observations.

Thirty distinct upper fronts (duration greater than 12 h and temperature gradient greater than 2°C/100km) were identified and tracked from the NORAPS analyses during the period of the study. In general, the analyzed temperature gradient was weaker than that observed in the ACARS data. The latter depicted a temperature gradient of 8°C/100 km for two cases, whereas the analyzed gradient did not exceed 6°C/100 km. Most upper fronts (47%) attained maximum intensity in the base of the upper-level trough, although 33% (13%) did so just downstream (upstream) of the trough line. Most of the useable aircraft tracks were near 200-300 mb, therefore the portion of the upper front above the tropopause was examined in greater detail than that below the tropopause, although the latter would be expected to contain stronger temperature gradients.

TABLE OF CONTENTS

ACKNOWLEDGEMENTS

I. INTRODUCTION

An upper-level front is defined as a narrow transition zone located in the upper troposphere, where variations in temperature and wind fields are concentrated (Keyser and Shapiro 1986). Upper-level fronts are characterized by large horizontal temperature gradients, static stability, absolute vorticity and vertical wind shear. Sanders et al. (1991) presented an upper-front case in which the 500 mb temperature gradient increased from 2°C/100km to 18°C/100km in a 48 h period (Fig. 1) When viewed on constant pressure charts, fronts appear as long, narrow features, whose along- front scale (1000-2000 km) is typically an order of magnitude larger than its cross-front scale (100-200 km). Therefore, the thermal and wind gradients are typically much greater across the front than along the front. When depicted in vertical cross section, fronts appear as sloping zones with a vertical thickness of one to two km. Fronts exist because of differential advection of the thermal and wind patterns resulting from the sheared horizontal and vertical velocity fields associated with baroclinic waves. Shears in the three-dimensional velocity field are associated with deformation in both the horizontal and vertical planes, which stretches and contracts broad regions of air into narrow zones.

Upper-level fronts are of interest because their divergence patterns play an integral role in midlatitude cyclogenesis. Furthermore, the vertical circulations associated with upper-level fronts are a key component in the development and organization of midlatitude cloud and precipitation systems (Keyser and Shapiro 1986). Additionally, upper-level fronts are preferred regions of small-scale mixing caused by gravity waves, Kelvin-Helmholtz

instabilities (KHI), and turbulent eddies, all of which are commonly known as clear air turbulence (CAT; Keyser and Shapiro 1986). The location and intensity of upper-level fronts and jets are of critical importance to aviation safety not only for avoiding areas of turbulence, but also for efficient flight routing in order to minimize fuel consumption (Ellrod and Knapp 1991). An additional hazard associated with upper level fronts is high surface winds resulting from the transport of high momentum air downward to mid-levels where boundary layer processes may mix it to the surface (Pauley et al. 1996).

However, the current network of upper-air reporting stations is barely adequate to provide data to analyze and track upper-level fronts. Presently, the mean spacing of rawinsonde (RAOB) stations within North America is 400 km, which cannot resolve the 200 km width of upper-level fronts. RAOBs do capture the vertical structure of upper-level fronts. But it is only with considerable difficulty that this vertical structure can be exploited to improve the analysis of the horizontal structure as demonstrated by Sanders et al. (1991). Their technique consisted of manually analyzing RAOBs on virtual potential temperature surfaces at an interval of 4°K, before converting to isobaric analyses.

Today's high-resolution primitive equation mesoscale models contain adequate resolution (less than 100 km and greater than 15 levels) and physics to collapse broad temperature gradients into realistic frontal zones as the forecast time progresses (Benjamin et al. 1991). The challenge lies in accurately depicting upper fronts in the initial conditions, which depends on providing accurate observations at an adequate resolution to the model's data assimilation system. One source of such data exists in the form of aircraft reports collected and transmitted automatically by Aeronautical Radio Inc. (ARINC)

Communications, Addressing and Reporting System (ACARS).   ACARS observations consist of : latitude/longitude (tenths of a minute), time (nearest minute), temperature (nearest tenth degree Celsius), flight level (nearest hundred feet), wind direction (nearest degree), and wind speed (nearest knot). The typical horizontal resolution of ACARS data is less than 100 km for level flight (an observation every 5-7.5 minutes) and during ascent/descents as fine as 100 m. One airline has its fleet reporting observations every 3 minutes (40 km resolution) during cruise flight. The quality of ACARS reports is excellent; only 1.3% of the observations are rejected on average (Moninger 1995).

The objective of this thesis is to evaluate the temperature gradients generated from the Navy Operational Regional Atmospheric Prediction System (NORAPS) analyses in the vicinity of upper-level fronts with aircraft observations crossing these upper-level fronts. This study is a preliminary, predominantly qualitative examination of upper-level fronts with a more rigorous statistical examination planned for the future.   Turbulence generated from upper fronts can be a hazard to aircraft that cruise in the upper troposphere. Therefore, the presence and strength of turbulence from aircraft reports located near or within the upper-level front will be examined.

To meet this objective, this thesis is organized as follows. Chapter II presents background information on aircraft reports and turbulence. Descriptions of the data and the decoding methods used for this study are given in Chapter III. Results are presented in Chapter IV, including a summary of all the fronts identified during the study and a case study of a well-developed upper-level front. Chapter V contains conclusions and recommendations.

II. BACKGROUND

A.   AIRCRAFT REPORTS

Since the mid- 1940s, meteorological data collected from research aircraft have been an important source of information for the study and analysis of upper-level fronts. For example, studies by Briggs and Roach (1963), Danielsen (1964), and Shapiro (1974, 1976) utilized instrumented aircraft to probe the structure of upper-level fronts.   However, until recently, aircraft data were not widely available on a routine basis. Not until the mid-1970s were observations taken aboard commercial aircraft deemed to be a valuable source of upper-air data. The Aircraft to Satellite Data Relay (ASDAR) system used during the FGGE demonstrated the feasibility of using commercial aircraft for gathering meteorological data (Kruus 1986).   Prior to 1975, the wind vector data was suspect because of prevailing air navigation methods; however the introduction of the inertial navigation system (INS) resulted in much improved wind vector data (Julian 1989). INS winds are not only much more accurate than the older computed winds, but they are, for all practical purposes, instantaneous rather than averaged winds. Schwartz and Benjamin (1995) reported that aircraft temperature measurements are accurate to the nearest 0.25°C and winds to the nearest knot.

The next hurdle to be overcome was that the main source of error in an aircraft meteorological report-- man. The conventional air reports (AIREP) and pilot reports (PIREP) require a series of manual actions which introduce considerable error. PIREPS are

5

voice-transmitted reports of weather from a pilot to a Flight Service Station (FSS) or Air Route Traffic Control Center (ARTCC) specialist who must record the observation and enter it into the National Weather Service's (NWS) communication gateway (Schwartz 1996). Problems with PIREPs include non-standardization and non-conformity to the reporting regulations. Specifically, the most common problems are: location, aircraft type, time, and /or altitude reported as "unknown"; use of non-standard abbreviations; non-standard locations; and turbulence reported in the remarks section rather than in the turbulence section (Schwartz 1996). Conventional AIREPS received at FNMOC under the bulletin header XRXX are routine inflight voice weather reports which contain temperature, wind, turbulence and icing parameters. Since these reports are relayed by voice in much the same way as PIREPS, they are subject to the same types of errors.

The development of avionics which automatically record and transmit the meteorological data from the in-flight aircraft to a central collection site was instrumental in improving the accuracy of aircraft observations. The proof-of-concept ASDAR units utilized in FGGE demonstrated the feasibility and accuracy of automated aircraft observations. Now, the advent of ACARS has greatly facilitated the collection of automated aircraft observations.

ACARS has an advanced bi-directional datalink communication system that operates in the VHF band. The datalink allows automatic transfer of meteorological data between onboard systems and the user's (airline) ground-based computer (*Jane's Avionics* 1996). The VHF ACARS is adequate for data retrieval within the continental United States. A high frequency (HF) datalink extension to ACARS that was certified in 1992 provides a

communication link beyond the line of sight limitations of VHF, which then has the potential for worldwide coverage (*Jane's Avionics* 1996). The HF system is fully automatic and makes use of the existing aircraft HF radio and antenna, with data transmission rates that are comparable to those of low-data-rate satellite communications (Satcom), relaying data that are digitally formatted. Satcom is also an alternative to the HF datalink. ARINC passes the data to National Center for Environmental Prediction (NCEP) via modem and phone lines. NCEP further disseminates the data to other operational numerical prediction centers such as FNMOC that ingest the data into their regional and global data assimilation systems (Schwartz and Benjamin 1995).

The specific parameters measured by an ACARS unit include: latitude/longitude (tenths of a minute), time (nearest minute), temperature (nearest tenth degree Celsius), flight level (nearest hundred feet), wind direction (nearest degree), and wind speed (nearest knot). Wind measurements are obtained via the aircraft Inertial Navigation System (INS), which measures aircraft acceleration, velocity, position, and angles of attitude. Measurements taken by the aircraft's pitot-static system and outside air temperature thermometers are combined to determine a true airspeed vector. This vector is fed into the INS computer and subtracted from the ground speed vector to obtain the wind velocity (Lord et al. 1984).

In addition to the manual AIREPS transmitted under the XRXX bulletin header, FNMOC also receives AIREPS under the bulletin header YRXX. The latter consist of ACARS and Aircraft Meteorological Data Relay (AMDAR) reports reformatted at Tinker AFB to AIREP format. These observations are fully automated and include temperature and wind (speed and direction) reports and sometimes turbulence reports.

The ACARS dataset is of very high quality; usually only 1.3% of the data contain errors (Moninger 1995). A study by Brewster et al. (1989) revealed rejection rates for fully automated observations (i.e., ACARS and YRXX) of 2.6% for temperatures and 0.9% for winds. The same study reported rejection rates for voice reports (i.e., PIREPS and XRXX) of 31% for temperatures and 34% for winds. Lord et al. (1984) compared ACARS wind measurements with radiosonde, cloud motion (satellite-derived), and VISSR Atmospheric Sounder (VAS) thermally derived winds. The study concluded that ACARS provide an independent source of wind data that complements other sources and is of comparable quality. A comparison of ACARS reports collected during ascent/descent with rawinsondes was also conducted by Schwartz and Benjamin (1995). Overall, statistics indicate that the accuracy of ACARS data was higher than rawinsonde data.

NOAA's Forecast Systems Laboratory (FSL) has the most experience with the quality control of ACARS data. First, a series of checks and corrections are performed when the data arrives at FSL by scrutinizing the temporal and spatial continuity of reports from individual aircraft. Second, FSL develops a "reject list" of aircraft (by tail number) whose data have consistently proven inaccurate. This is accomplished by comparing the data from each aircraft with expected values produced by the Mesoscale Analysis and Prediction System (MAPS; Moninger 1995). Also, a geographic display system has been developed to monitor in real time and for the last 30 days, the locations of ACARS-capable aircraft and the meteorological data reported. The geographic display system is available to government users over the Internet on FSL's home page, while the reject list is available via e-mail to interested users.

Every hour the ACARS data are analyzed for the preceding two hours, several checks and corrections are made, and data deemed acceptable from the last hour are recorded. The previous hour's data are utilized to provide time continuity. The ACARS data receive the following checks (Moninger 1995):

- Temperature within a specified range for the particular aircraft altitude.

- Wind direction in range from 0 to 360 degrees.

- Ground speed less than 700 knots.

- Wind speed positive and less than a specified maximum for the particular aircraft altitude.

- Aircraft latitude or longitude difference between adjacent observations.

- Changes in aircraft altitude consistent with typical commercial aircraft maneuvers.

In addition, aircraft data are corrected for (Moninger 1995):

- Aircraft that report position in thousandths of a degree of latitude/longitude instead of the expected degrees, minutes, and tenths of minutes. The program flags these aircraft, maintains a list of such aircraft, and corrects the position.

- Aircraft that report temperature in degrees instead of tenths of degrees. A manual list is generated; the program adjusts temperature from aircraft on this list.

- A particular fleet of aircraft that reports longitude reversed around 90 degrees West, v component of wind reversed, and u component of wind stuck on easterly. The program uses a manually created list of these aircraft to correct the longitude and change the direction by 180 degrees.

Every three hours, FSL runs a special cycle of the MAPS data ingest that receives corrected and quality controlled-data from all ACARS-producing aircraft, even those on the

9

reject list. This special cycle generates quality control information, which is maintained in a database and allows FSL to detect when rejected aircraft begin to produce acceptable data (Moninger 1995). The database consists of long-term histories of error statistics for each ACARS aircraft back to December 1993. Every week, FSL produces a report of rejected, new, and suspicious aircraft during the past two weeks. The data are e-mailed internationally to interested parties.

The current volume of this high quality, asynoptic data is already sufficient to produce improvements in upper-level wind forecasts over the United States (Benjamin et al. 1991). Currently, only the United States has an operational 3-h analysis/forecast cycle- primarily because of the ACARS meteorological data (Fleming 1996). As of 1996, over 22,000 automated aircraft observations per day were reported by commercial aircraft over the continental United States (Fleming 1996). The number of observations processed each day is expected to increase to 50,000 in the near future (National Weather Service Modernization Committee 1994). Currently, most of the major U.S. airlines (e.g., American, United, Northwest, and Delta) operate aircraft with ACARS equipment. Roughly 2000 aircraft from American, United, Northwest, and Delta are ACARS equipped. Many international airlines also have ACARS equipped aircraft. Interestingly, FSL receives much more ACARS data than FNMOC and other numerical centers.

Today the temporal scale of most ACARS reports is 5-7.5 min, which equates to a horizontal spatial scale of approximately 100 km. However, the new "enroute" format (presently utilized by United Parcel Service) has a standard sampling rate of 3 min, which at typical aircraft cruise speeds, yields about a 40-km horizontal resolution (Fleming 1996).

Furthermore, ACARS reports during ascent and decent may be reported every 300 feet (100 m). ACARS-equipped aircraft, therefore, are capable of resolving mesoscale events such as upper-level fronts which are discernable from wind and temperature data.

Figure 2 shows the spatial coverage of ACARS reports over a 12 -h period in November 1995 (Moninger 1995). Geographically, the continental United States is well covered. However, a few areas like south Texas and northern New England have poor coverage. A significant point is that most ACARS observations are from aircraft at cruising altitude, which means the altitudes of the reports are predominantly in the 29,000 to 42,000 foot range. Temporally, the reports have a distinct maximum over the continental U.S. during peak commercial aircraft activity from 1800 UTC to 0600 UTC daily.

ACARS meteorological data are very valuable to airline meteorologists, dispatchers, and load planners (National Weather Service Modernization Committee, 1994). Airlines are particularly interested in upper-level winds which are critical for operational planning, fuel conservation, and payload calculations. Analyzed peak jet stream winds from today's high resolution numerical models are still too weak by about 10% when compared to automated commercial aircraft reports (Tennenbaum 1996). Additionally, these commercial aircraft "pseudo" soundings are very valuable sources of mesoscale data for aviation meteorology forecasters in terminal areas.

Barwell and Lorenc (1985) assessed the impact of aircraft observations on analyses and forecasts from the First GARP Global Experiment (FGGE) on the U.K. Meteorological Office and the European Center for Medium Range Weather Forecasts (ECMWF) data assimilation systems. Parallel runs with and without aircraft observations show significant

11

analysis differences in the upper troposphere over northern hemisphere oceans; using aircraft data gave a better representation of jet strengths and less reliance on poorer quality observations. This positive impact extends to the shape and position of upper tropospheric features in forecasts from these analyses. Numerous other studies such as Benjamin et al. (1991), Tenenbaum (1991, 1996), Smith and Benjamin (1994), and Bell (1994) have evaluated the impact of aircraft reports on numerical model analyses and forecasts.

Benjamin et al. (1991) evaluated the impact of ACARS on the Mesoscale Analysis and Prediction System (MAPS). The MAPS 3-h intermittent data assimilation system configured in isentropic coordinates was developed and implemented in real-time operation. Isentropic coordinates were used to take advantage of the improved resolution near frontal zones and greater spatial coherence of data that this coordinate system provides. MAPS output was compared to National Center for Environmental Prediction's (NCEP) Regional Analysis and Forecast System (RAFS). Analyses generally fit mandatory-level observations more closely in MAPS than in RAFS. Three-hour forecasts from MAPS, incorporating asynoptic aircraft reports, improve on 12-h MAPS forecasts valid at the same time for all levels and variables, and also improve on 12-h RAFS forecasts of upper-level winds. This result is due to the quality and volume of the aircraft data as well as the effectiveness of the isentropic data assimilation used.

Tenenbaum (1991) reported on an ensemble of eleven cases where cruise-level wind data from commercial aircraft were compared to analyses from the ECMWF, NCEP, and United Kingdom Meteorological Office (UKMO) centers and revealed that the subtropical jet in southwest Asia was 11%, 17%, and 17% weaker, respectively, than aircraft

observations. Tenenbaum (1996) revisited his 1991 study utilizing data obtained from commercial aircraft crossing the 1992 winter subtropical jet streams over southwest and east Asia. Comparisons of these data with new, high-resolution analyses from four of the major operational centers (ECMWF, NCEP, UKMO, and Japan Meteorological Agency (JMA)) show that the peak analyzed winds are still too weak by about 10 %. In addition, about 17% of the cases show larger errors in which the analyses substantially miss the location or magnitude of individual jet streaks.

Smith and Benjamin (1994) compared the impact of ACARS and wind profiler data on MAPS short-range forecasts over the Continental United States (CONUS). The methodology consisted of parallel runs of the 3-h MAPS assimilation cycle, with and without individual data sources, to determine the various contributions of each source. The study concluded that ACARS data provide the most impact on wind forecasts at the important jet levels and contribute to significant improvements in temperature forecasts. The impact of both types of data is strong in 3-h and 6-h forecasts, but not detectable at 12 h.

Bell (1994) assessed the impact of ACARS data on the UKMO operational data assimilation system and center forecasts. During 1993 large volumes of high-quality ACARS data became available to UKMO from internal U.S. flights. Bell's hypothesis was that this large increase in data volume upstream of the UK should improve their 2-5 day forecasts. Bell's subjective assessment identified clear improvements in the structure, phase and strength of the upper flow as features moved out into the Atlantic. Objective verification of four forecasts (15-18 Dec 1992) gave average reductions in root mean square scores of 4% at T+48. The improvements seemed greater at longer forecast range.

13

The Federal Aviation Administration (FAA) is supporting a program to explore the possibility of using commercial aircraft to sense humidity (National Weather Service Modernization Committee 1994). Also, in situ turbulence estimates derived from algorithms that use existing vertical acceleration data on the aircraft can be made without adding any new hardware (Fleming 1996). As the processing capability of aircraft avionics improves the turbulence information can be down linked in real time via ACARS (Fleming 1996). A demonstration by United Airlines is scheduled for 1997. Airlines are very interested in including turbulence data in routine ACARS reports and a few (e.g., Ansett Airlines of Australia) have achieved this goal.

The main advantage of ACARS data is that it is automated and therefore very few serious problems are inherent in the data. The removal of manual intervention by the pilot improves the quality and consistency of the reports. Another significant advantage of ACARS data is the volume of these high-quality asynoptic observations, which is critical to the success of MAPS because it is designed for three-hour updates (Brewster et al. 1989). Including ACARS data has been shown to increase the accuracy of short term forecasts from mesoscale models such as MAPS (Brewster et al 1989).

A general disadvantage of ACARS for mesoscale observations is that the data can be hard to retrieve or may be unavailable for the average aviation forecaster. These data are proprietary in nature because the cost of retrieving the data is borne by the airlines. The airlines pass the data to ARINC, which distributes it to other government users. Until the data are available to all users, including the public, the full value of the data will not be realized.

Another disadvantage is the possibility for a single airline to set up their wind sensing equipment in a different manner which results in wind directions that are 180 degrees off. The standardization of ACARS output among airlines should be pursued by the FAA. The biggest limitation for NWP application is that the data are predominantly "single-level" because airliners spend most of their flight time at a single cruise altitude. Fleming (1996) reported that of the 22,000 daily ACARS reports, 95% are at flight level. Models require three-dimensional data like RAOBs to fully define their three-dimensional initial conditions.

Overall, the advantages of ACARS data greatly outweigh their disadvantages. As more ACARS-equipped aircraft come on line over the next few years, a greater volume of valuable mesoscale observations will be available. The bottom line value of ACARS data is that it provides a large quantity of high-quality upper-level wind reports in the vicinity of upper-level jets that are vitally important to aviation and weather forecasters.

B.   TURBULENCE

The turbulence examined in this study includes the jet stream turbulence and Clear Air Turbulence (CAT) associated with upper-level fronts, which are generated by strong horizontal and vertical temperature gradients and wind shears. CAT/jet stream turbulence is a mesoscale, high-altitude phenomenon normally occurring above 15,000 feet above ground level (AGL). This type of turbulence was determined to be the cause of 68 out of 189 weather-related aviation accidents in the U.S. (Ellrod 1985), making prediction of areas of high-level, non-convective turbulence one of the major problems an aviation forecaster must face. Scientists have estimated that commercial aircraft encounter up to 1.5

15

million CAT events each year based on the current annual flight hours flown which means that a major airline will experience an average of one substantial CAT encounter every month (Ellrod 1993). These incidents may cause passenger injury, structural damage, and airframe fatigue. They also cause increased fuel usage attributed to course alterations, reduced air speeds, and landing diversions. A steady increase in domestic and international high-altitude flights is projected to continue into the next century, which places a high priority on improving our ability to detect and predict CAT/jet stream turbulence.

Significant CAT/jet stream turbulence is prevalent in regions of: 1) vertical wind shear; 2) horizontal wind shear; 3) convergence; 4) horizontal deformation; 5) strong horizontal temperature gradients; and 6) lapse rate discontinuities (Ellrod 1985). All of the above occur near sloping upper-level frontal zones and jet streams where horizontal temperature gradients are strong and where large vertical and horizontal wind shears exist (Fig. 3). Mountain wave and other mechanical sources of upper-level turbulence are not of interest to this study.

The principal mechanism responsible for turbulence is Kelvin-Helmholtz instability (KHI), which is an atmospheric phenomena that resembles a breaking ocean wave. KHI occurs when vertical wind shear within a stable layer exceeds a critical value. This critical value is best represented by the nondimensional Richardson number (Ri) which is often used as a measure of possible turbulent conditions, since Ri is related to both shear and stability (Ellrod and Knapp 1991). The Richardson number can be defined as

$$Ri = \text{Static stability (vertical wind shear)}^{-2} \qquad (2.1)$$

16

Vertical wind shear (VWS) can cause turbulent eddies to develop and propagate into regions of slower wind speed at lower levels. VWS evolves into turbulence by amplifying shear waves along a stable layer (KHI) that results in mixing and decreased thermal instability within the layer (Ellrod and Knapp 1991). Once the critical shear value is reached (Ri=0.25), the laminar flow breaks down into turbulent eddies.

Deformation (DEF) and upper-level convergence (CVG) are also key ingredients in turbulence production. Deformation is a property of a fluid that transforms a circular shaped area of fluid to an elliptical shape and so acts to strengthen upper-level frontal zones. Convergence in the vicinity of the jet stream and tropopause induces strong subsidence and in some cases turbulence.

Observations of turbulence are available primarily from the manually-reported PIREPS and AIREPS as discussed in the previous section. As in many human-observed data sets, these reports are subject to limitations. They are intermittent in both space and time and are particularly scant at night when few aircraft are flying. Turbulence can be reported in numerical category codes or in plain-language abbreviations varying from light to extreme turbulence. Reports of turbulence are highly subjective and uncalibrated because they depend upon a pilot's perception of the degree of turbulence, which depends upon the weight, speed, and handling characteristics of the aircraft (Reap 1996). Despite these limitations, PIREPS and AIREPS are useful in identifying significant areas of turbulence.

Certain cloud and moisture boundaries are indicative of CAT and jet stream turbulence. Some common characteristics of turbulence-producing cloud signatures as observed in infrared satellite imagery are: the sharpness of cloud boundaries, transverse

banding in cirrus clouds, or scalloping along the cirrus edge (Ellrod 1985). The 6.7 micron water vapor imager on geostationary satellites is useful in locating turbulence-producing upper-level features such as shortwave troughs, deformation zones (upper level fronts), jet streams, and vorticity centers. Also, turbulence outbreaks have been correlated with a darkening trend in water vapor imagery. The darkening is a result of dynamic processes such as a tropopause fold or break, and their associated subsidence and resultant drying. The turbulence is observed within the region of darkening and immediately adjacent to it; when the darkening ceases the turbulence diminishes (Ellrod 1985).

The National Oceanic and Atmospheric Administration (NOAA) developed a climatology of turbulence (Ellrod 1993) designed to help airlines avoid potentially dangerous encounters with turbulence at high altitudes. The goal of the NOAA study was to improve existing upper- atmospheric forecasts by diagnosing where CAT and/or jet stream turbulence is likely to occur-- between the altitudes of 25,000 to 40,000 feet. Results indicate that regions in the Northern Hemisphere at risk for CAT and/or jet stream turbulence are remarkably consistent from year to year. Data for the Northern Hemisphere was based upon long period averages of a turbulence index (TI). TI is defined as the product of deformation and vertical wind shear derived from numerical model forecast winds aloft (Ellrod 1993). TI was calculated daily at 0000 UTC and averaged monthly, seasonally, and annually over a three-year period. The study indicates that the most vulnerable altitudes for severe turbulence are between 30,000-35,000 feet, where most aircraft fly.

The CAT/jet stream turbulence climatology also has some distinct geographic and seasonal variations (Ellrod 1993). CAT/jet stream turbulence is minimal in the tropics and

in polar regions. In winter, a number of high risk areas exist in an east-west direction across the mid-latitudes. These areas, where strong jet streams often merge and frequent cyclogenesis occurs, include the southwestern U.S., the Canadian maritime provinces, the north-central Pacific, eastern China and Japan, Scandinavia, as well as North Africa to Southwest Asia. For example, one out of every four flights from Atlanta to Los Angeles is likely to encounter significant CAT/jet stream turbulence over the southwestern U.S. during the winter (*Aviation Week and Space Technology* 1994). During the winter a dramatic increase and southward shift in CAT/jet stream turbulence occurs, because the jet stream is stronger and migrates further south. Figure 4 is from Ellrod (1993) and depicts the average winter TI value which would be valid during the period of this study. The index on the figure is multiplied by a factor of 10 and is valid for the 250-300 mb layer. The geographic distribution discussed above is readily apparent in Fig. 4.

III. METHODOLOGY

This study examines upper fronts occurring in a two-month period from 1 March 1996 to 30 April 1996 both from the perspective of analyses from the Navy's mesoscale model and from available aircraft data over the continental United States (CONUS) and adjacent waters (Fig. 5). Upper-level fronts are expected to be frequent in the Northern Hemisphere during late winter/early spring. The following sections describe the characteristics of these data and the data-handling procedures employed in this study.

A. DATA

The data used in this study include four types of aircraft reports-- AIREPS (both conventional XRXX and automated YRXX types), PIREPS, and ACARS data-- as well as Navy Operational Regional Atmospheric Prediction System (NORAPS) model analyses all of which were obtained from FNMOC. ACARS data are primarily available in Binary Universal Form for the Representation of Meteorological Data (BUFR), which is the World Meteorological Organization's (WMO) standard code for observational meteorological data (Martin et al. 1993). XRXX AIREP data consist of routine inflight voice weather reports which were encoded in the ASCII AIREP format. YRXX AIREP data is made up of ACARS and AMDAR automated observations which have been reformatted as AIREPs. The YIXX bulletin contains PIREPS which are non-routine, inflight weather reports also encoded in ASCII. Table 1 is a summary of the parameters contained in the ACARS, AIREP (XRXX and YRXX), and PIREP data.

21

Figure 6 depicts the number of ACARS observations by day for the entire period of this study. The total number of observations is 453,132 and the daily mean is 7428. Note that the data stream received by FNMOC is only approximately one third of the daily ACARS data (22,000). Figure 7 displays the daily average number of ACARS observations by hour and reveals the diurnal variation in the data. Note that the minimum occurs during the night-time hours from 0500 to 1200 UTC, which implies that the 1200 UTC analysis is less impacted by ACARS than the 0000 UTC analysis which follows the data maximum. Figure 8 depicts the percentage of total ACARS observations by flight level. Note the maximum of reports in the 28,000' to 41,000' range, which is favorable for the purposes of studying upper-level fronts. The banded nature of the distribution at lower levels is an anomaly caused by United Airlines aircraft which report every 2000 feet during ascents and descents. Some banding is apparent at higher flight levels as well. This is caused by the fact that all aircraft operating under Instrument Flight Rules (IFR) are required to fly at odd flight levels beginning at FL290 spaced every 2000 feet (i.e., eastbound aircraft fly at FL290, FL330, FL370 etc while westbound aircraft fly at FL310, FL350, FL390, etc.).

Figures 9-11 represent the same figures as above except for the YRXX observations. The total number of observations for this database during the period of interest was 485,786 with a daily mean of 7964. Note that on 14-15 April little or no data was received (Fig. 9). This data void is present for the other ASCII data types (XRXX and YIXX) as well and likely represents a data transmission problem. Figure 10 depicts the diurnal variation in YRXX observations and the daily maximum and minimum expected with typical airline operations. This distribution is similar to that for ACARS (Fig. 7), except for the maximum occurring

later at approximately 0000 UTC which likely reflects the inclusion of foreign airlines in the YRXX dataset and their departures for Europe from the East Coast in early evening hours. Figure 11 depicts the distribution by flight level and is very similar to the ACARS distribution (Fig. 8) for the reasons stated previously.

Figure 12 depicts the daily number of XRXX observations. Total XRXX observations were 71,017 with a daily mean of 1164, which is appreciably smaller than the ACARS or YRXX datasets. Figure 13 portrays the hourly distribution of XRXX observations and is consistent with typical aircraft activities and the automated observations. Figure 14 depicts the percentage of total XRXX observations by flight level. The distribution is dominated by flight levels above 29,000 feet, which is advantageous to the analysis of upper-level fronts and associated turbulence as previously stated.

The number of YIXX (PIREP) reports for the period is even smaller, with a total of 37,371 and a daily mean of 613. Figure 15 depicts the daily number of YIXX observations during the period. The asynoptic nature and daytime maximum of YIXX observations is apparent in Fig. 16 . Figure 17 depicts the percentage of total YIXX observations by flight level and reveals the low-level bias of this data type. This is caused by the fact that many of these reports came from general aviation aircraft, which are smaller and unpressurized, and therefore tend to operate at lower altitudes. Also, ATC facilities tend to solicit PIREPS during the ascent/descent portion and low-level portions of a flight because these are the critical phases of flight where weather often has its largest impact on aircraft operations. However, a second maximum does occur at higher flight levels from 31,000 to 41,000 feet

which should contain numerous upper-level turbulence reports. Although the overall number of reports is small, they are significant because most PIREPS contain turbulence information.

All turbulence codes were converted to a numerical format unique to this study (Table 2). Figure 18 displays the percentage of XRXX reports by turbulence type. Note that a large percentage (64%) of XRXX observations did not report turbulence and that 25% of the observations reported no turbulence. This distribution is not surprising, considering that XRXX reports are routine reports, and overall, turbulence is an infrequent event (11% of observations). Reports of light turbulence dominate over all other in the XRXX database. Chop is defined as rhythmic or jolt-like turbulence that does not alter the altitude or attitude of the aircraft (Gleim 1993). Regular turbulence, reported in varying degrees, is differentiated from chop because it causes an alteration in the aircraft's altitude and/or attitude. In contrast, Figure 19 depicts the turbulence reports form the PIREP database. Note that 34% of these observations did not report turbulence and 30% reported no turbulence leaving 36% of the observations that contained turbulence information. PIREPS are non-routine reports which are solicited during significant meteorological events and therefore should have more positive turbulence reports than XRXX. Light and moderate turbulence intensities dominated the distribution of positive PIREP turbulence reports.

The NORAPS model represents the Navy's current capability in terms of short-range, regional modeling and forecasting guidance. Table 3 provides a brief description of the characteristics of the NORAPS model (Bayler and Lewit 1992).

24

B. DATA DECODING AND PROCESSING

Each of the data types (ACARS, AIREPS, and PIREPS) were independently decoded since each employs a unique format. A BUFR decoder for the ACARS data was provided by Mr. Tom Beeck of FNMOC and modified to output the data in ASCII form rather than writing the output to the database used at FNMOC. The decoder successfully read all reports and output three files for each day's worth of data: a file containing all reports in the NORAPS CONUS domain, a file containing all reports outside of the CONUS domain, and a log file documenting program performance. An AIREP decoder was obtained from Prof. Wendell Nuss and modified to include the decoding of the turbulence reports as well as accommodating variations in the AIREP format present in the YRXX data. To improve the percentage of AIREP turbulence reports successfully decoded, a two-stage process was used. First, individual words were examined for spelling errors or inconsistencies and standard abbreviations were substituted (e.g., LGT was used for LITE, LIGHT, LTG, SLIGHT, etc.). After this was accomplished, the decoder was able to look for a smaller set of keywords in assigning the numerical codes listed in Table 2. In addition, numerical scales were obtained and verified by the meteorology departments in several airlines for numerical turbulence codes in use. These were also re-encoded using the turbulence values in Table 2. This decoder was used for both the XRXX and YRXX datasets and successfully decoded 99.9% of YRXX reports and 97.9% of XRXX reports. A PIREP decoder was developed using similar logic and was able to successfully decode 94.7% of the reports. The AIREP and PIREP decoders produced the same output files as the ACARS decoder as well as a fourth "edit" file which contained the reports which the decoder could not completely decode. These edit files were

25

especially useful for the XRXX AIREP and PIREP data, because these observations contain numerous, non-standard abbreviations and a long remarks section. Many of the reports in the edit files were manually corrected and inserted into the database. Figures 20 and 21 represent the number of manually corrected reports added to the database from the XRXX and YIXX (PIREP) bulletins. A total of 490 XRXX and 1259 PIREP observations were added which yields daily means of 8 and 21, respectively.

Next, the decoded data for each data type were sorted into daily files containing observations form 0000 UTC to 2359 UTC in chronological order. The program also removed exact duplicates within each data type. The main purpose of this step was to ensure that the daily files all represented the same 24 h period to facilitate both quality control and plotting.

The final preparatory step applied to the aircraft data was quality control. Since PIREPS contain neither flight number nor tail number, the track-checking portions of the quality control program could not be applied. Therefore only a gross check was performed for the PIREP data. However, the daily files for ACARS, YRXX, and XRXX data (819,634 total observations) were input together into a quality control/track formulation program which performs a series of tests looking for data errors.

The first step in the quality control program is to arrange the data by 1) data type, 2) flight number, 3) date and time, and 4) altitude. This results in approximate tracks within each data type. Then the program conducts a gross check of the data and removes near duplicates. It was found that the XRXX data sometimes truncated 7-character flight numbers to 6 characters and included the same observation with both 7 and 6 characters. The latter

were removed when both were present. The data were then sorted again, this time according to 1)flight number, 2)date and time, and 3) altitude. This results in combining the data types into approximate tracks. Duplicates between data types were then removed. During this 61-day period approximately 35% of the YRXX data duplicated ACARS reports and were therefore rejected. Note that bad temperatures or winds found in the gross check were set to missing rather then rejecting the whole report. Next, the observations are checked for a stuck clock. A stuck clock means the aircraft track shows the same time (typically 0000 UTC) for the entire or large portions of the track, which occurred in 2,223 of 819,634 total observations (0.27%). Next, the track is checked for inconsistent heights by identifying reports near in time with very different altitudes, which occurred in 1545 observations (0.19% of total). For example, the first report of a track sometimes had a pressure near 500 mb, followed by a report a minute or two later with a pressure report near 1000 mb. This was followed by a check of the ordering of the observations within the high-resolution ascent/descent portions of the track, where consecutive reports could have had the same time to the nearest minute, which occurred in 559 observations (.07%of total). Next, a check for bad platform speeds is done which indicates a bad position report for that observation, which occurred in 2714 observations (.33% of total). Next, the vertical speeds are checked to weed out improper pressure or flight level reports, which occurred in 508 observations (.06% of total). All of the rejected observations (1.59% of total) excluding duplicates were written to one file, while the observations that passed the quality control checks were written to a separate file. Final rejection rates for each data type following all of the checks and duplicate removals were: ACARS 2.0%, XRXX 5.6%, and YRXX 36.3%.

27

The aircraft tracks (from ACARS, YRXX and XRXX data) and the turbulence reports from XRXX and PIREPS (see Table 2 for turbulence codes) were then plotted on the NORAPS 0000 and 1200 UTC height/temperature and height/wind fields. Aircraft reports were plotted using a simple station model which displayed the type of report (P for PIREP, Y for YRXX, A for ACARS, and X for XRXX) within the circle, the wind in knots, the temperature in °C above and to the left, turbulence information below the temperature, and the airline and flight number below the station. All reports which contained turbulence information were plotted in red. PIREPS were used strictly for their turbulence information with the aircraft type plotted to the lower right of the report.

This program calculates and then contours and shades (at 2 degree Celsius per 100 km) the potential temperature gradient based on the NORAPS analysis (e.g., Fig. 22). The program also contours and shades the isotachs utilizing the NORAPS analysis data. The NORAPS temperature and wind analyses were generated at 50 mb increments from the 500 mb level up to the 200 mb level at 0000 and 1200 UTC for the period 4 March 1996 to 30 April 1996 (NORAPS data for 1-3 March 1996 were not available). The appropriate aircraft tracks and turbulence reports for each level were also plotted on the NORAPS analysis charts. An excellent example of an aircraft track traversing an upper front is Delta Flight 821 over Tennessee and Kentucky (Fig. 22).

IV. RESULTS

For the period 4 March 1996 to 30 April 1996, 30 distinct upper-level fronts were subjectively identified and tracked. Typically, throughout the period of the study, the upper-level fronts entered the domain (CONUS) in the Pacific Northwest and exited the domain in the vicinity of the Atlantic Coast/Canadian Maritime Provinces. The results of this analysis are presented in terms of a summary section and a detailed case study.

A. SUMMARY

Table 4 summarizes the key parameters for each of the 30 fronts. To qualify as distinct the front had to last a minimum of 12 hours and attain a minimum temperature gradient of 2°C/100 km. The mean duration of all fronts was 52 hours. During the period, the maximum temperature gradient depicted by the NORAPS analysis at any level was between 4°C/100 km and 6°C/100 km which occurred quite frequently for strong fronts. Typically, weak or developing fronts possess a horizontal temperature gradient of 2°C/100 km. Of the 30 fronts only eight failed to attain a 4°C/100 km temperature gradient at some point during their life cycle. Aircraft reports revealed that 22 of the 30 fronts had temperature gradients of at least 4°C/100 km with a maximum temperature gradient of 8°C/100 km for two fronts. Keep in mind that the temperature information from aircraft reports is not currently utilized by the NORAPS data assimilation system. Overall, the existing NORAPS data assimilation system does an adequate job of depicting the existing temperature gradients for most upper-level fronts but under-analyzes the strongest fronts.

There is also room for improvement concerning the location and areal coverage of the temperature gradients generated by upper-level fronts. With respect to level, NORAPS depicted the 4°C/100 km contour most often at the 200 mb level followed by the 250/500 mb levels, then 400 mb, 450 mb, and 300 mb respectively. NORAPS never depicted a 4°C/100 km at the 350 mb level for any of the 30 upper-level fronts which is consistent with a check of the aircraft reports which indicated a maximum temperature gradient of 3°C/100 km at 350 mb on a few occasions. Strong fronts possess a 4°C /100 km gradient at most levels.

Column 5 of Table 4 represents the position of the upper-level fronts with respect to the long wave trough when the upper-level front was the strongest. The numerical values in Column 5 are represented graphically in Fig. 23. Of the 30 fronts studied the majority (47%) reached their maximum intensity at the base of the upper-level trough (position 5), 33% just downstream of the upper-level trough (position 6), 13% just upstream of the upper-level trough (position 4) and 3% each for positions 7 and 3. Two of the 30 upper-level fronts and its associated long wave trough became cutoff during the period.

Column 6 of Table 4 displays the maximum wind speed of the jet (m/s) associated with each upper-level front and the level of maximum winds. The strongest jet speed attained was 85 m/s by three fronts, two at 200 mb and one at the 250/300 level. Most frequently the level of maximum winds was at both 250/300 mb simultaneously (40%), followed by 250 mb (23%), 200 mb (13%), 300 mb (10%), 300/250/200 mb simultaneously (10%), and 300/200 mb simultaneously (3%).

Column 7 represents the maximum turbulence reported within the vicinity of each upper-level front during its life span. Aircraft reports of turbulence coincided with every front except for two. 73% of the fronts had aircraft reports indicating moderate or greater turbulence while 27% of upper-level fronts had aircraft reports indicating severe or greater turbulence. One front produced extreme turbulence, here encoded "98". This single report of extreme turbulence occurred over the desert southwest (central Arizona) in association with a robust upper-level front with a 4°C/100 km contour at 200 mb (Fig. 24). A close-up of this area (Fig.25) reveals that the report of extreme turbulence was reported via a PIREP by a Cessna Citation at 200 mb, which was in close proximity to the 4°C/100 km contour (light green) but was within the 2°C/100 km (dark green) NORAPS contour. Note the zero turbulence report within the 4°C/100 km contour which may indicate that the NORAPS analysis places the strongest temperature gradient too far east.

Throughout the period of the study most reports of moderate or greater turbulence occurred within or very close to a strong NORAPS analysis temperature gradient. For example, Figs. 26 and 27 depict a north-south orientated upper-level front at 300 mb which was traversed by United Airlines Flight 31. This example is an ideal case to demonstrate the use of aircraft reports. This aircraft track is traversing the upper-level front (2°C/100 km contour) at a right angle while in the cruise portion of flight and is a solitary, discernable track. Most importantly, the temperatures reported by UAL 31 over Iowa show a consistent 2-3°C/100 km temperature gradient along the western edge of the NORAPS contour. Also note the three PIREP turbulence reports of moderate (30) and moderate-severe (40) by a Boeing 727 and a report of light turbulence by a C141 on the western edge of the shaded

31

region (Fig.27). Another typical example of turbulence reports within a temperature gradient maximum associated with an upper-level front is Fig. 28 which shows three PIREPS by a Boeing 727 over the Minnesota-Wisconsin-Iowa border reporting moderate and moderate-severe turbulence. Note the two XRXX reports over southwest Minnesota and southeastern South Dakota which report light-moderate (20) and continuous chop (68) turbulence, respectively.

Fig. 29 depicts a moderately strong upper-level front over the Great Lakes region at 200 mb. A close-up of the southern portion of the 2°C/100 km contour reveals a clean track of United Airlines (UAL) Flight 38 flying west to east from South Dakota along the Minnesota-Iowa border (Fig. 30). The temperatures reported by UAL 38 depict a consistent 2°C/100 km temperature gradient with up to a 5°C/100 km temperature gradient which is well outside the NORAPS 2°C/100 km temperature gradient contour . All tracks cited in this study were checked for consistency in level and direction utilizing the appropriate log files which were generated daily and contain detailed information on each individual aircraft track.

The vast amount of useable aircraft tracks occur in the 300 mb to 200 mb levels. Quite often the 200 mb level contains so many aircraft tracks that many of them are unreadable. At the lower levels (500 to 400 mb) very few tracks are evident because most commercial airliners cruise at higher altitudes. Fig. 31 depicts a robust upper-level front over the Inter-mountain-West at 500 mb. Unfortunately, only portions of aircraft tracks and numerous single reports (from aircraft ascending or descending through the 500 mb level) are available which was typical throughout the study at the lower levels.

B.   CASE STUDY

The case study was undertaken in order to evaluate the effectiveness of NORAPS in depicting an intense upper front as compared to numerous aircraft tracks which traversed the front.   Of the 30 fronts analyzed during the study, upper-level front number 23 (refer to Table 4) was chosen for closer inspection because of its duration (144 hr) and track over the CONUS, its strong temperature gradients (4-8°C/100 km), numerous turbulence reports, and the 26 quality aircraft tracks which traversed the front. Front 23 entered the domain in the vicinity of the Pacific Northwest and traversed the entire CONUS along an upper-level longwave trough and exited the domain in the vicinity of the Canadian Maritime Provinces.

Figures will be presented depicting the initial location in the Pacific Northwest at 1200 UTC 12 April 1996, the mid-point location in the Midwest at 1200 UTC 15 April 1996, and the final location in the Canadian Maritime Provinces at 1200 UTC 18 April 1996 of front 23 on NORAPS temperature analyses as it transits the CONUS.   Additionally, quality aircraft tracks crossing the upper-level front throughout the duration of front 23 (1200 UTC 12 April 1996 to 1200 UTC 18 April 1996) are presented and discussed in chronological order.

Figures 32-36 depict the temperature analyses of front 23 from 500 mb to 200 mb when it initially entered the domain at 1200 UTC 12 April 1996. The windspeed analyses (not shown) always place the jet streak/jet maximum upstream of the maximum temperature gradient at all levels. Figures 32, 33, 35 and 36 show a 2°C/100 km contour on the 500 mb, 400 mb, 250 mb, and 200 mb NORAPS temperature analyses, respectively, in the vicinity of the Pacific Northwest. Note that the tightest packing of the isotherms (thin lines) and the

largest shaded region occurs at the 200 mb level, while the temperature analysis at 300 mb (Fig. 34) indicate weak temperature gradients with no shaded regions in the Pacific Northwest implying that this level is at or near the tropopause. Also notice the disparity of the positions of the 2°C/100 km contour/upper-level front from level to level with respect to the long wave trough (not consistent with the expected slope of the trough) which may indicate an analysis problem within NORAPS.

Figure 37 illustrates an example of an aircraft track traversing the 2°C/100 km contour over California and Nevada at 200 mb at 0000 UTC 13 April 1996, 12 h after the front's initial appearance. Note that British Airways (BA) Flight 025 indicates temperature gradients of 2-5°C/100 km across the front while the shaded region on the NORAPS analysis depicts a gradient between 2°C/100km and 4°C/100km). BA025LFZ is plotted in red because the observations contain turbulence information which in this case reported no turbulence along the front.

A close-up of the Northern Idaho region at 1200 UTC 13 April 1996 (Fig. 38) shows UAL Flight 2147 southbound along the Pacific Coast indicating an abrupt temperature change of 4°C over Central Oregon while NORAPS indicates a weak gradient in this region. Figure 39, valid at the same time, is a close-up of the leading edge of the upper-level front at 200 mb showing Northwest (NW) Flight 936 crossing the temperature gradient maximum and indicating temperature changes of 2-3°C along the track, in agreement with the analysis.

At 0000 UTC 14 April 1996 the 300 mb temperature analysis (Fig. 40) reveals an excellent example of an aircraft track. UAL 1648's temperature observations indicate weak gradients of 0-1°C along the length of the track which matches very well with the NORAPS

analysis which lacks a strong temperature gradient. Figure 41 portrays a close-up in the vicinity of the upper-level front and shows a report of light-moderate turbulence (20) by a Boeing 737 within the 2°C/100 km temperature gradient maximum in Colorado. Note the various other reports of turbulence in the base of the trough including: continuous moderate turbulence (38) by an MD80; occasional light turbulence (14) by a Boeing 727; continuous chop (68) by Delta Flight 1895 (WA1895); and severe turbulence (50) by an MD80. Figure 42 depicts UAL 1170 crossing the temperature gradient maximum at 200 mb at the same time as above and indicating an abrupt 7°C temperature change over Western Nevada within the 2°C gradient contour. The NORAPS analysis depicts tight packing of the isotherms across Central Utah which UAL 1170 temperature reports do not support.

Figures 43-47 depict the temperature analyses of front 23 during the mid-point of its transit across the CONUS at 1200 UTC 15 April 1996. The large amplitude longwave trough was positioned over the Central United States with the upper-level front positioned at the base of the trough (position 5 Fig. 23) or just to the west of the trough axis (position 4 Fig. 23). The 2°C/100 km shaded contours adequately represent the position of the upper-level front at 500, 400, 250 and 200 mb in Figs. 43, 44, 46, and 47 respectively. Again, the 300 mb level lacks a strong thermal gradient and therefore does not depict a 2°C/100 km shaded temperature gradient contour (Fig. 45). Note the existence of two separate areas of a 4°C/100 km gradient (light green contour) on Fig. 47 over Nebraska and Arkansas on the NORAPS 200 mb temperature analysis. Figure 48 is a close-up of the 4°C/100 km temperature gradient maximum over Nebraska and depicts Northwest Flight 586 passing just to the northwest of the contour. NW 586's ACARS temperature reports show

35

temperature changes of 2-4°C/100 km on the western portion of the track (west of the NORAPS 4°C/100 km temperature gradient maximum) but then an increase in temperature at the eastern end of the track nearer to the NORAPS 4°C/100 km temperature gradient maximum. Here it is apparent that the NORAPS temperature analysis cannot depict the detail evident in the aircraft track.

An elongated region of strong temperature gradient stretching from Saskatchewan to Oklahoma at 250 mb is depicted by Fig. 46. A close-up of the southern portion of the temperature maximum (Fig. 49) reveals two aircraft tracks crossing the shaded region of front 23. UAL 1270 over Oklahoma shows a 2°C/100 km temperature gradient within the shaded region, and UAL 99 over Northwest Kansas shows a consistent 2°C temperature gradient across the contour except for a 5°C/100 km change on the western border. Again, the NORAPS temperature analysis does an adequate job overall, however it does not depict the 5°C/100 km change on the western border.

Figure 50 depicts a myriad of aircraft tracks crossing upper-level front 23 over the central United States at 0000 UTC 16 April 1996. Note the strong temperature gradient at 200 mb as represented by the numerous 4°C/100 km (light green) maximum along the western portion of the longwave trough (positions 3 and 4 from Fig. 23). A close-up of the northernmost 4°C/100 km temperature gradient maximum over North Dakota (Fig. 51) shows NW 843 bisecting the contour from NW to SE. The ACARS temperature observations from NW 843 show temperature gradients of 1-3°C/100 km over North Dakota. Also note the track of BA025LFZ which depicts a consistent 2-3°C/100 km temperature change along the track while reporting no turbulence (red zero). This illustration indicates

that the NORAPS analysis depicts a temperature gradient that is too strong compared to the observations from NW 843 but agrees well with BA025LFZ.

A close-up of the NORAPS 250 mb temperature analysis at 1200 UTC 16 April 1996 (Fig. 52) reveals a large 4°C/100 km (light green) temperature gradient maximum over Minnesota and Wisconsin which represents a portion of front 23. UAL 29 is crossing the 2°C/100km contour just north of the 4°C/100 km contour. UAL 29's observations reveal a 0-8°C/100 km temperature gradient across the front over Minnesota while NORAPS depicts a maximum gradient of 5°C/100 km. Here, clearly, the NORAPS analysis would have been more accurate if UAL 29's temperature data were input into the model. Also note the PIREP for light turbulence (10) on the western edge of the 2°C/100 km contour.

Figure 53 portrays the NORAPS 200 mb temperature analysis at the same time which is very similar to the 250 mb chart discussed above. This close-up of the same 4°C/100 km maximum over Minnesota and Wisconsin reveals the track of DL 565 crossing the region from west to east. In this case DL 565's observations show a 1-4°C/100 km temperature change across the front which is in good agreement with the NORAPS analysis, except that the aircraft shows the 4°C/100 km maximum slightly to the east of the NORAPS 4°C/100 location. Note the negative report of turbulence within the frontal region (0) over Minnesota.

By 1200 UTC 17 April 1996 the 250 mb analysis depicts a cutoff with the upper front encircling the trough (Fig. 54). The longwave trough is located over the Atlantic Coast and the strongest temperature gradient (4°C/100 km) at the base of the trough with another small maximum over New Brunswick. A close-up of the 4°C/100 km contour over New

37

Brunswick (Fig. 55) reveals the tracks of Royal Dutch Airlines (KLM) Flight 012 and BA009BMZ across the temperature gradient contour. KLM012UMZ crossed the 4°C/100 km maximum and reported temperatures which varied by 2-6°C/100 km. The 6°C/100 km change (from -42 to -48°C) was reported just north of the NORAPS 4°C/100 km contour. BA009BMZ's YRXX temperature observations reveal a temperature gradient of 1-5°C north and west of KLM012's track. The density of the aircraft tracks over the Mid-Atlantic prevented closer inspection of the temperature gradient at the base of the trough.

By 0000 UTC 18 April 1996 the trough and upper front drifted slightly eastward and weakened significantly (no 4°C/100 km contour). Figure 56 zooms in on the base of the trough and displays tracks from UAL871 and DL210. UAL871 is descending as it heads northward, however the southern portion of the track was level and reveals a consistent 1-3°C/100 km temperature change along the track south of and within the temperature gradient contour. The short track of Delta flight 210 reveals a 1-2°C/100 km gradient within the NORAPS 2 °C/100 km temperature gradient maximum.

At 1200 UTC 18 April 1996 (the final NORAPS analysis depicting front 23) the longwave trough and upper front continue to weaken as they exit the domain. The 200 mb level (Fig. 57) depicts a large, mature temperature gradient maximum and a broad upper-level front. Note the circular shape of the temperature gradient maximum around the trough which was typical of a mature front and a filling longwave trough. Figure 58 (a close-up of Fig. 57) depicts KL013UPZ crossing the front over the Canadian Maritime Provinces reporting a 0-2°C/100 km temperature change across the front with no turbulence reported.

The NORAPS temperature analysis and the temperatures from the KLM track match very well over New Brunswick.

Although front 23's duration was much longer than the mean (52 hours), its evolution was fairly representative of the majority of the upper-level fronts. It was a vigorous front from the temperature gradient perspective and had a jet maximum of 70 m/s at 300 mb. Front 23 was distinctive because of the numerous quality aircraft tracks that bisected the front and the temperature gradients they revealed. This front (along with front 13) possessed an aircraft track which had a temperature gradient of $8°C/100$ km which was the greatest detected during the period of the study. During the entire period, the largest temperature gradient contour depicted by NORAPS was $4°C/100$ km (light green) which allows for a maximum gradient of $6°C/100$ km. Therefore, NORAPS under-analyzed the strongest upper fronts which supports the case for including aircraft temperature observations in NORAPS analyses.

V. CONCLUSIONS

The goal of this study was to examine the temperature gradients associated with upper fronts as depicted by NORAPS and to compare these to aircraft-observed temperature gradients. A secondary goal was to observe and document the type and magnitude of turbulence associated with upper fronts as reported by aircraft.

For the period 1 March to 30 April 1996 data volumes for the study were 453,132 ACARS; 485,786 YRXX/AIREP; 71,017 XRXX/AIREP; and 37,371 PIREP observations for a total of 1,047,306.

Thirty distinct upper fronts (defined as having a duration greater than 12 h and a temperature gradient greater than 2°C/100km) were identified and tracked from the NORAPS analyses during the period of the study. In general, the analyzed temperature gradient was weaker than that observed in the ACARS data. The latter depicted a temperature gradient of as high as 8°C/100 km for two cases, whereas the analyzed gradient did not exceed 6°C/100 km. Most upper fronts (47%) attained maximum intensity when located in the base of the upper-level trough, although 33% (13%) did so just downstream (upstream) of the trough line. Most of the useable aircraft tracks were near 200-300 mb, therefore the portion of the upper front above the tropopause was examined in greater detail than the portion below the tropopause, although the latter would be expected to contain stronger temperature gradients.

There were a total of 108,388 aircraft observations that contained turbulence information (almost exclusively from XRXX and YIXX). Of the 71,017 XRXX reports

64% did not report turbulence or were missing turbulence information, 25% reported no turbulence, leaving 11% of observations with a positive report of turbulence. Of the 11% a large majority of the reports were for light turbulence. Of the 37,371 PIREPS (YIXX) 34% did not report or were missing turbulence information, 30% reported no turbulence leaving 36% of observations with a positive report of turbulence. Of the 30% most of the reports were for light or moderate turbulence. Throughout the study the YIXX observations verified that turbulence is generated by upper-level fronts and most often, reports of moderate or greater turbulence occurred within the NORAPS temperature gradient maxima or in close proximity to them. Aircraft reports show that not all upper-level fronts are turbulence producers and that overall, upper-level turbulence is a rare event. An interesting observation concerning aircraft turbulence reports was the fact that almost every automated (ACARS) report from British Airways and KLM Airlines reported while crossing an upper-level front reported zero turbulence despite nearby positive reports of turbulence which may indicate that the algorithm utilized by these airlines needs some refining.

Front 23, which was the subject of the case study, lasted longer than any of the other fronts (144 hr), had numerous readable aircraft tracks crossing the front, and possessed, along with one other front, the largest observed temperature gradient during the study-- 8°C/100 km. The case study revealed that the NORAPS model does an adequate job of depicting upper-level fronts overall, however, aircraft reports consistently revealed larger temperature gradients than the NORAPS analyses rendered. Also, slight position disagreements of these upper-level features were common between the NORAPS analyses and aircraft reports. Occasionally, NORAPS depicted upper-level temperature gradients in

regions where crossing aircraft showed no temperature changes across the feature. Also, the aircraft tracks often revealed smaller scale temperature differences within the NORAPS temperature gradient contours which tended to be smoothed by NORAPS analyses. The high quality, sheer number, and utility of aircraft observations have improved upper-level wind analyses and have the potential to improve NORAPS temperature analyses if utilized by the NORAPS data assimilation system, which may then lead to improved depiction of upper-level fronts in NORAPS analyses.

A recommendation for future study is to complete a more rigorous statistical examination of the NORAPS model temperature analyses as compared to aircraft temperature reports and apply this to evaluate other models as well. Another recommendation would be to compare and contrast the late winter-early spring period of this study to a late fall-early winter period to determine if the observed temperature gradients and turbulence reports vary. Also a study during a mid-summer period may demonstrate the shift of the jet stream/upper fronts northward and the expected weakening of the thermal gradients and turbulence. Finally, because increasing numbers of "pseudo-soundings" are available from airliners during the ascent/descent stage of flight a study comparing conventional rawinsonde soundings to aircraft soundings would be interesting.

Data type	Automated	Latitude/long. units	Temp units	Winds	Turbulence
ACARS	Yes	tenths&hundreds of degrees	tenths °K	dir- whole deg spd- tenths of m/s	Some
AIREP- XRXX	No	tenths of degrees	whole °C	dir- whole deg spd- whole kts	Yes
YRXX	Yes	tenths of degrees	whole °C	dir- whole deg spd- whole kts	Some
PIREP	No	tenths&hundreds converted from NAVAIDS	whole °C	dir- whole deg spd- whole kts	Yes- plain language

Table 1. Characteristics of Aircraft Reports.

0	No Turbulence
10	Light
12	Isolated Light
14	Occasional Light
16	Intermittent Light
18	Continuous Light
20	Light to Moderate
22	Isolated Light to Moderate
24	Occasional Light to Moderate
26	Intermittent Light to Moderate
28	Continuous Light to Moderate
30	Moderate
32	Isolated Moderate
34	Occasional Moderate
36	Intermittent Moderate
38	Continuous Moderate
40	Moderate to Severe
42	Isolated Moderate to Severe
44	Occasional Moderate to Severe
46	Intermittent Moderate to Severe

Table 2. Turbulence Codes

48	Continuous Moderate to Severe
50	Severe
52	Isolated Severe
54	Occasional Severe
56	Intermittent Severe
58	Continuous Severe
60	Chop, Light Chop
62	Isolated Chop, Isolated Light Chop
64	Occasional Chop, Ocnl Light Chop
66	Intermittent Chop, Intmt Light Chop
68	Continuous Chop, Cont Light Chop
70	Light to Moderate Chop
72	Isolated Light to Moderate Chop
74	Occasional Light to Moderate Chop
76	Intermittent Light to Moderate Chop
78	Continuous Light to Moderate Chop
80	Moderate Chop
82	Isolated Moderate Chop
84	Occasional Moderate Chop

Table 2. continued

86	Intermittent Moderate Chop
88	Continuous Moderate Chop
90	Low Level Wind Shear
91	Light Clear Air Turbulence (CAT)
92	Light to Moderate CAT
93	Moderate CAT
94	Moderate to Severe CAT
95	Severe CAT
96	Mountain wave or Mechanical
97	Severe Chop
98	Extreme
99	No Report

Table 2. continued

Coverage Area	Forecast Length	Data Assimilation	Model Grid Characteristics	Numerical Aspects	Physical Parameterizations
CONUS 9000X4000km	48 hours	First guess: 6h forecast Objective Analysis: Multivariate Optimum Interpolation Analysis (MVOI)	Horizontal Resolution: 45 km Vertical Resolution: 36 levels Output Grid Projection: Mercator	Scheme C 4th order finite differencing of horizontal advection 2nd order finite differencing of vertical advection Centered time differencing with split explicit corrections	Boundary Layer: Detering-Etling 1.5 order Louis surface layer Tiedtke shallow cumulus mixing Harshrardhan radiation scheme Large scale lifting precipitation Kuo cumulus convection scheme

Table 3. Basic Characteristics of the NORAPS model.

Front #	Time span (hrs)	Posit. WRT to L/W trough	Max temp grad in °C/100km NORAPS (level in mb)	Max temp grad in °C/100km aircraft (level in mb)	Max jet speed in m/s (level in mb)	Max TB code from aircraft	# of good aircraft tracks
1	24	6	4 (500)	4 (250)	80 (300&250)	30	3
2	36	6	2 (500)	4 (250)	75 (300)	40	4
3	60	5 .	4 (500-400, 250&200)	5 (250)	75 (250)	50	16
4	60	5	4 (500, 450, 400&200)	4 (200)	85 (300&250)	20	8
5	90	6	4 (300&400)	4 (200)	70 (300&250)	30	11
6	24	7	2 (all levels)	2 (250)	70 (300, 250 &200)	50	1
7	120	5	4 (200&400)	5 (200)	75 (250)	50	15
8	72	4	4 (500, 400, 250&200)	5 (250)	75 (250)	50	14
9	24	5	2 (all levels)	3 (250)	80 (250)	20	6
10	24	5	2 (all levels)	2 (300)	65 (300&200)	18	4
11	72	5	4 (500, 250&200)	4 (200)	70 (300&250)	98	12
12	24	5	4 (200)	4 (250)	50 (300&250)	30	4
13	36	5	4 (500, 300, 250&200)	8 (200)	70 (200)	30	6
14	36	6	4 (250)	3 (200)	55 (250)	50	7
15	12	5	2 (all levels)	4 (200)	40 (300&250)	10	2

Table 4. Summary of Upper-level Fronts

Front #	Time span (hrs)	Posit. WRT to L/W trough	Max temp grad in °C/100km NORAPS (level in mb)	Max temp grad in °C/100km aircraft (level in mb)	Max jet speed in m/s (level in mb)	Max TB code from air-craft	# of good air-craft tracks
16	12	6	4 (250&200)	5 (200)	55 (300&250)	0	2
17	12	6	2 (all levels)	2 (300&250)	55 (250)	-	2
18	48	5	4 (250&200)	4 (250&300)	60 (300)	30	11
19	12	5	2 (all levels)	3 (300)	45 (300&250)	30	5
20	72	5	4 (500, 250&200)	5 (200)	85 (200)	30	17
21	60	6	4 (500, 450, 250&200)	5 (250)	85 (200)	40	13
22	24	4	2 (all levels)	5 (250)	60 (350, 300 &250)	10	2
23	144	5	4 (500, 250&200)	8 (250)	70 (300)	50	26
24	72	6	4 (200)	5 (250)	70 (200)	40	9
25	72	4	4 (400)	4 (300&200)	75 (250)	40	11
26	60	6	4 (500, 450, 400&200)	6 (250)	70 (300&250)	30	12
27	36	3	4 (200)	3 (200)	60 (250&300)	20	4
28	72	5	4 (500, 450, 400&200)	6 (200)	80 (300, 250 &200)	40	17
29	72	4	4 (400&200)	6 (250&200)	80 (300&250)	40	14
30	72	5	4 (500, 450, 400&200)	6 (200)	75 (300&250)	50	12

Table 4. continued
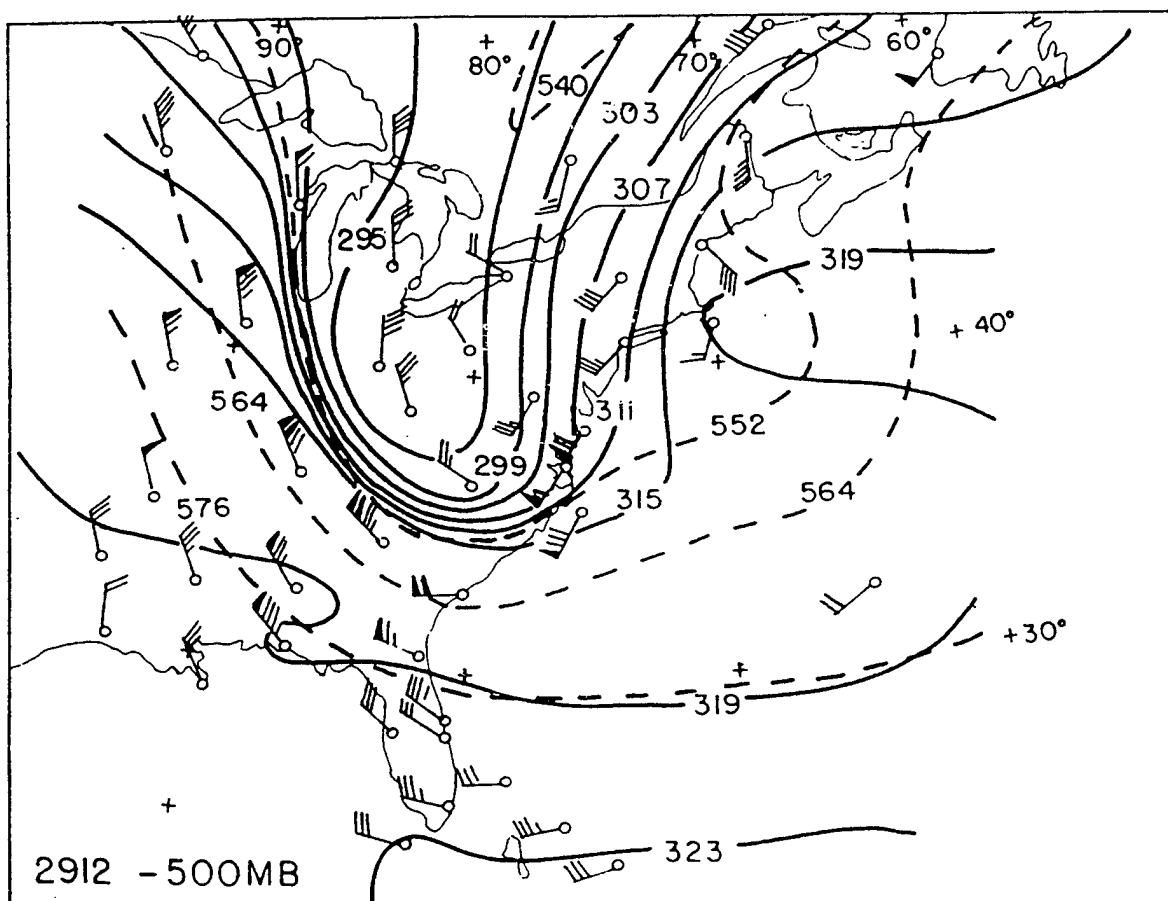
Figure 1. Analysis valid at 1200 UTC 29 October 1963 from Sanders (1991) depicting a strong upper front (18°C/100km) at 500 mb.
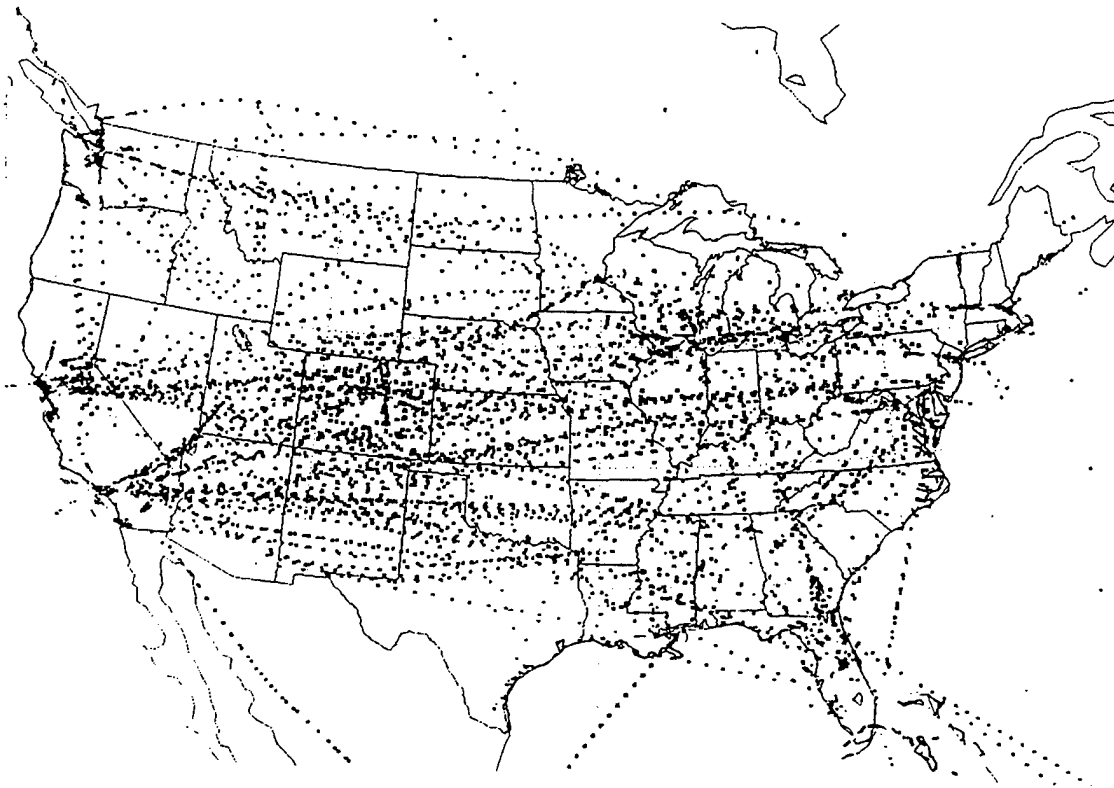
Figure 2. ACARS report locations (1239 observations) for all altitudes 0000-1200 UTC 20 Nov 1995 (Moninger 1995)

53
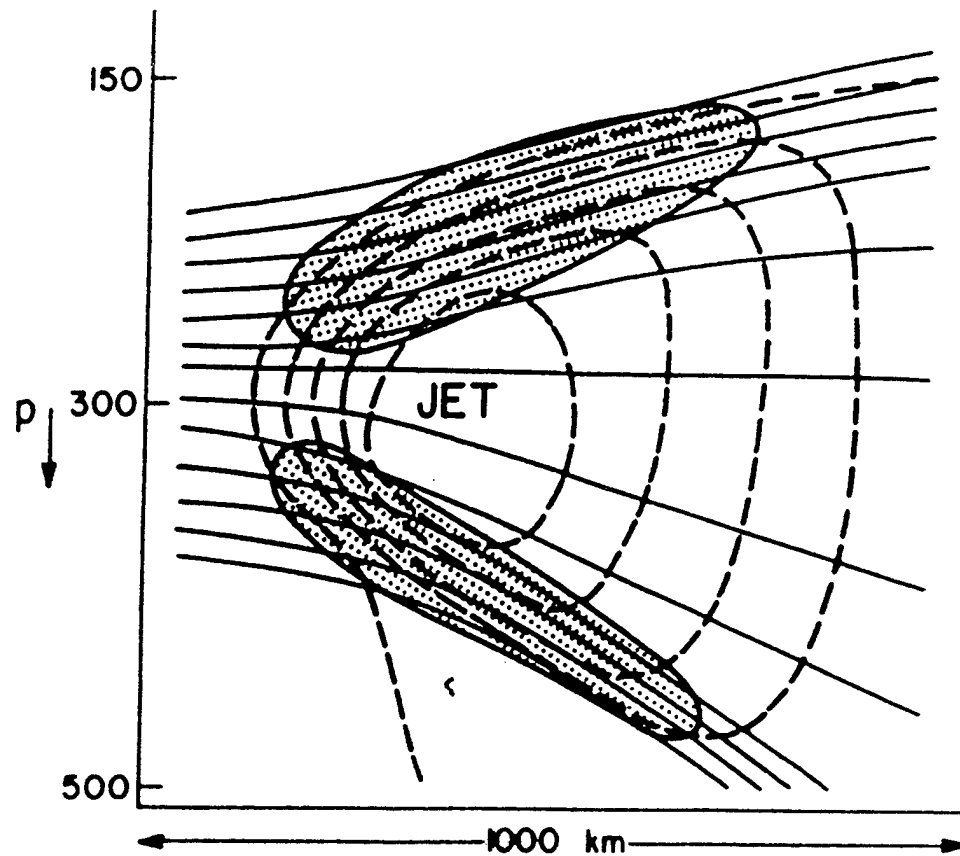
Figure 3. Schematic of regions of clear-air turbulence (stippled) in the vicinity of an upper-level frontal zone. Solid and dashed lines respectively indicate potential temperature and winds (Shapiro 1976)

54
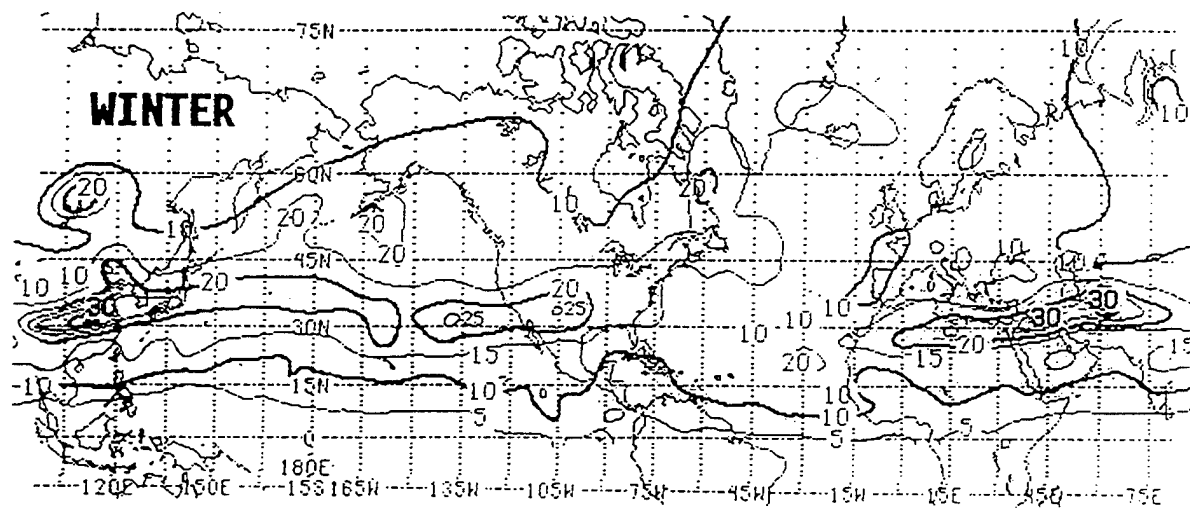
Figure 4. Average Turbulence Index (x10) for the winters of 1991-92 and 1992-93 for 250-300mb. Analysis based on 171 days of data (Ellrod 1993).
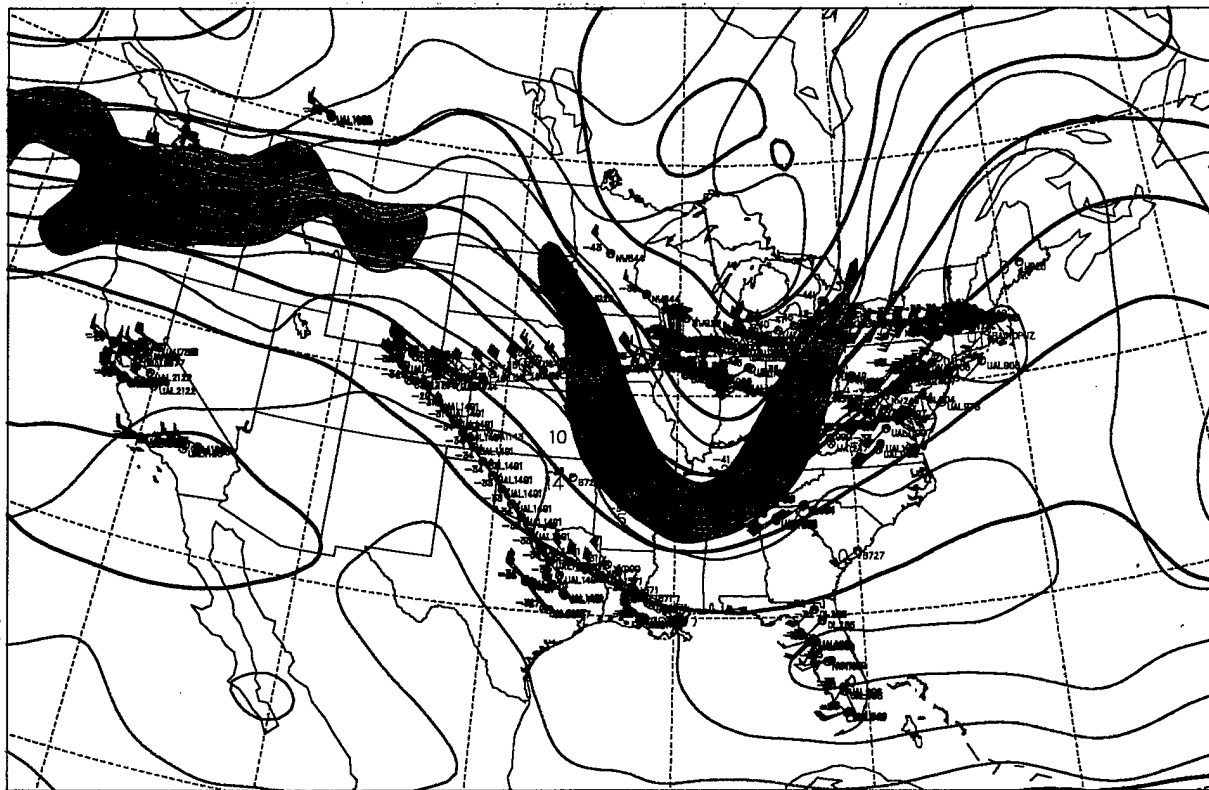
Figure 5. The domain examined in this study. Sample data and analyses are from 1200 UTC 26 April 1996.
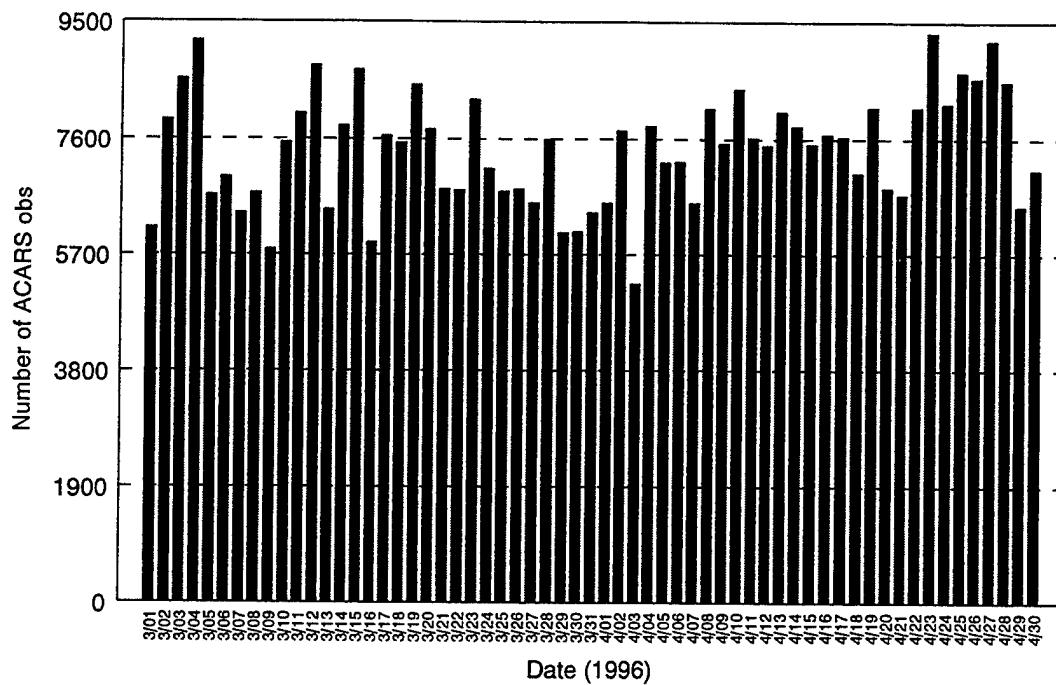
Figure 6. Number of ACARS reports per day during the study. The mean was 7428 per day for a total of 453,132.
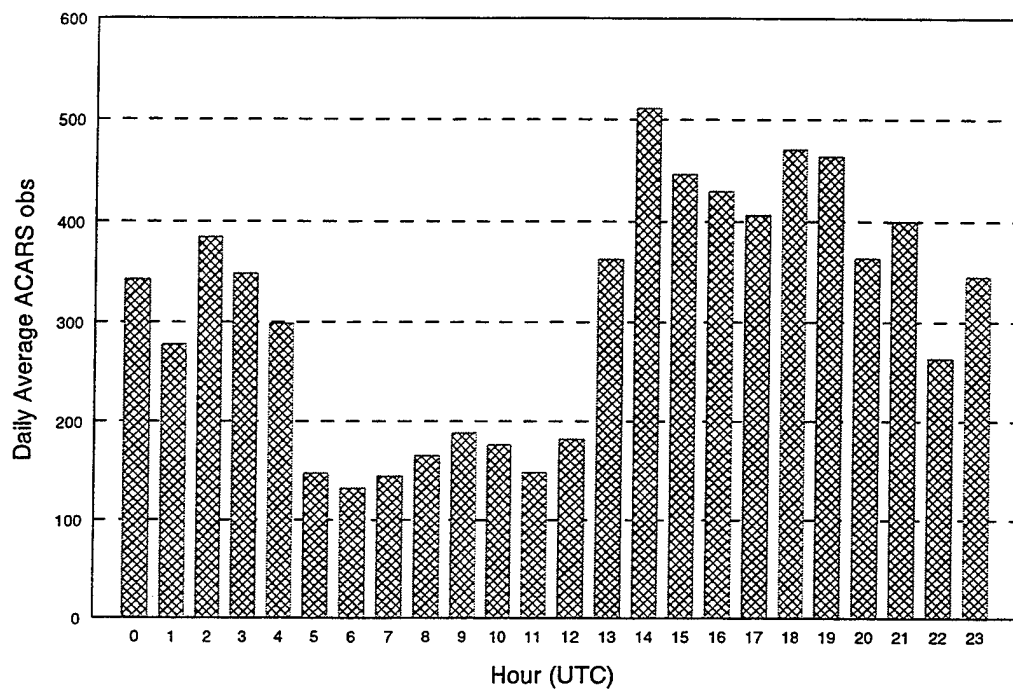
Figure 7. Daily average number of ACARS observations by hour during the study.
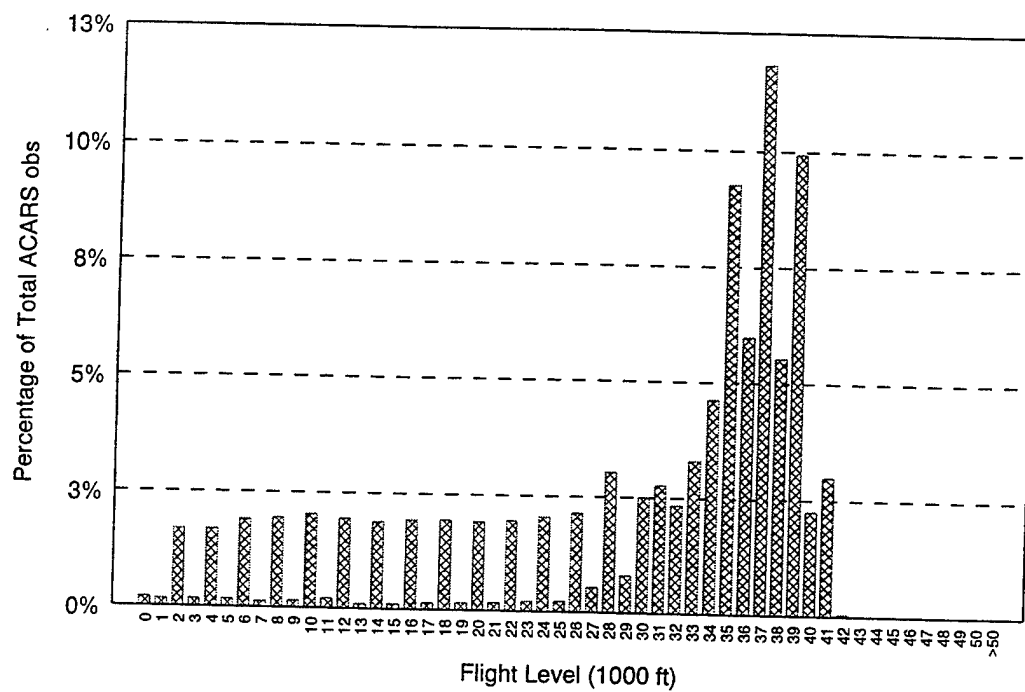
Figure 8. Percentage of total ACARS observations by altitude or flight level. Note that the large majority of observations occur above Flight Level (FL) 280.
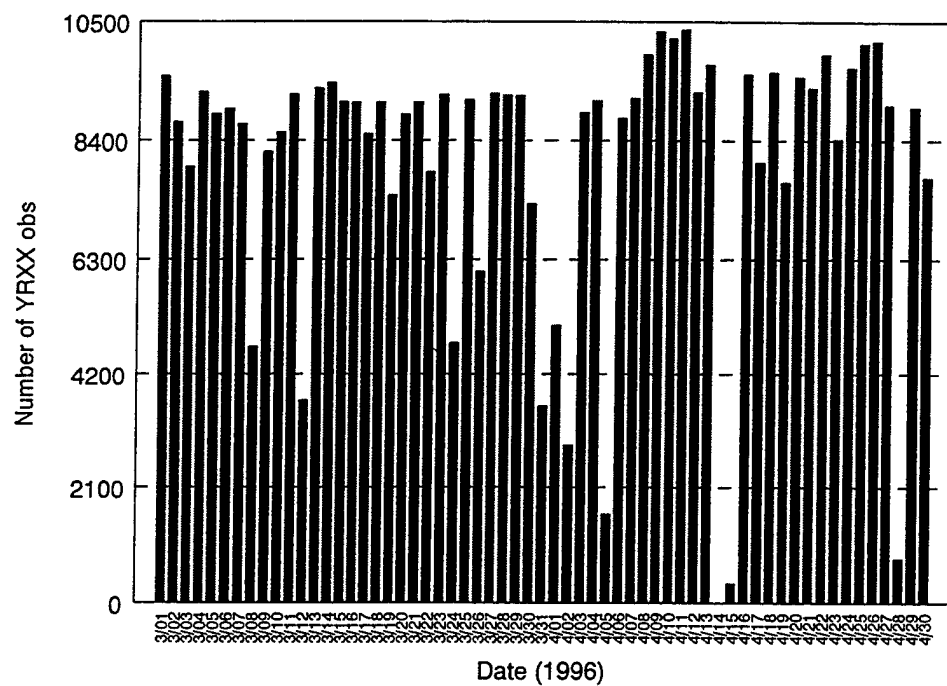
Figure 9. Number of YRXX reports per day during the study. The mean was 7964 per day for a total of 485,786.
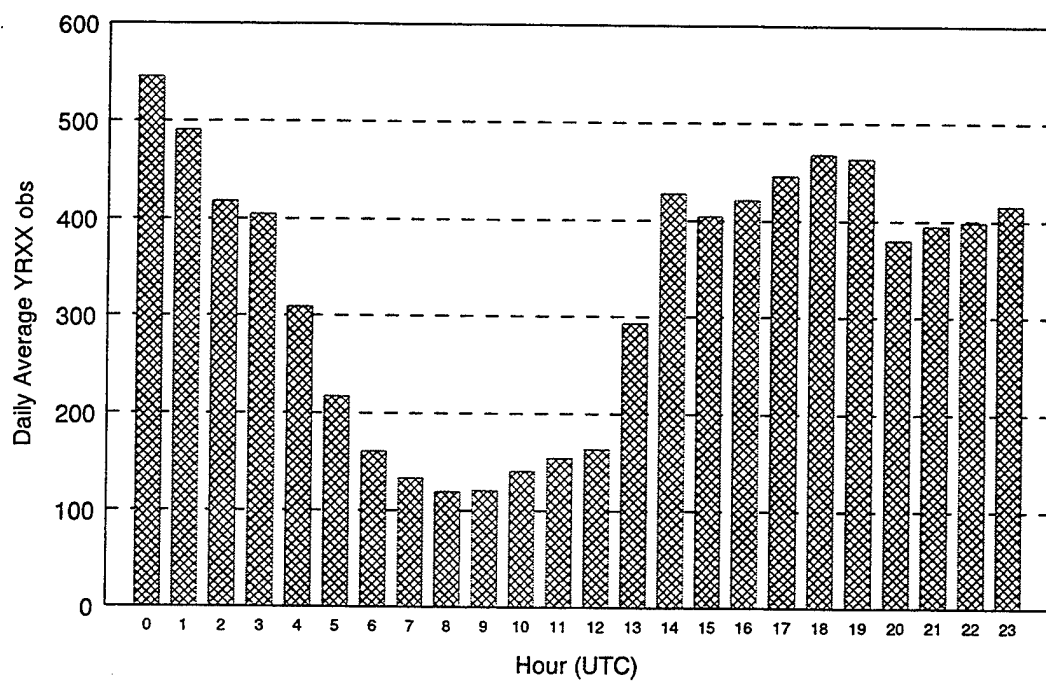
Figure 10. Same as Fig. 7 except for YRXX observations.
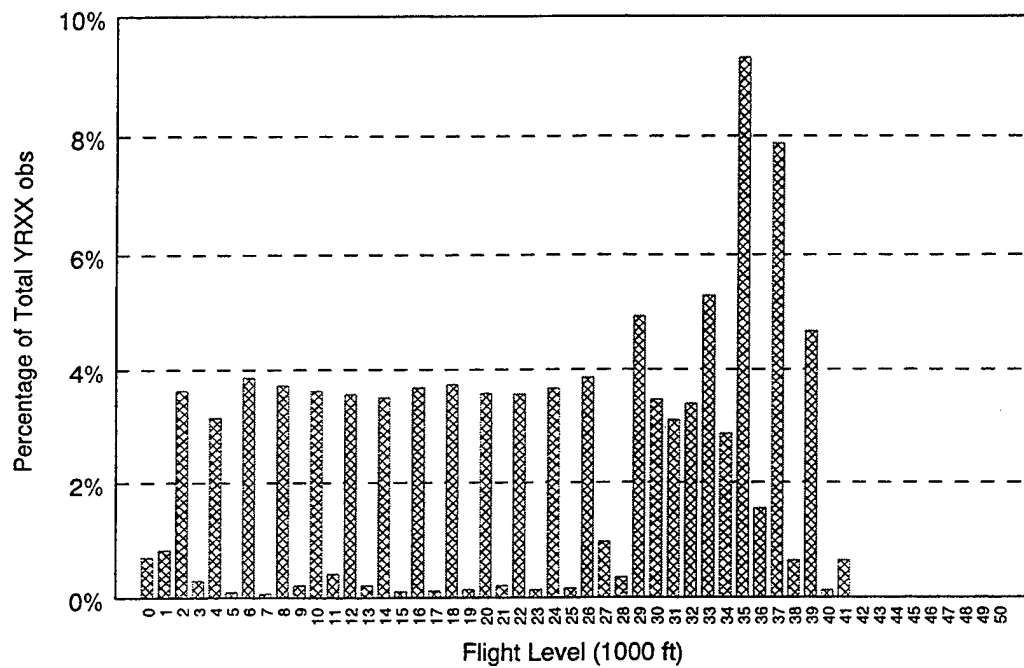
Figure 11. Same as Fig. 8 except for YRXX observations.
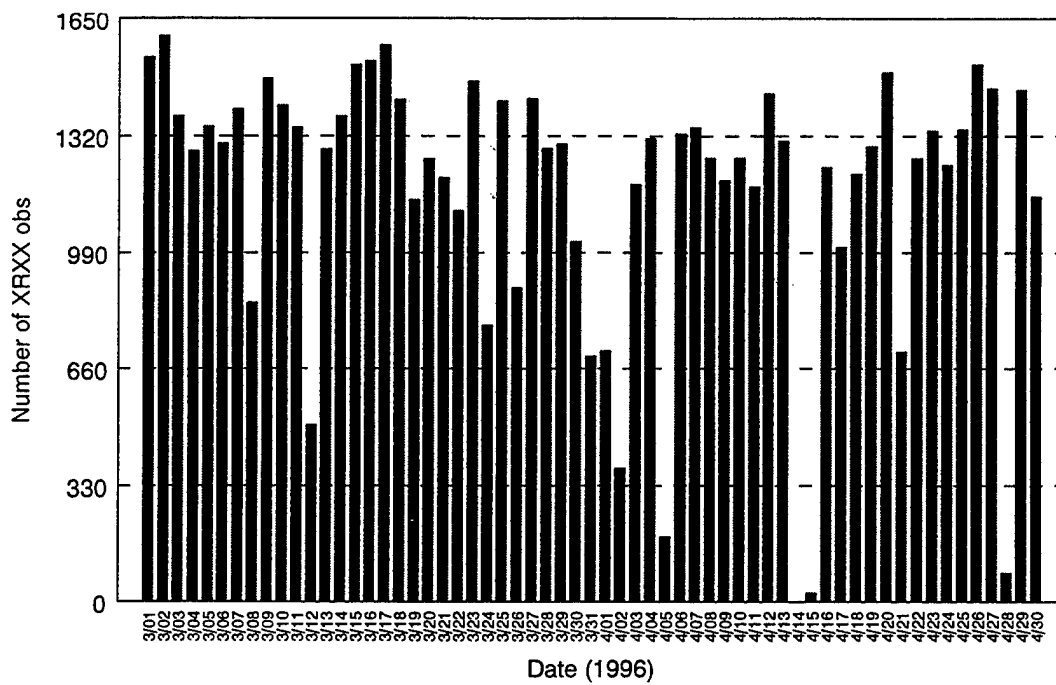
Figure 12. Number of XRXX reports per day during the study. The mean was 1164 per day for a total of 71,017.
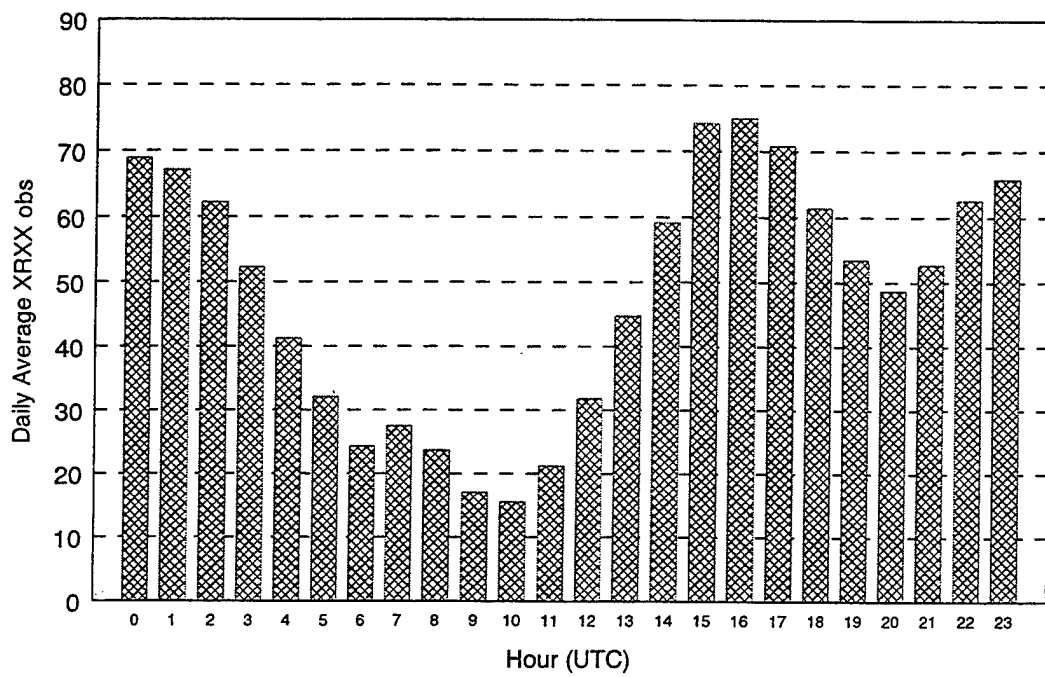
Figure 13. Same as Fig. 7 except for **XRXX** observations.
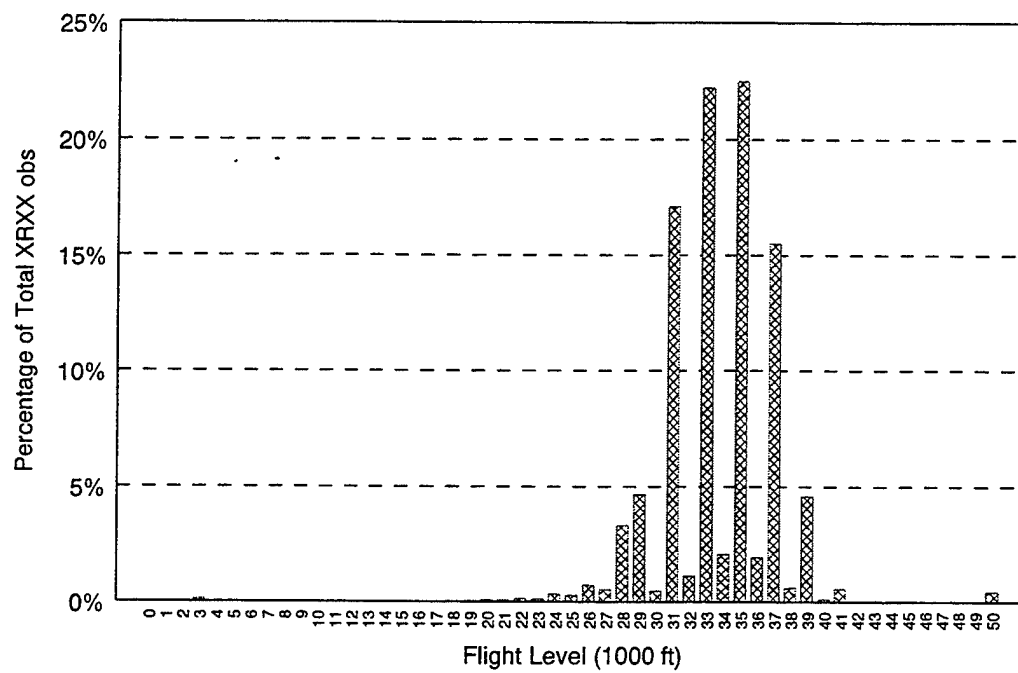
Figure 14. Same as Fig. 8 except for XRXX observations.
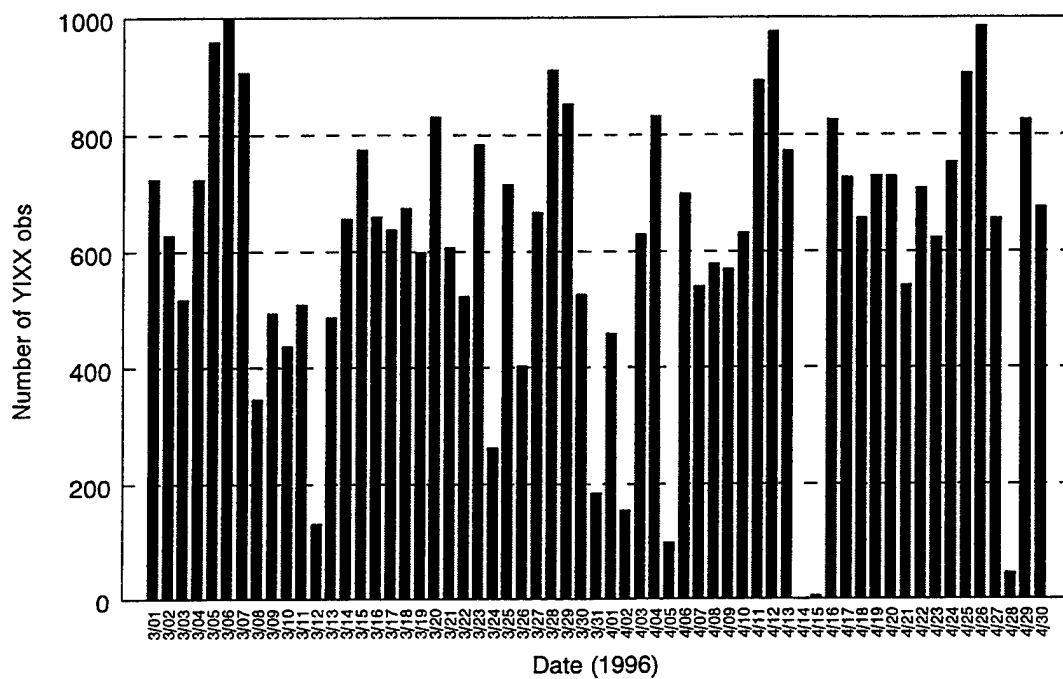
Figure 15. Number of YIXX reports per day during the study. The mean was 613 per day for a total of 37,371.
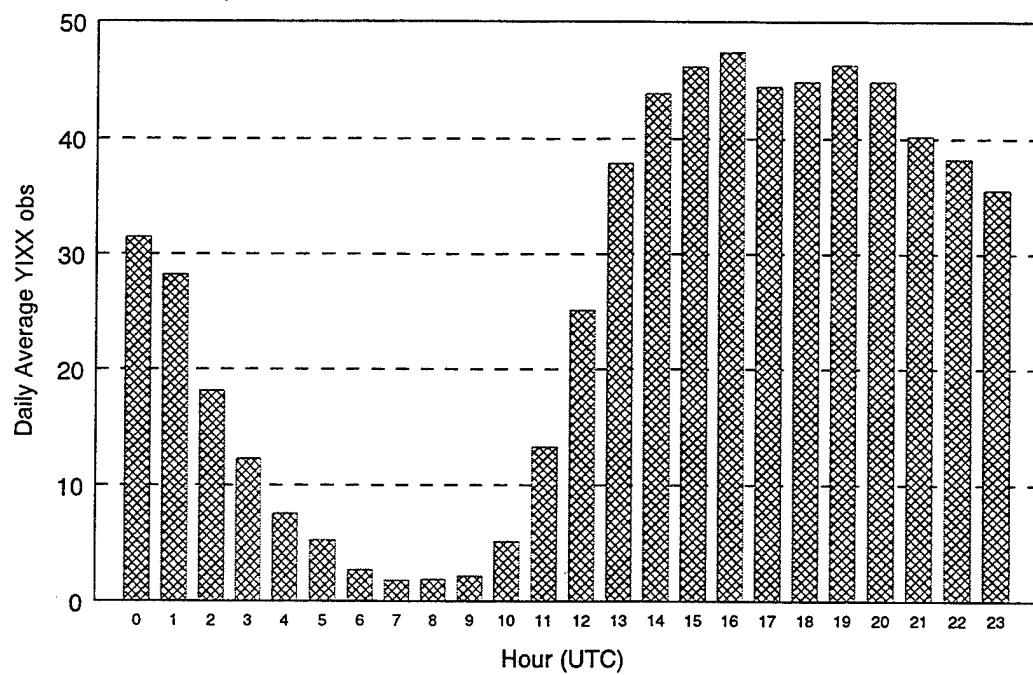
Figure 16. Same as Fig. 7 except for YIXX observations.
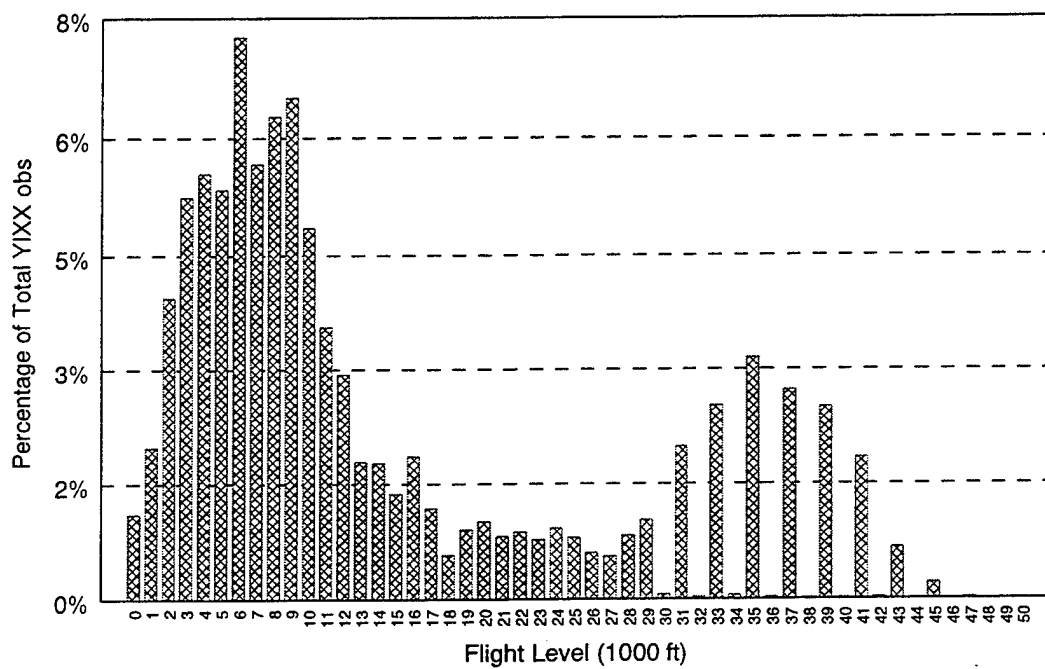
Figure 17. Same as Fig. 8 except for YIXX observations. Note that the majority of reports are at lower altitudes (below 10,000 feet) with a secondary maximum above FL280.

68
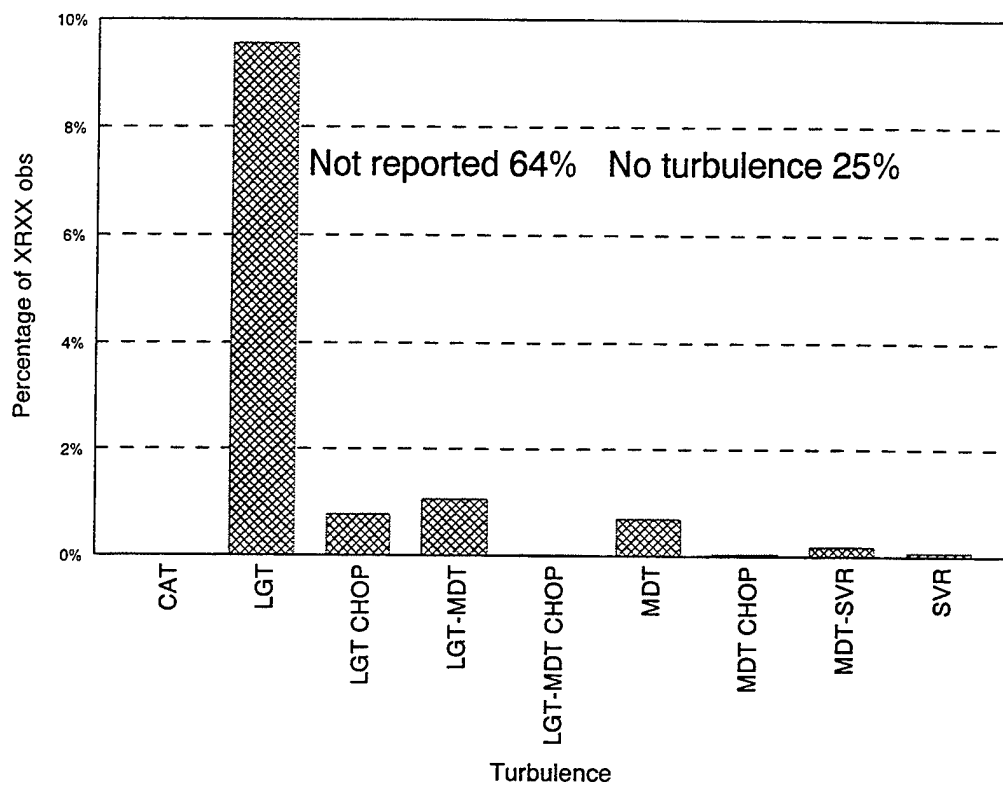
Figure 18. Percentage of XRXX turbulence reports by intensity level.
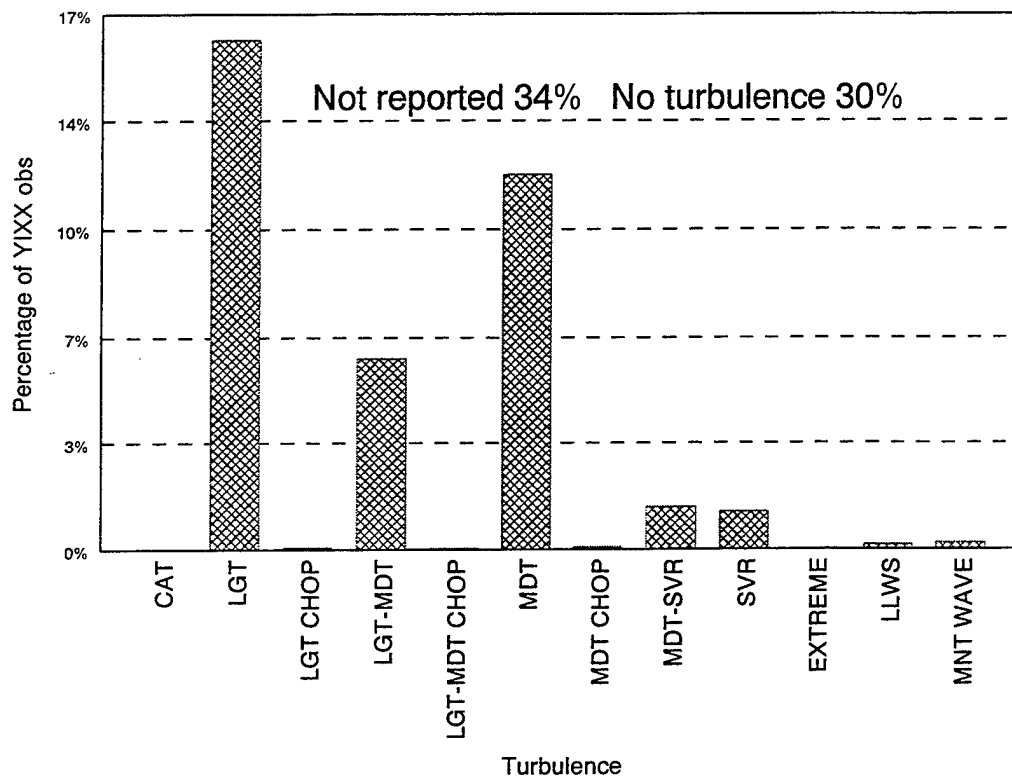
Figure 19. Percentage of YIXX turbulence reports by intensity level.
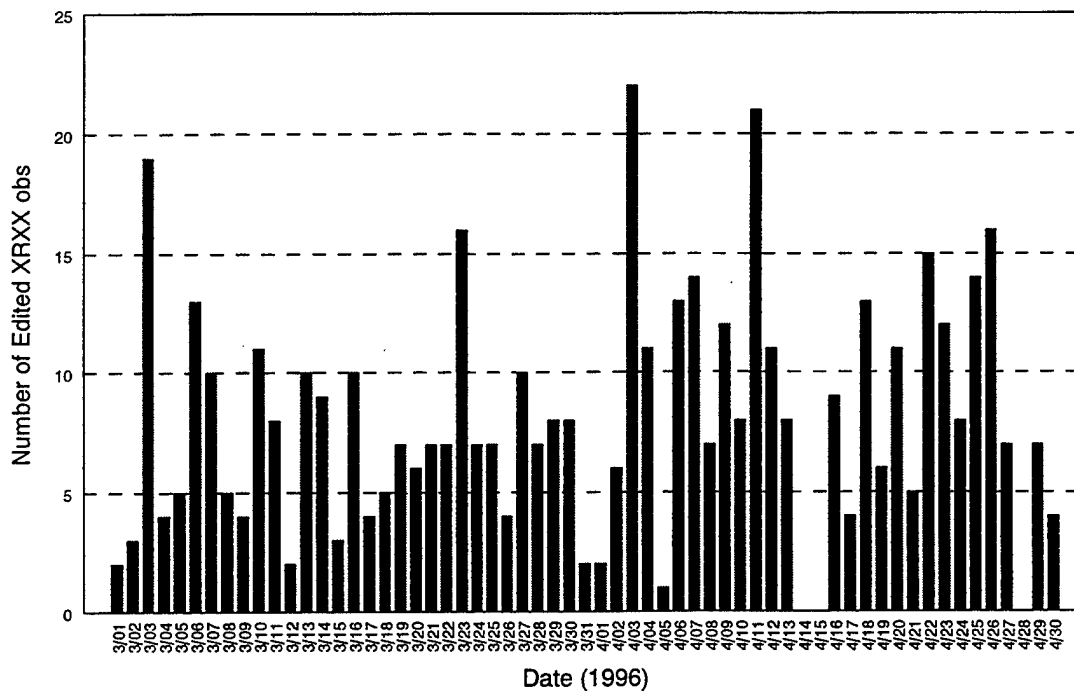
Figure 20. Number of hand edited XRXX observations, which were inserted into the database, by day during the period of the study. The mean was 8 per day for a total number of edited observations of 490.

71
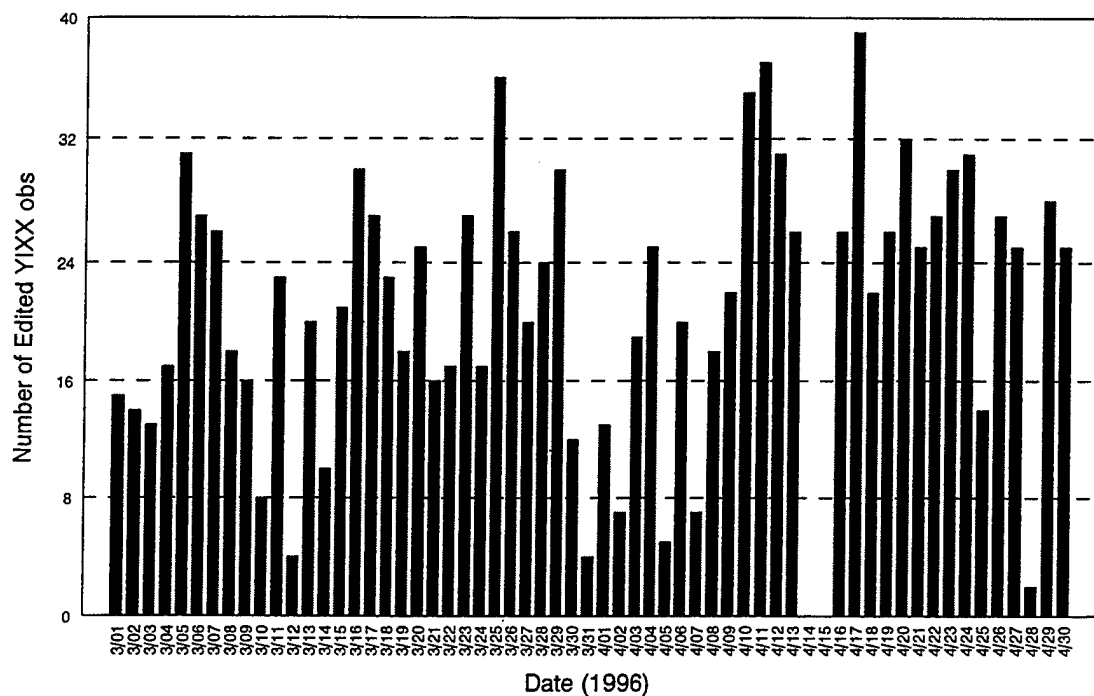
Figure 21. Number of hand edited YIXX observations, which were inserted into the database, by day during the period of the study. The mean was 21 per day for a total number of edited observations of 1200.
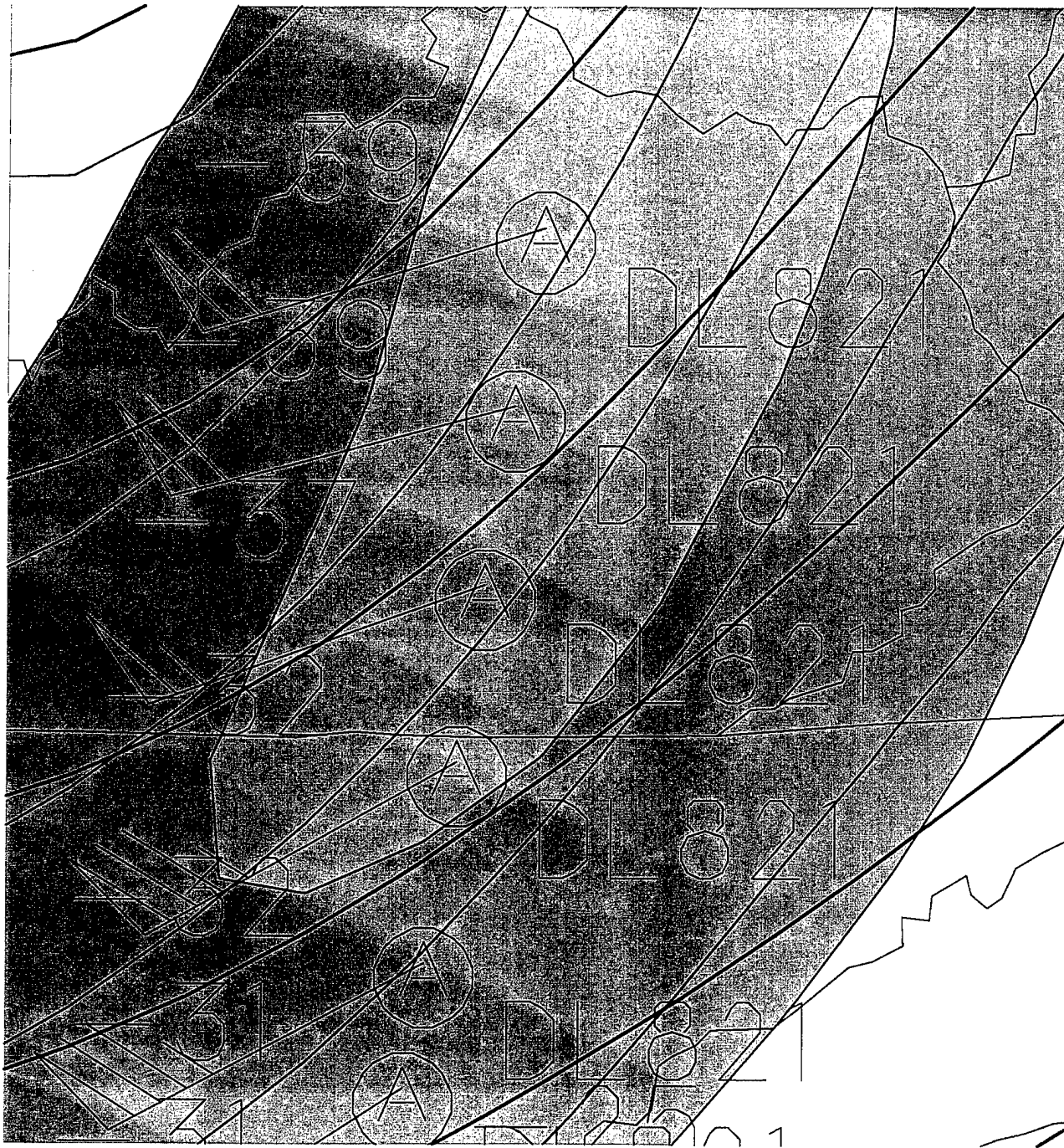
Figure 22. A close-up of Delta Flight 821 traversing an upper front over Tennessee and Kentucky on the NORAPS potential temperature analysis valid at 1200 UTC 26 April 1996 at 400 mb. The shading represents NORAPS temperature gradients of 2°C/100 km (dark green) and 4°C/100 km (light green).

73
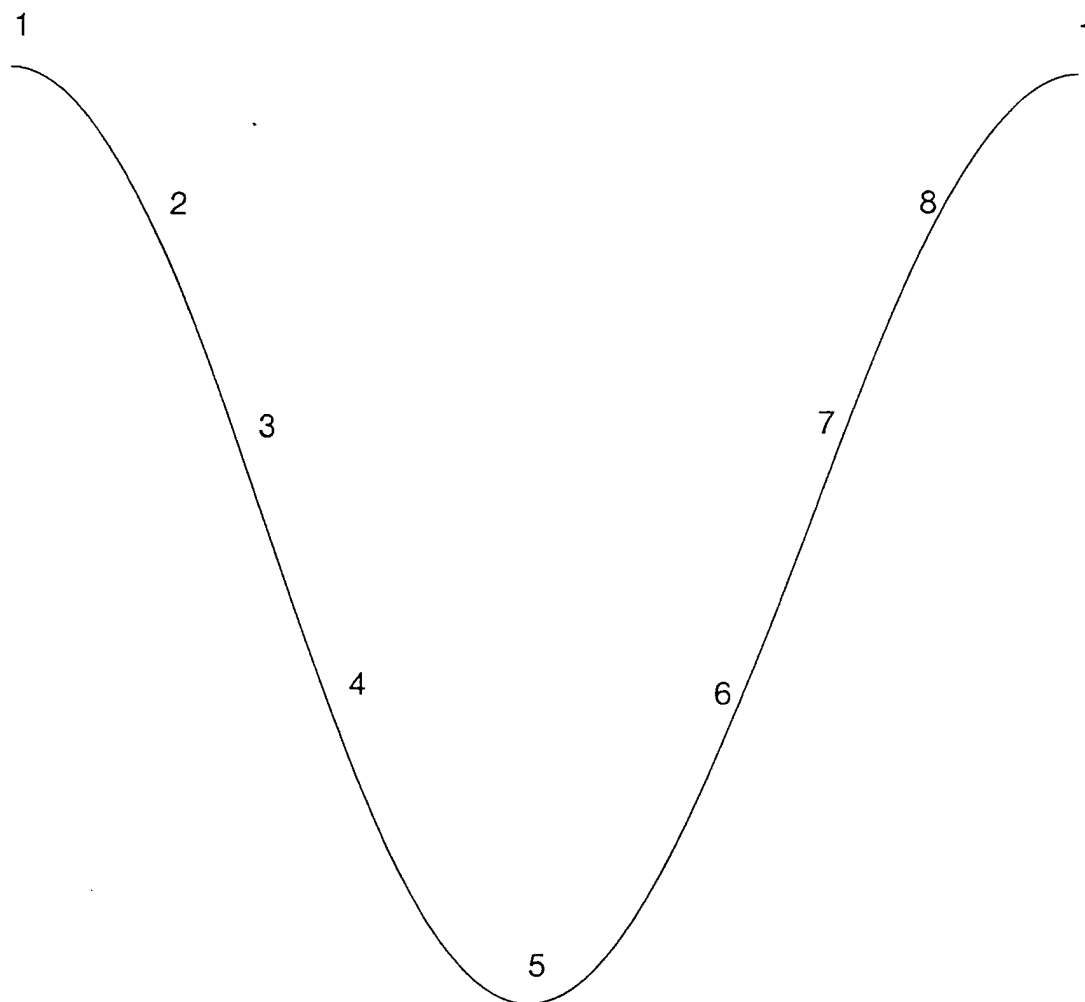
Figure 23. Schematic presentation of the positions of the upper front relative to the upper trough utilized throughout this study.

Figure 24. 200 mb NORAPS potential temperature analysis valid at 0000 UTC 24 March
1996. Dark green shading represents a 2°C/100 km gradient; light green shading
represents a 4°C/100 km gradient. The red observations indicate that turbulence
information was reported by that aircraft. The bold black lines are isoheights and the thin
black lines are isotherms.

Figure 25. Close-up of Fig. 24 which depicts an aircraft observation (PIREP) reporting extreme turbulence (98) over central Arizona by a Cessna Citation (C650).

Figure 26. Same as Fig. 24 except for 300 mb at 0000 UTC 30 April 1996.
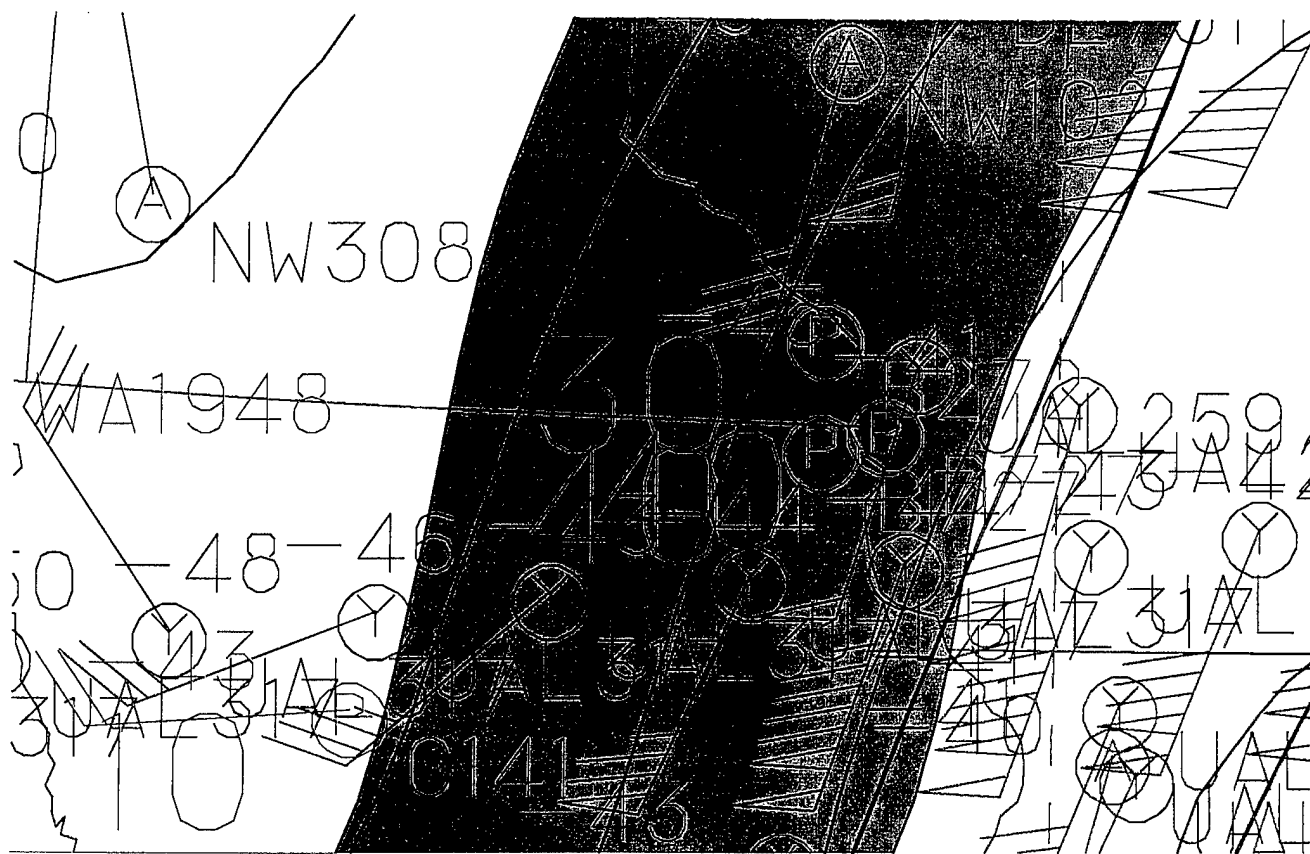
Figure 27. Close-up of Figure 26 in the vicinity of Iowa and southern Minnesota.
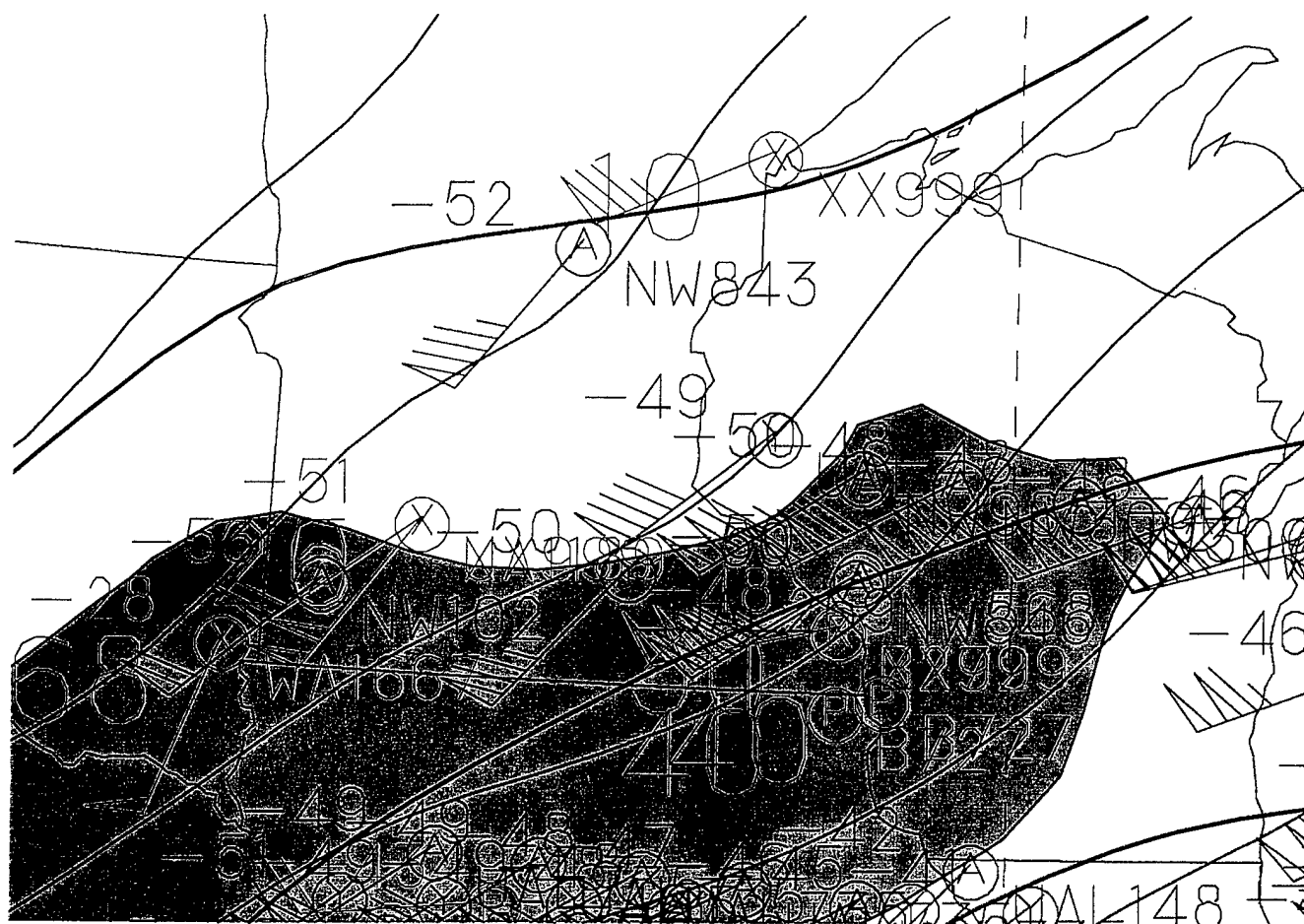
Figure 28. Close-up of 300 mb NORAPS potential temperature analysis valid at 0000 UTC 29 April 1996 in the vicinity of northern Iowa/southern Minnesota/central Wisconsin.
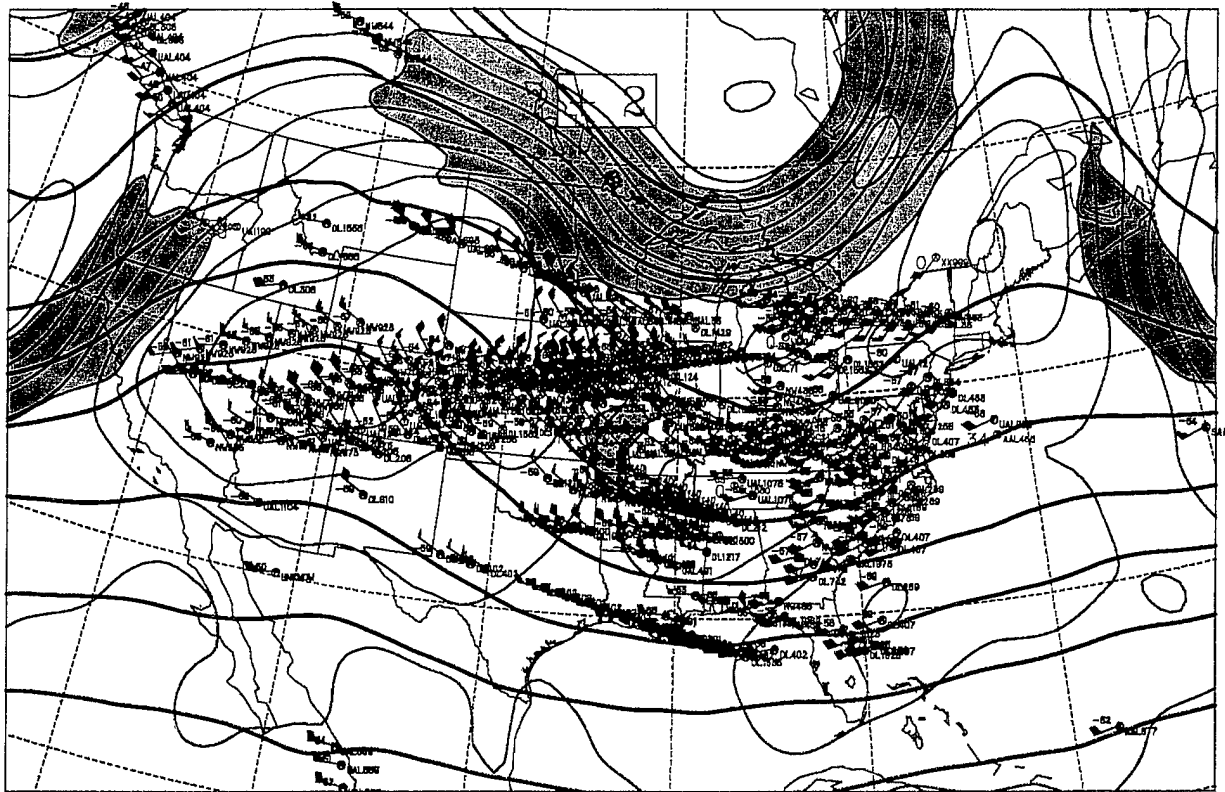
Figure 29. Same as Fig. 24 except for 1200 UTC 1 April 1996.

Figure 30. Close-up of Fig. 29 over the Upper Midwest.
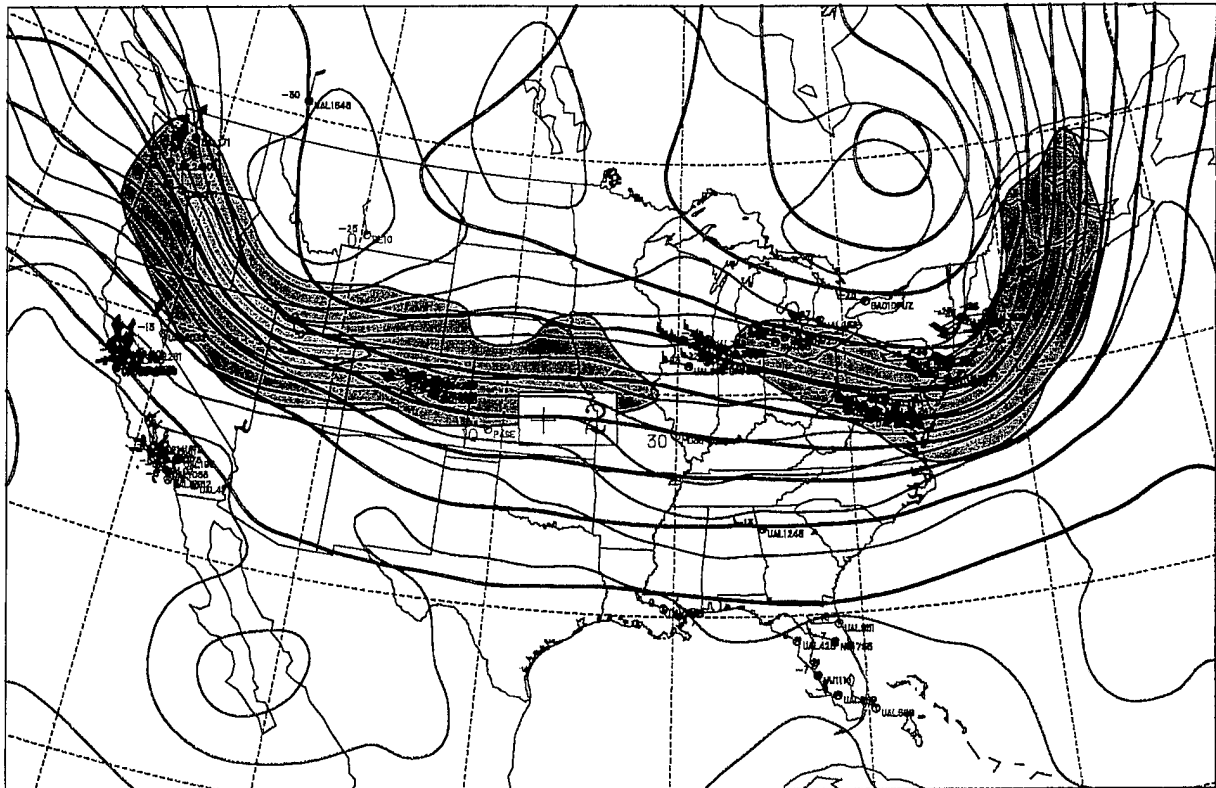
Figure 31. Same as Fig. 24 except for 0000 UTC 28 April 1996.
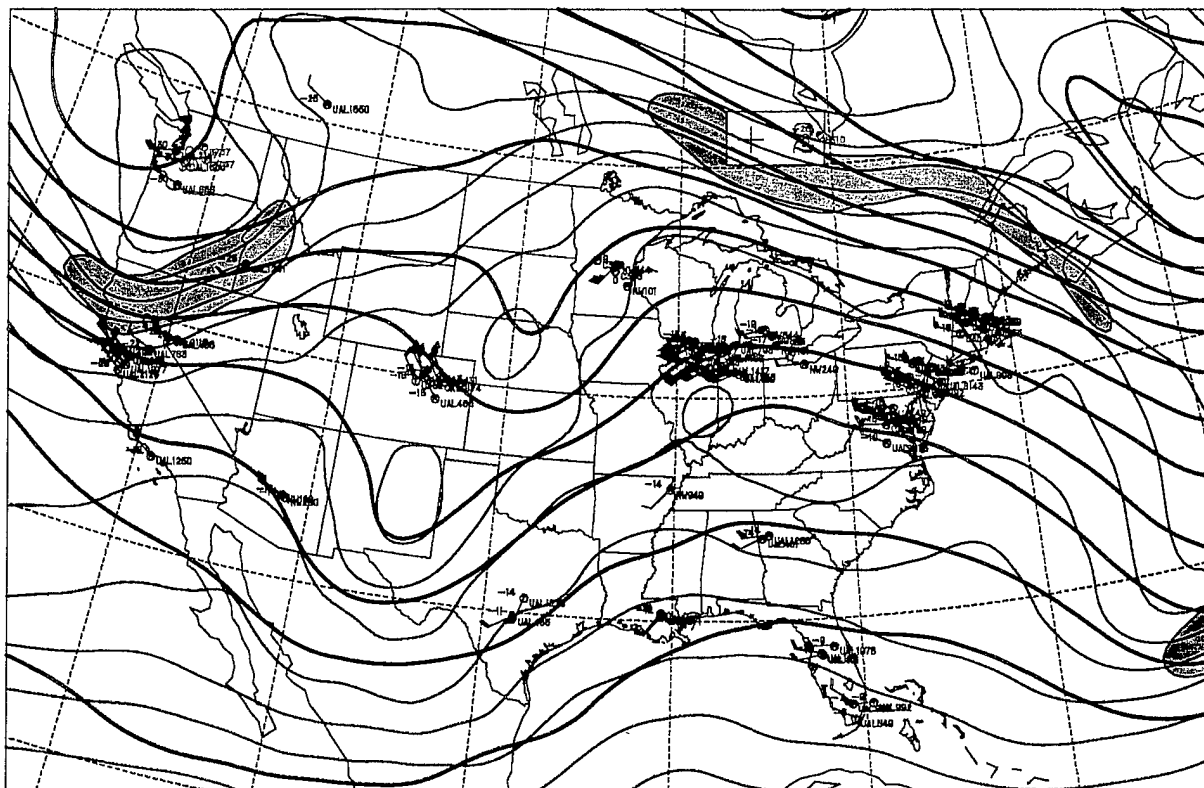
Figure 32. 500 mb NORAPS potential temperature analysis valid at 1200 UTC 12 April 1996. Dark green shading represents a 2°C/100 km; light green shading represents a 4°C/100 km gradient. The red observations indicate that turbulence information was reported by the aircraft. The bold black lines are isoheights and the thin black lines are isotherms.
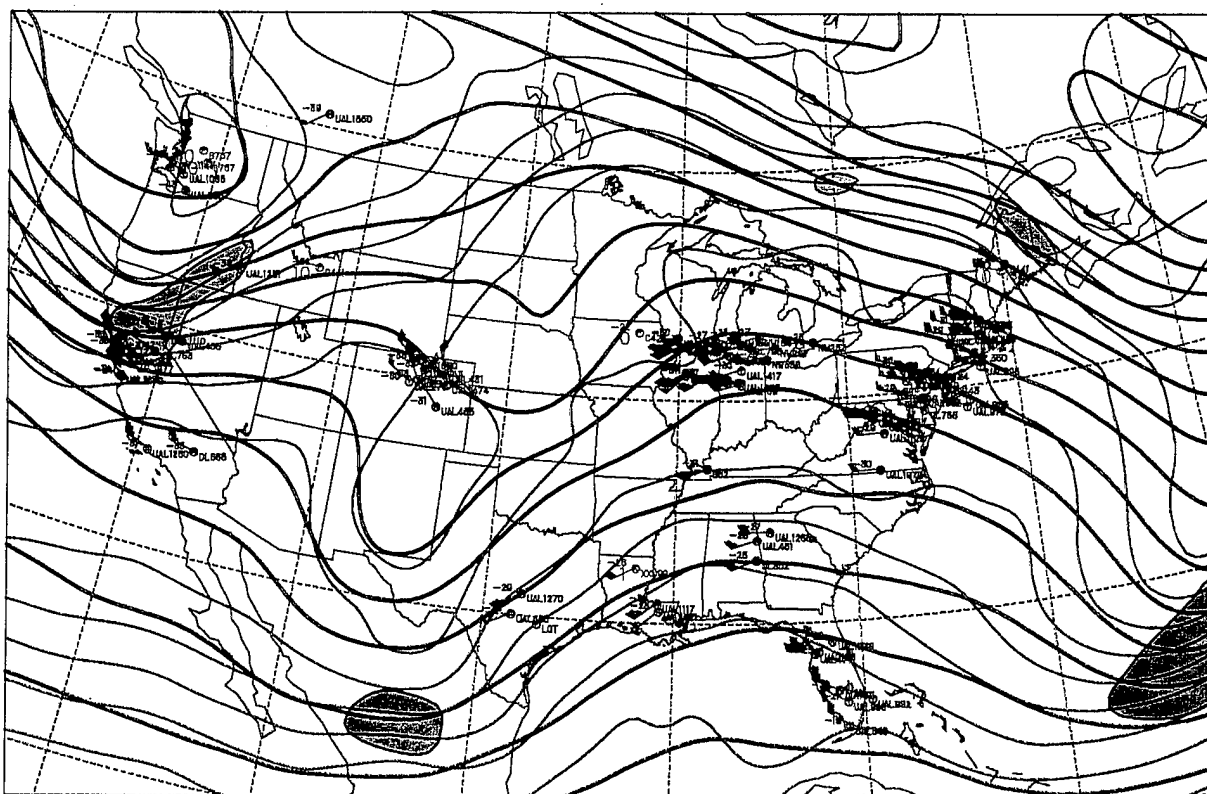
Figure 33. Same as Fig. 32 at 400 mb.

Figure 34. Same as Fig. 32 at 300 mb.
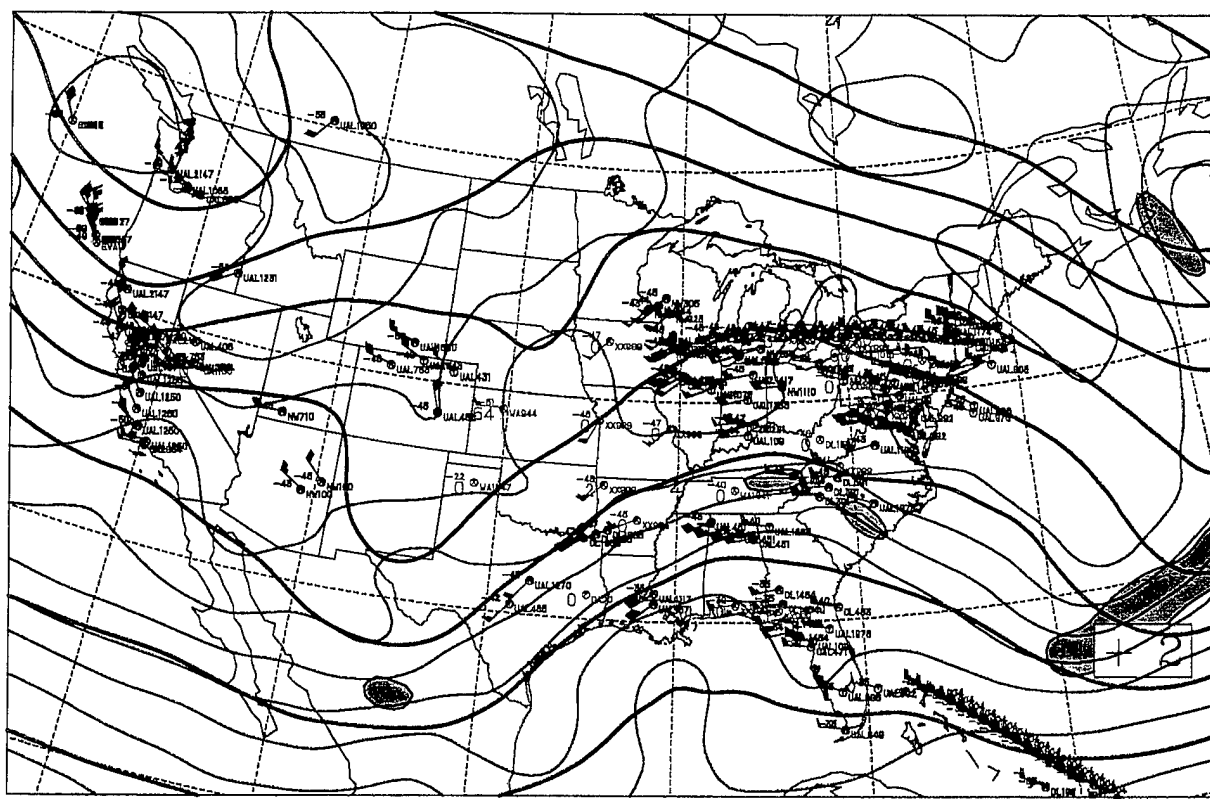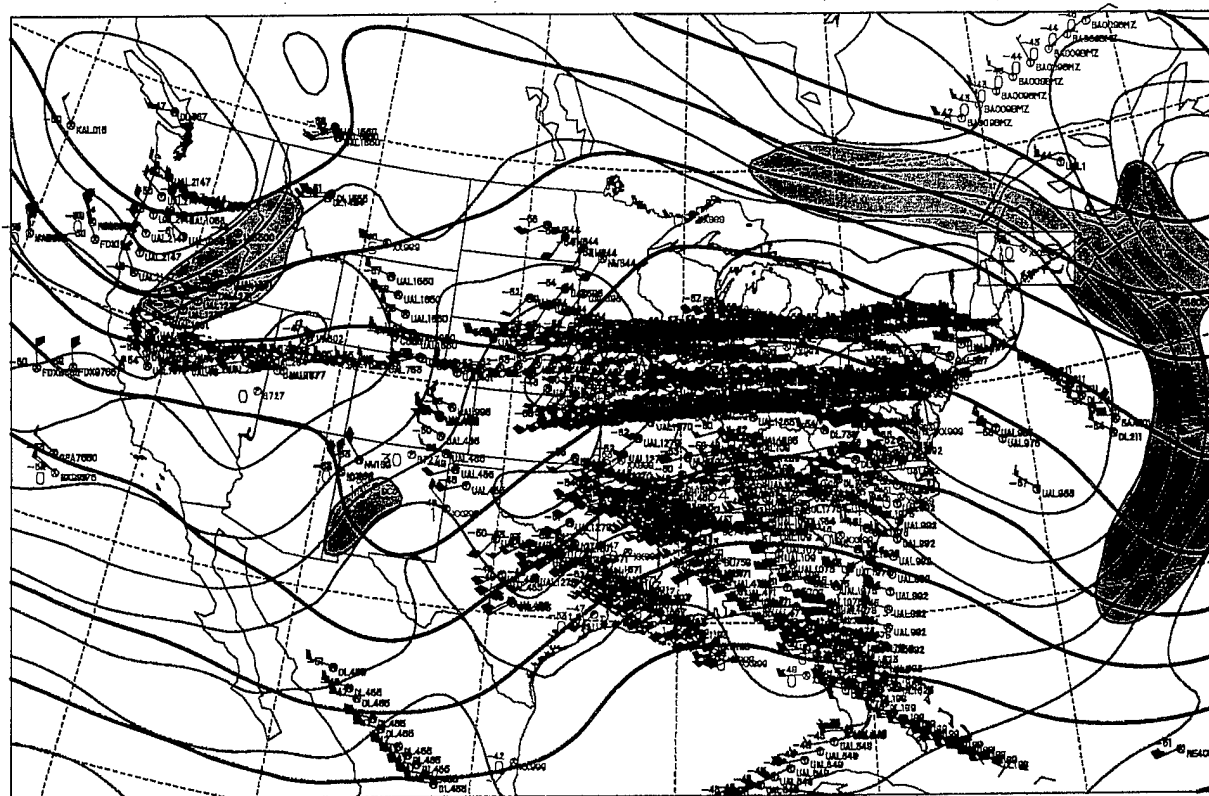
Figure 35. Same as Fig. 32 at 250 mb.
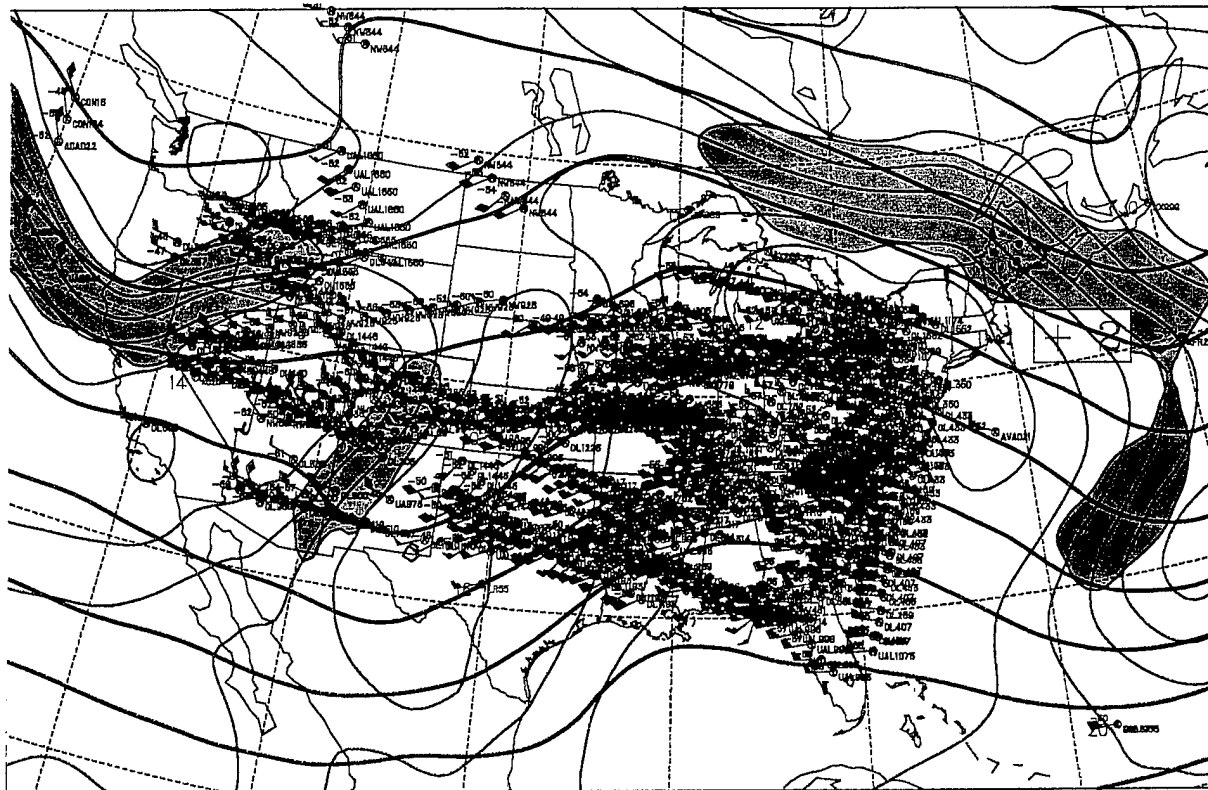
Figure 36. Same as Fig. 32 at 200 mb.

Figure 37. Close-up of the track of BA025LFZ over California and Nevada on the NORAPS 200 mb potential temperature analysis at 0000 UTC 13 April 1996.

88
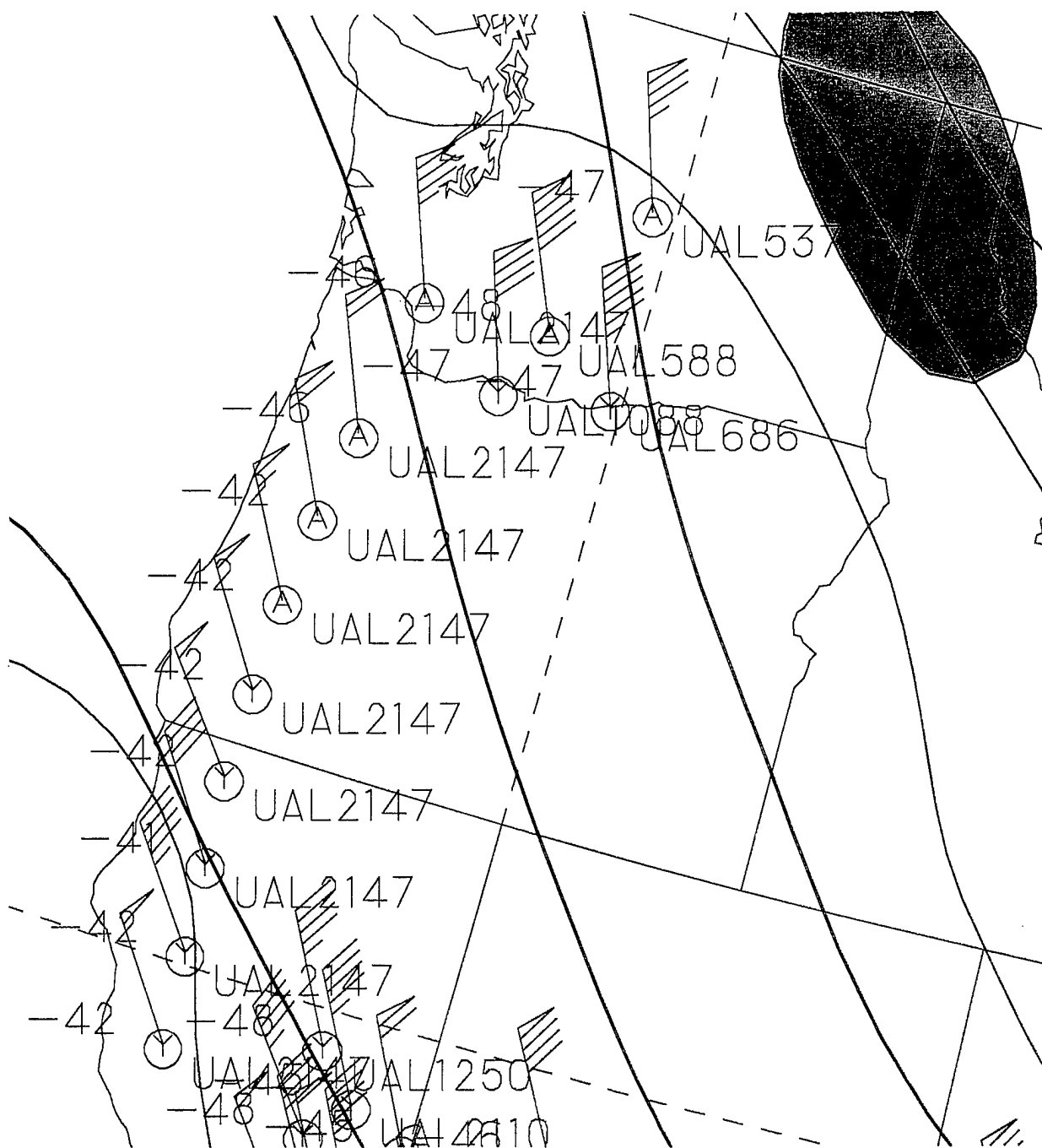
Figure 38. Close-up of the track of UAL 2147 over Oregon and California on the NORAPS 300 mb potential temperature analysis at 1200 UTC 13 April 1996.
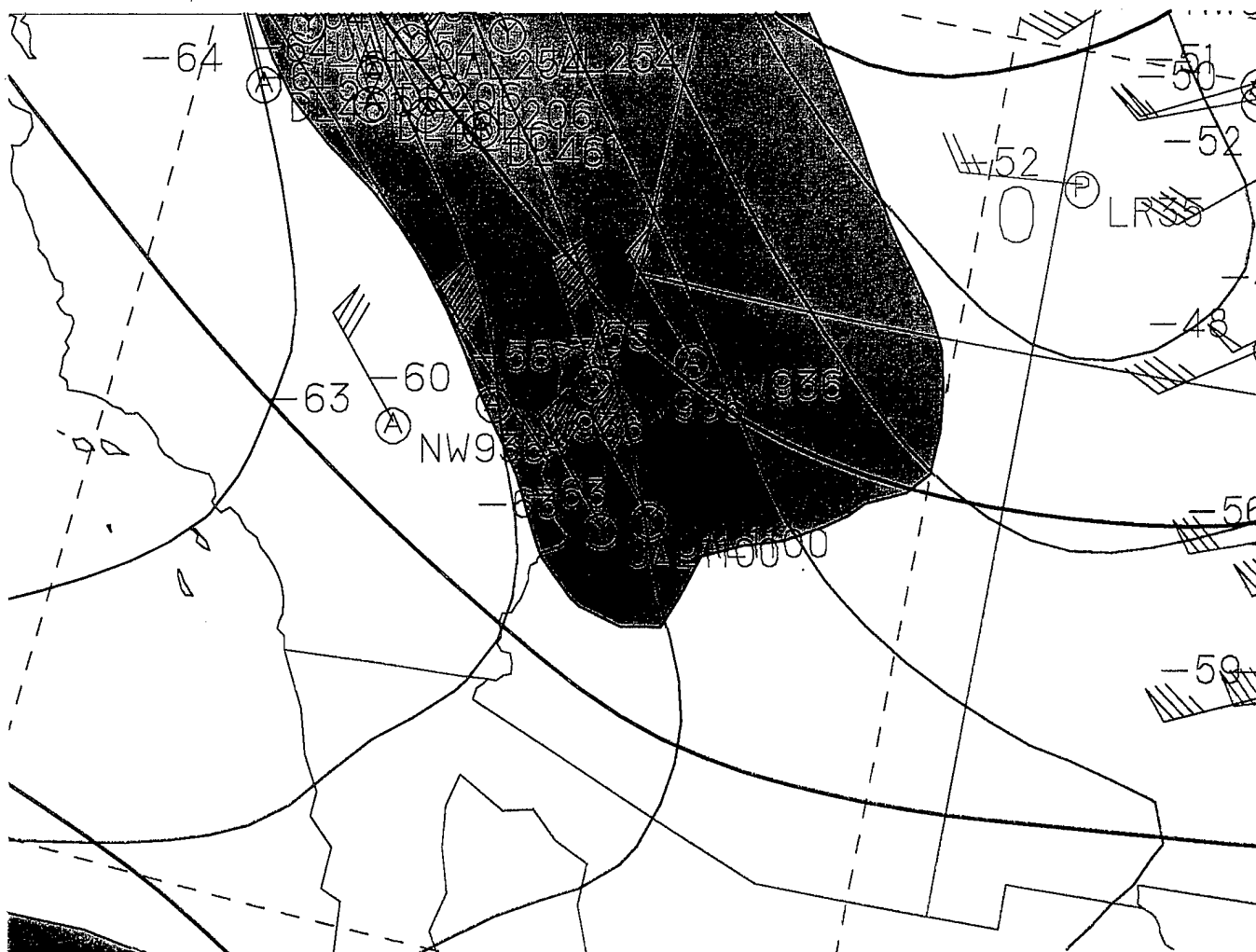
Figure 39. Close-up of the track of NW 936 over California and Nevada on the NORAPS 200 mb potential temperature analysis at 1200 UTC 13 April 1996.
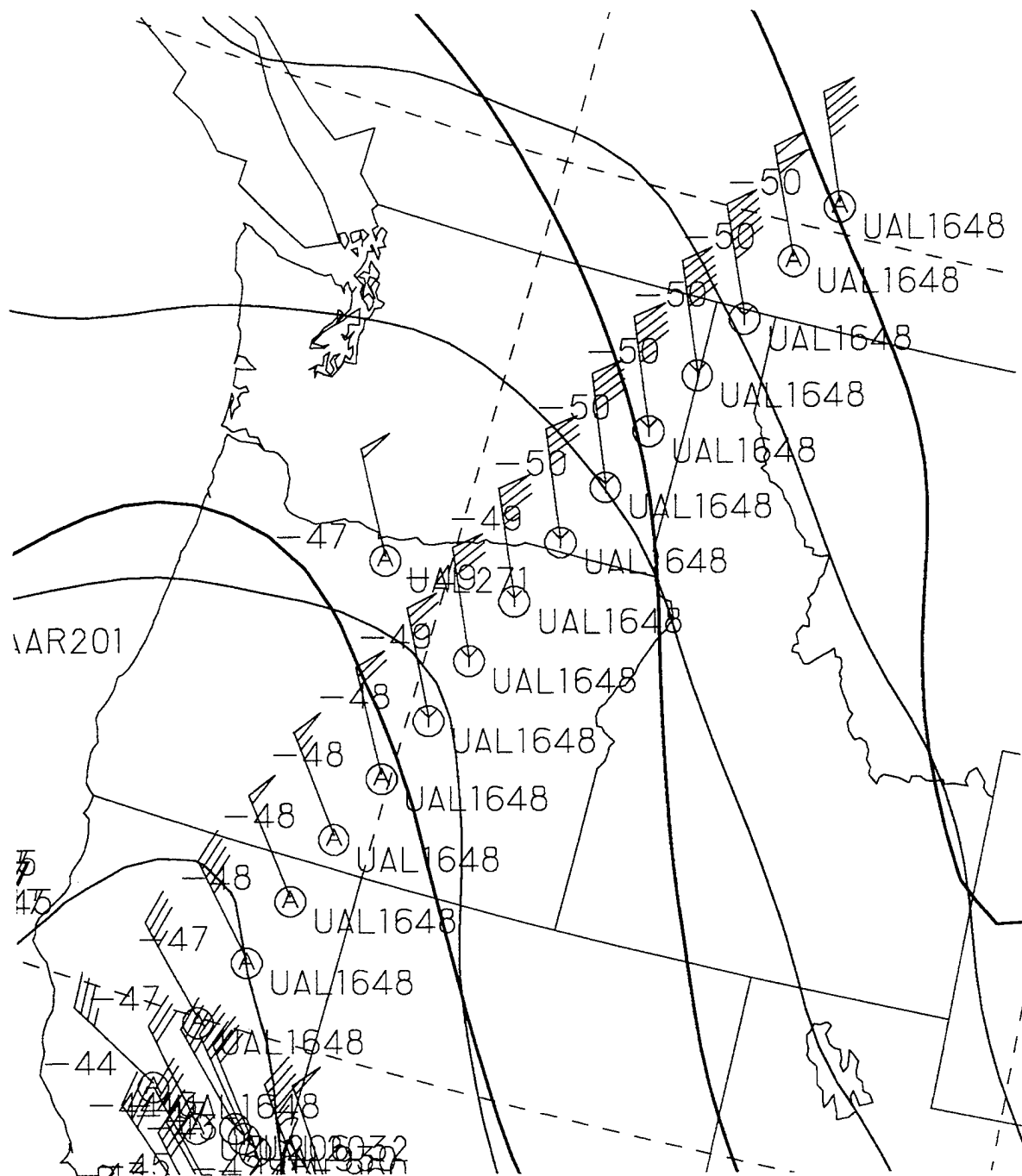
Figure 40. Close-up of the track of UAL 1648 over the Pacific Northwest on the NORAPS 300 mb potential temperature analysis at 0000 UTC 14 April 1996.
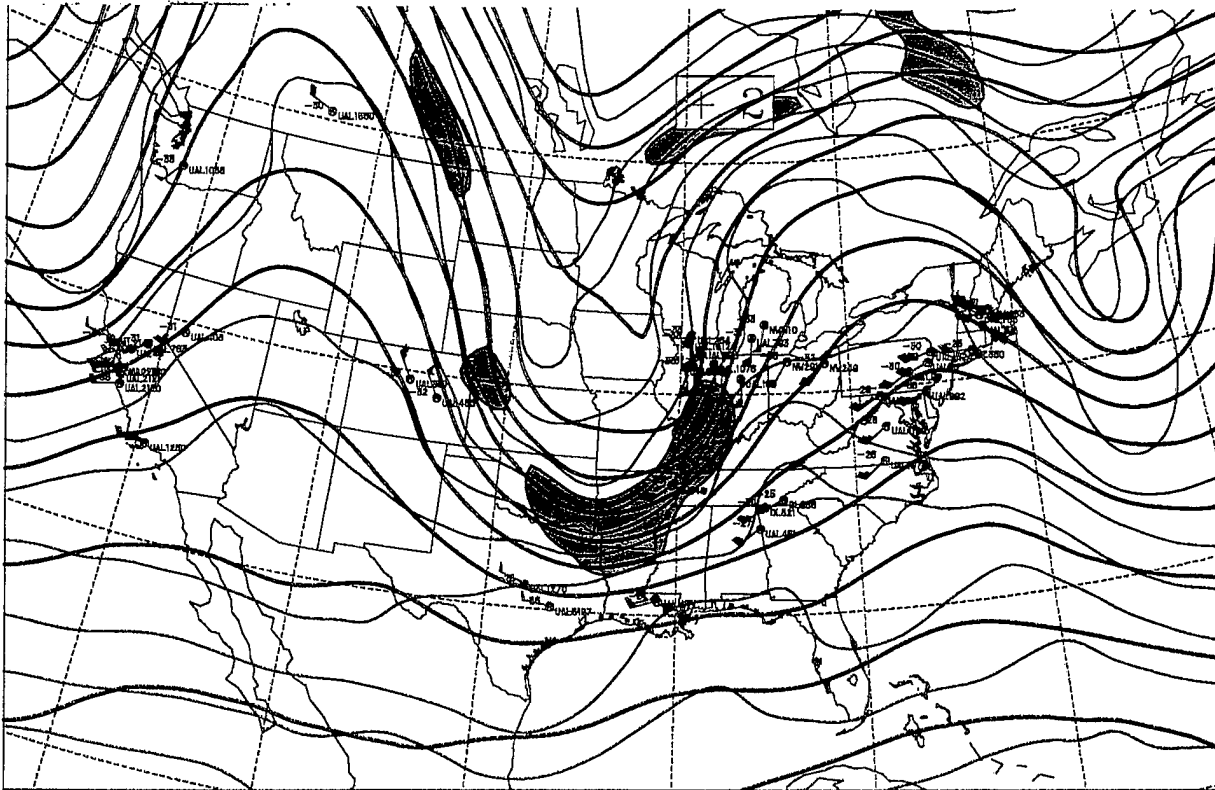
91
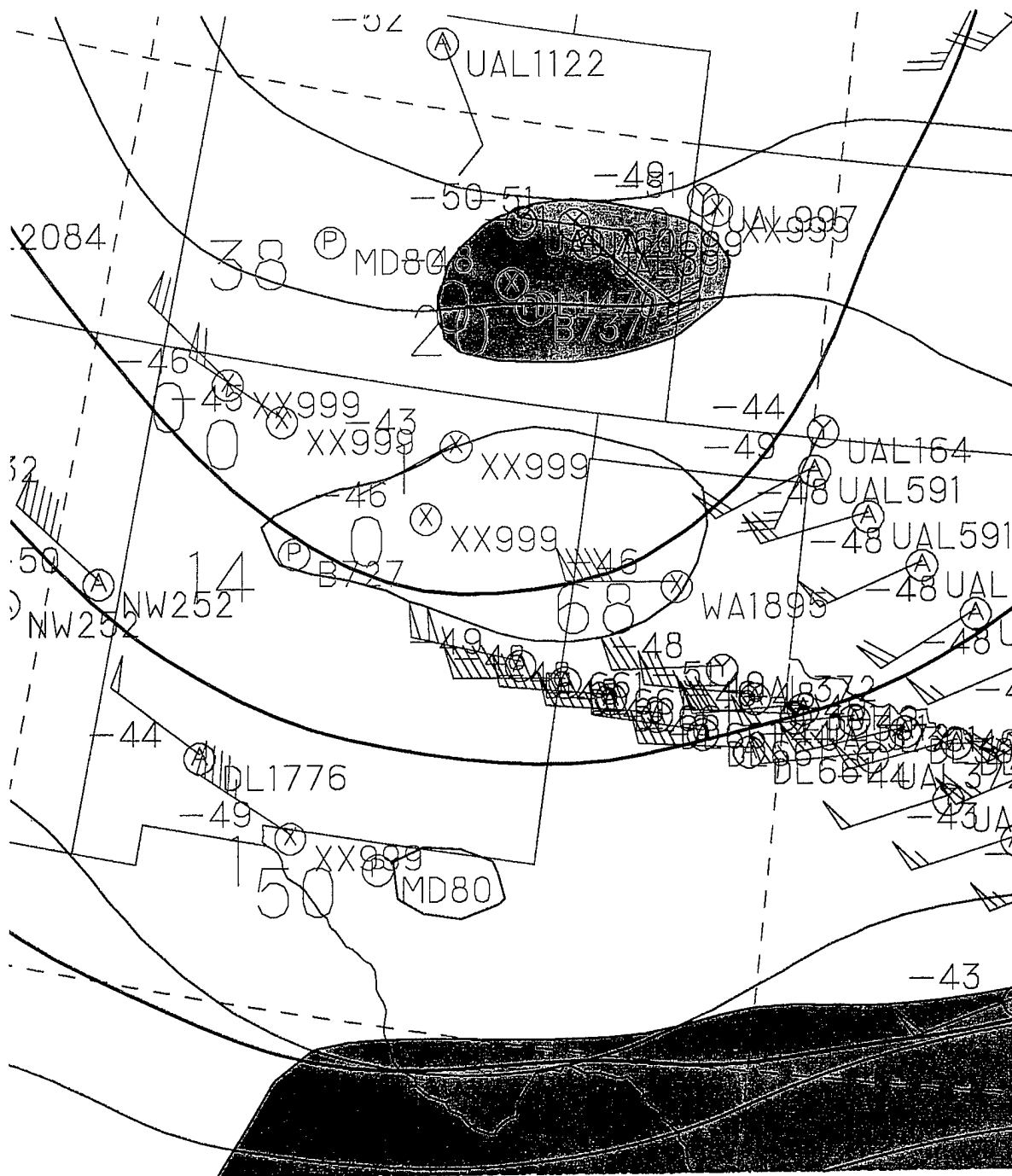
Figure 41. Close-up of the Desert Southwest on the NORAPS 300 mb potential temperature analysis at 0000 UTC 14 April 1996.
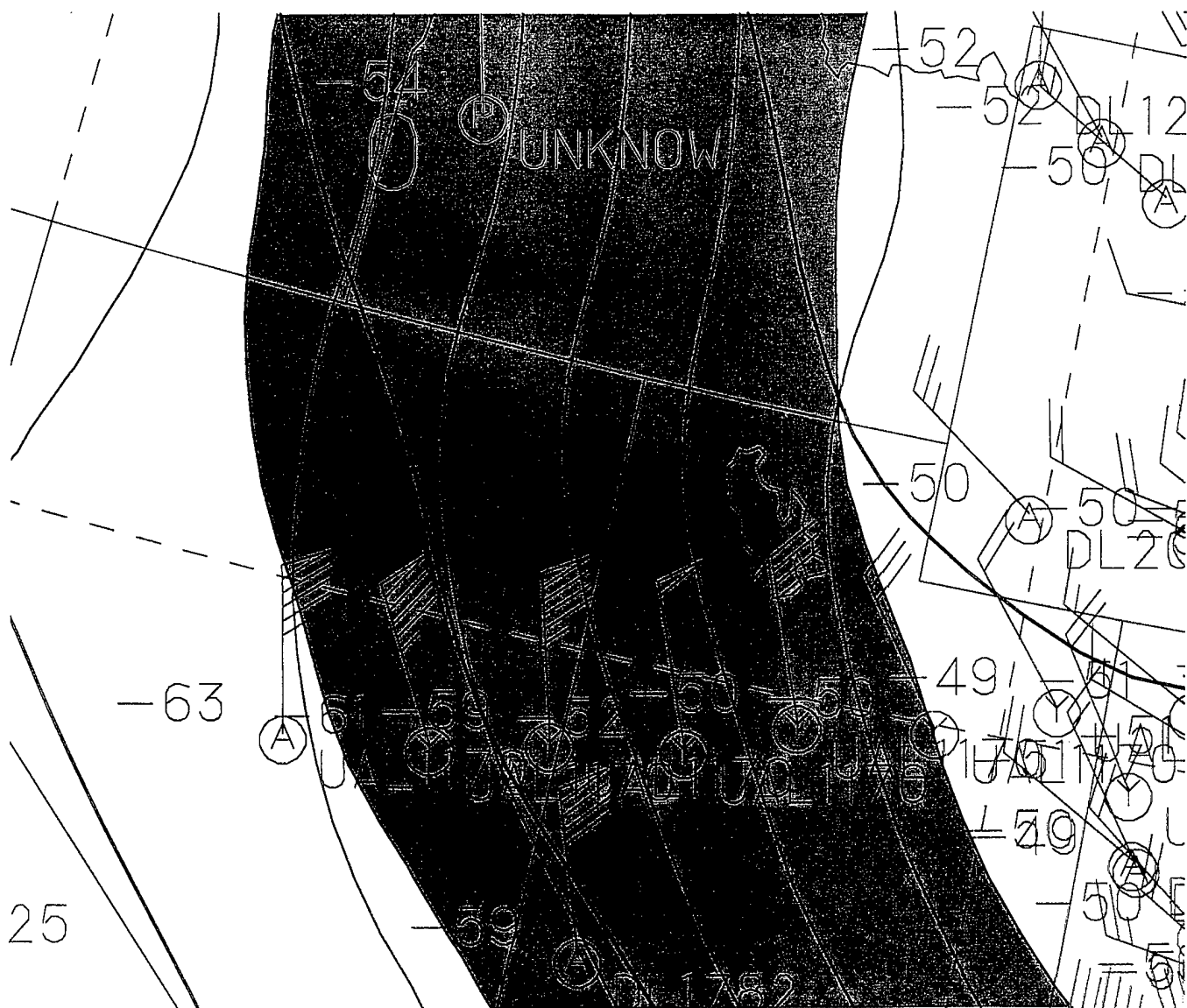
Figure 42. Close-up of the track of UAL 1170 over Nevada and Utah on the NORAPS 200 mb potential temperature analysis at 0000 UTC 14 April 1996.
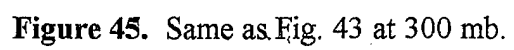
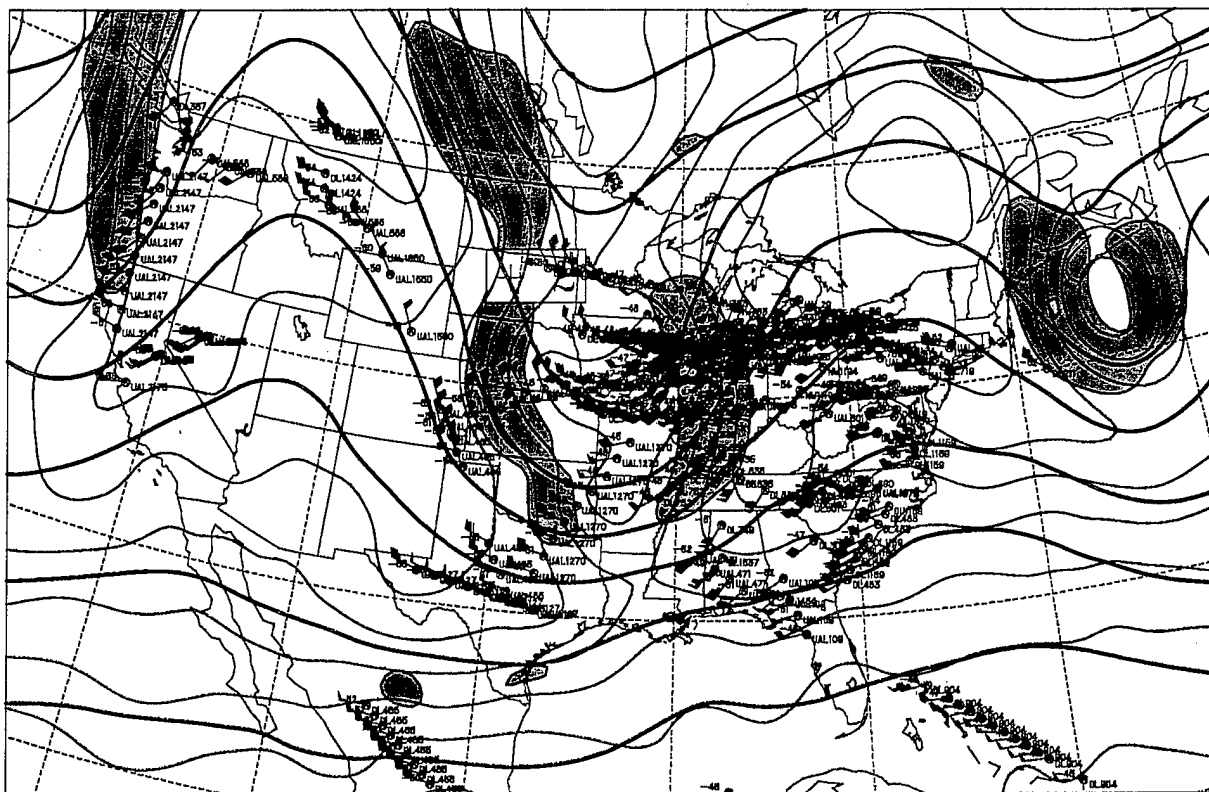**Figure 43.** 500 mb NORAPS potential temperature analysis valid at 1200 UTC 15 April 1996. Dark green shading represents a 2°C/100 km; light green shading represents a 4°C/100 km gradient. The red observations indicate that turbulence information was reported by the aircraft. The bold black lines are isoheights and the thin black lines are isotherms.

94
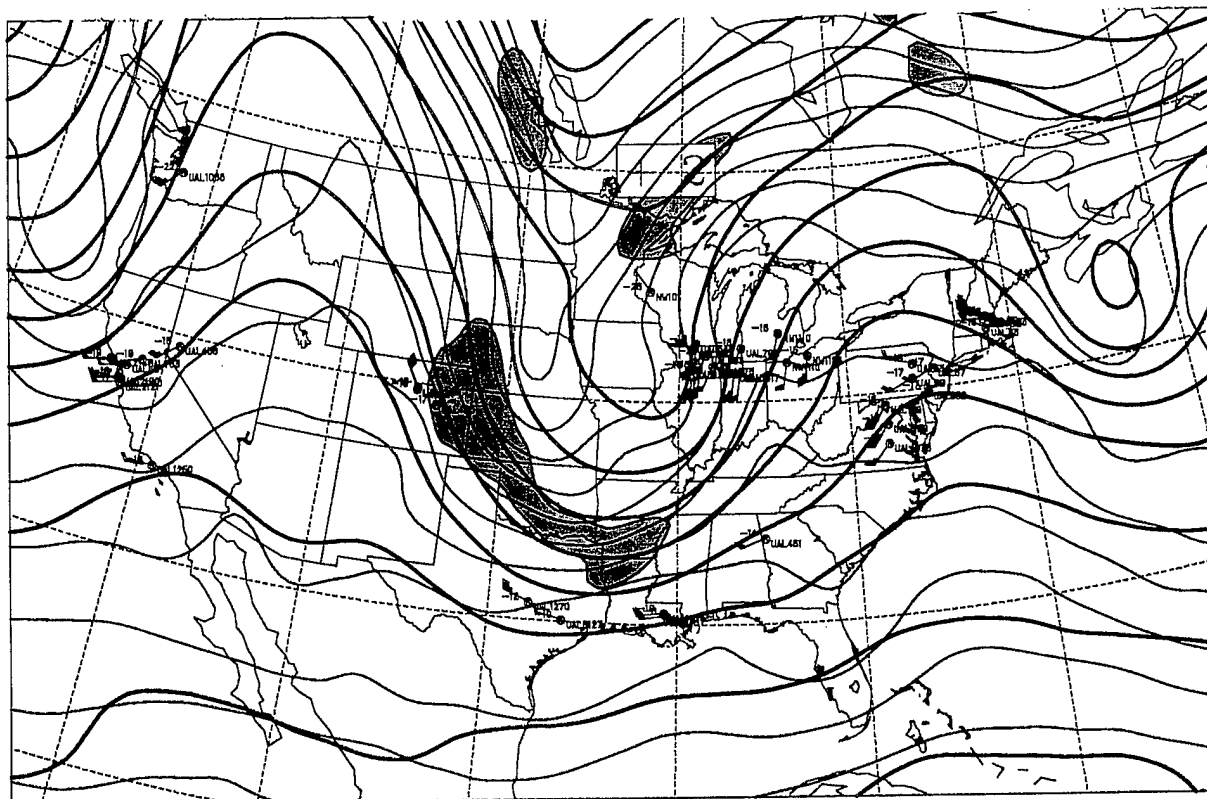
Figure 44. Same as Fig. 43 for 400 mb.

Figure 45. Same as Fig. 43 at 300 mb.

Figure 46. Same as Fig. 43 for 250 mb.
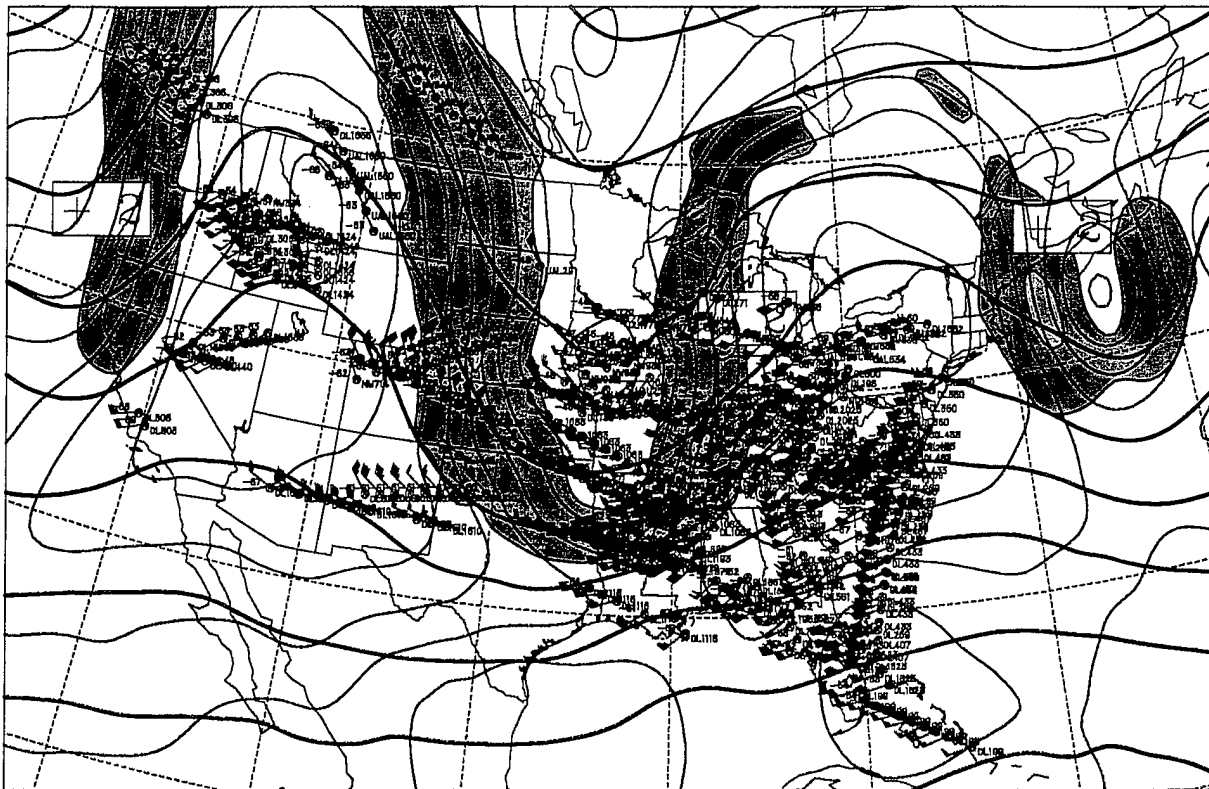
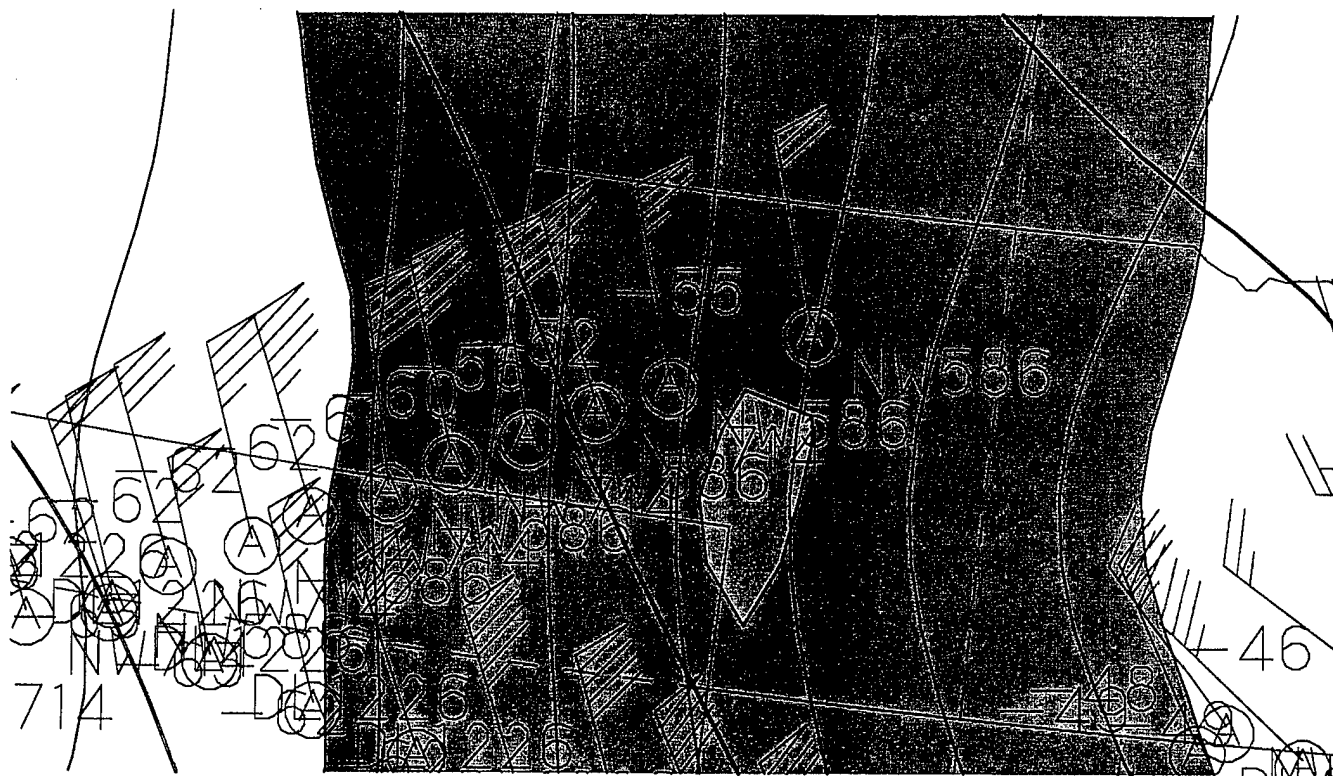**Figure 47.** Same as Fig. 43 for 200 mb.

Figure 48. Close-up of the track of Northwest Flight 586 over Wyoming and Nebraska on the NORAPS 200 mb potential temperature analysis valid at 1200 UTC 15 April 1996.
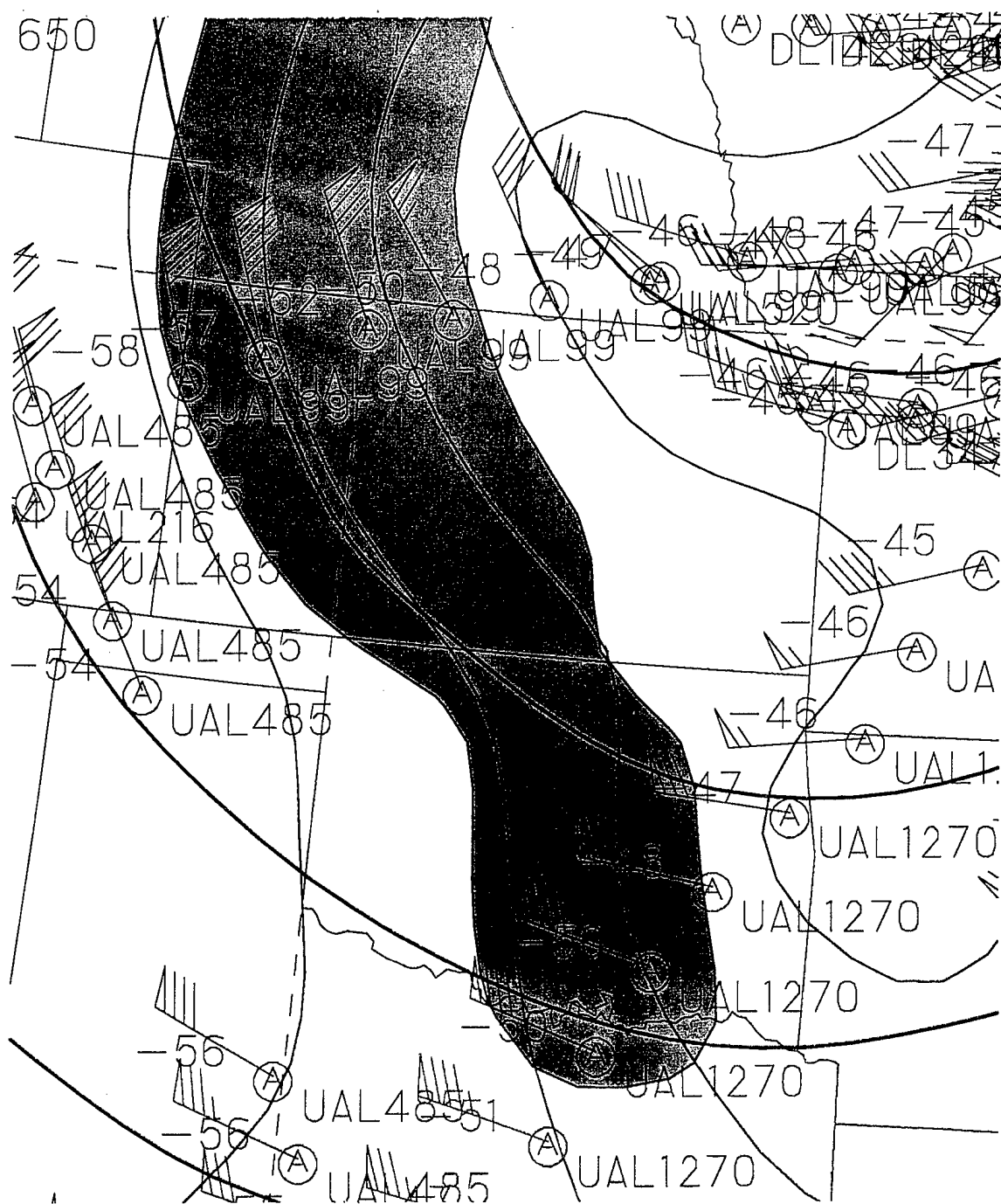
Figure 49. Close-up of the track of United Flights 99 and 1270 on the NORAPS 250 mb potential temperature analysis valid at 1200 UTC 15 April 1996.
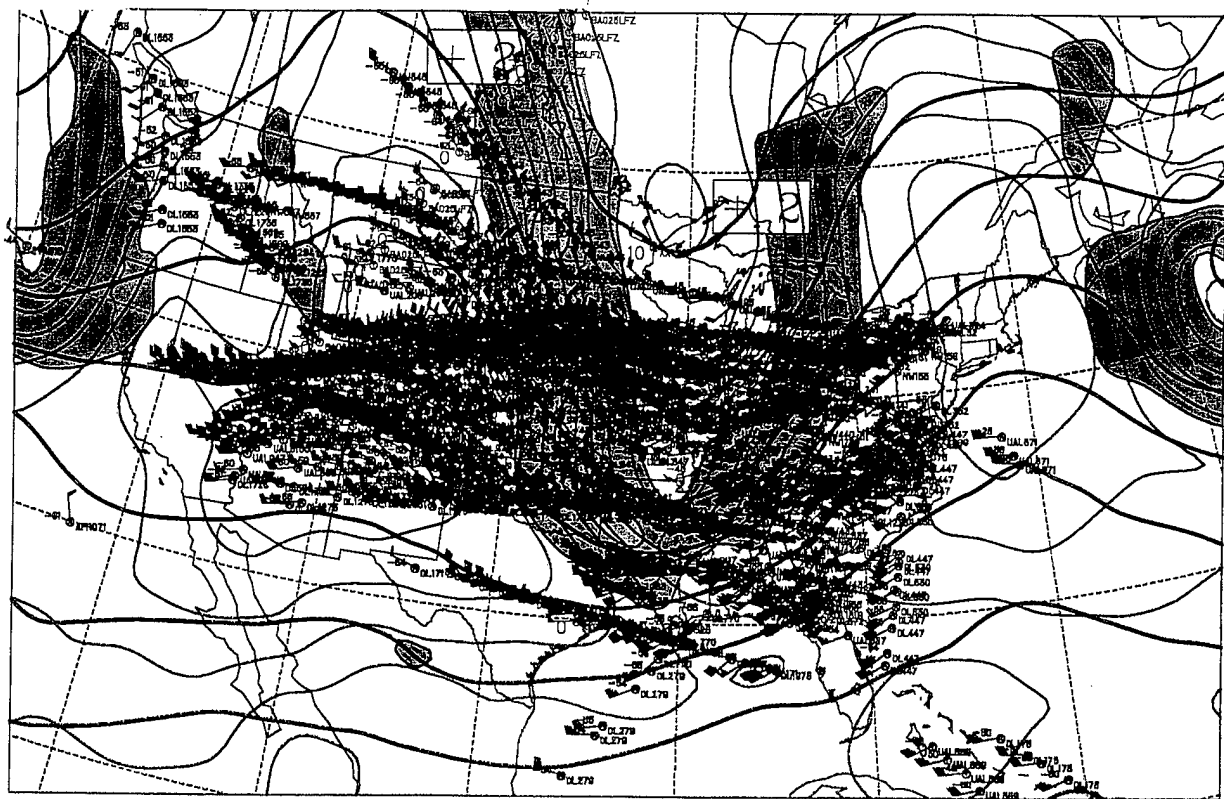
100

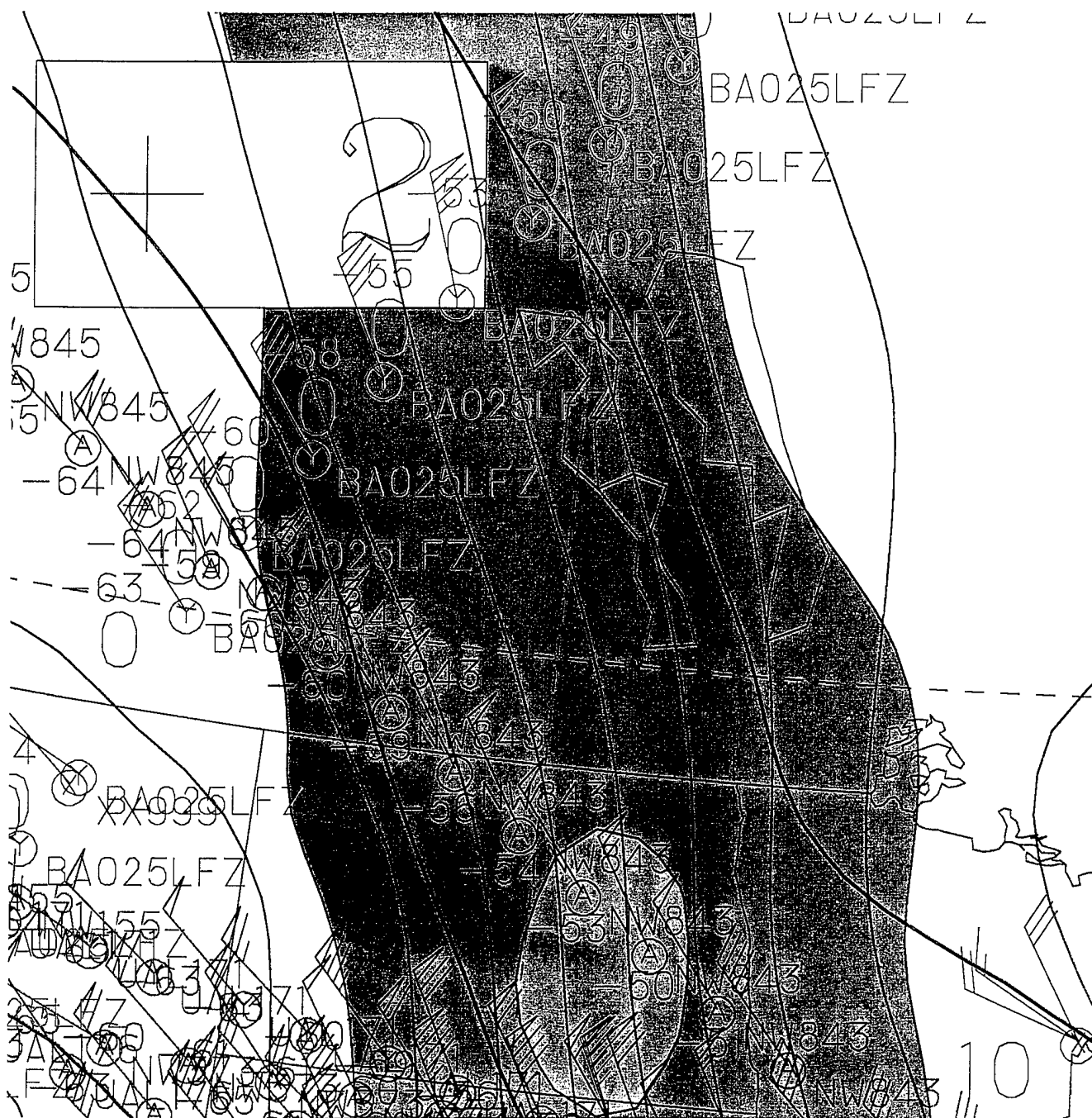**Figure 50.** Same as Fig. 24 at 0000 UTC 16 April 1996.

Figure 51. Close-up of the tracks of NW 843 and BA025LFZ over Saskatchewan, Manitoba and North Dakota on the NORAPS 200 mb potential temperature analysis at 0000 UTC 16 April 1996.
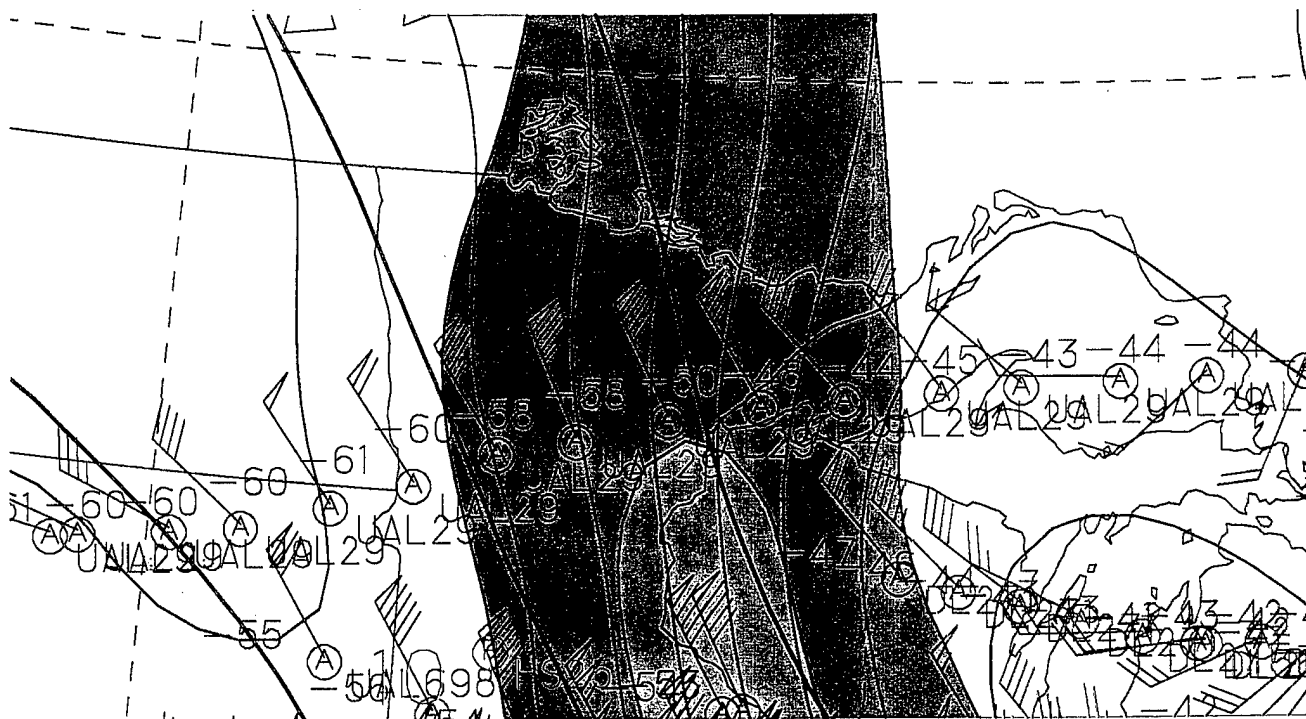
Figure 52. Close-up of the track of UAL29 over Minnesota and Michigan on the NORAPS 250 mb potential temperature analysis at 1200 UTC 16 April 1996.
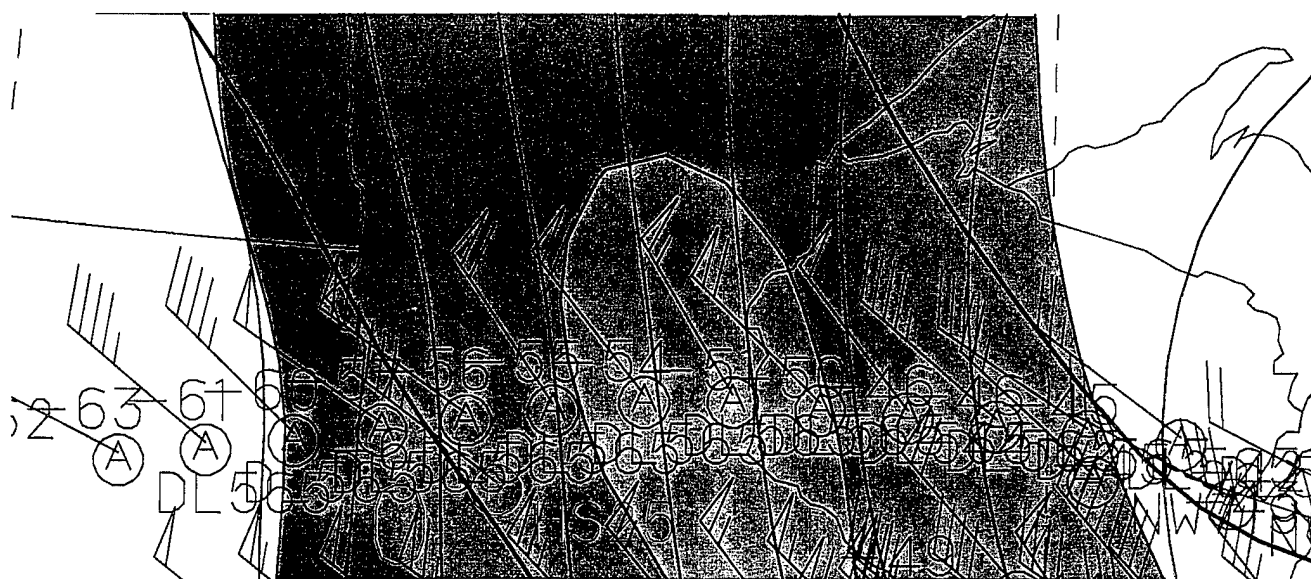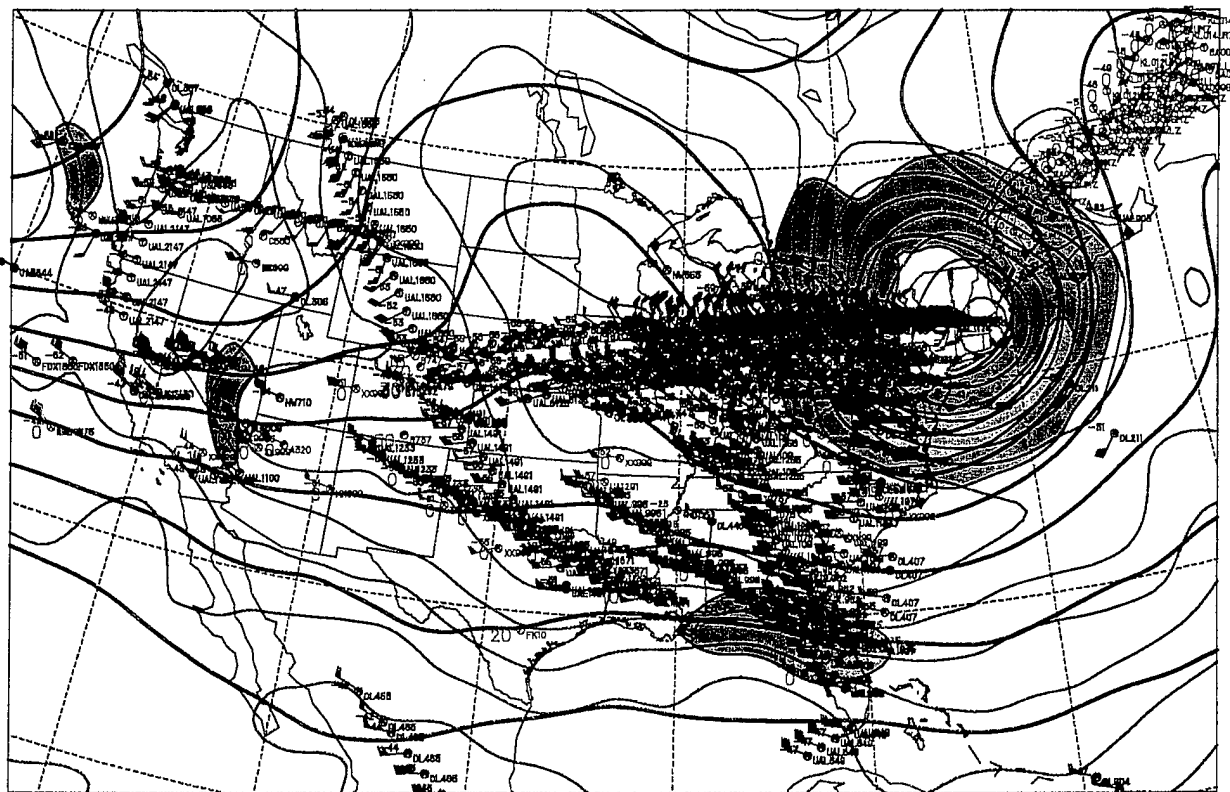
Figure 53. Close-up of DL565 over Minnesota and Wisconsin on the NORAPS 200 mb potential temperature analysis at 1200 UTC 16 April 1996.

Figure 54. Same as Fig. 24 except at 250 mb at 1200 UTC 17 April 1996.
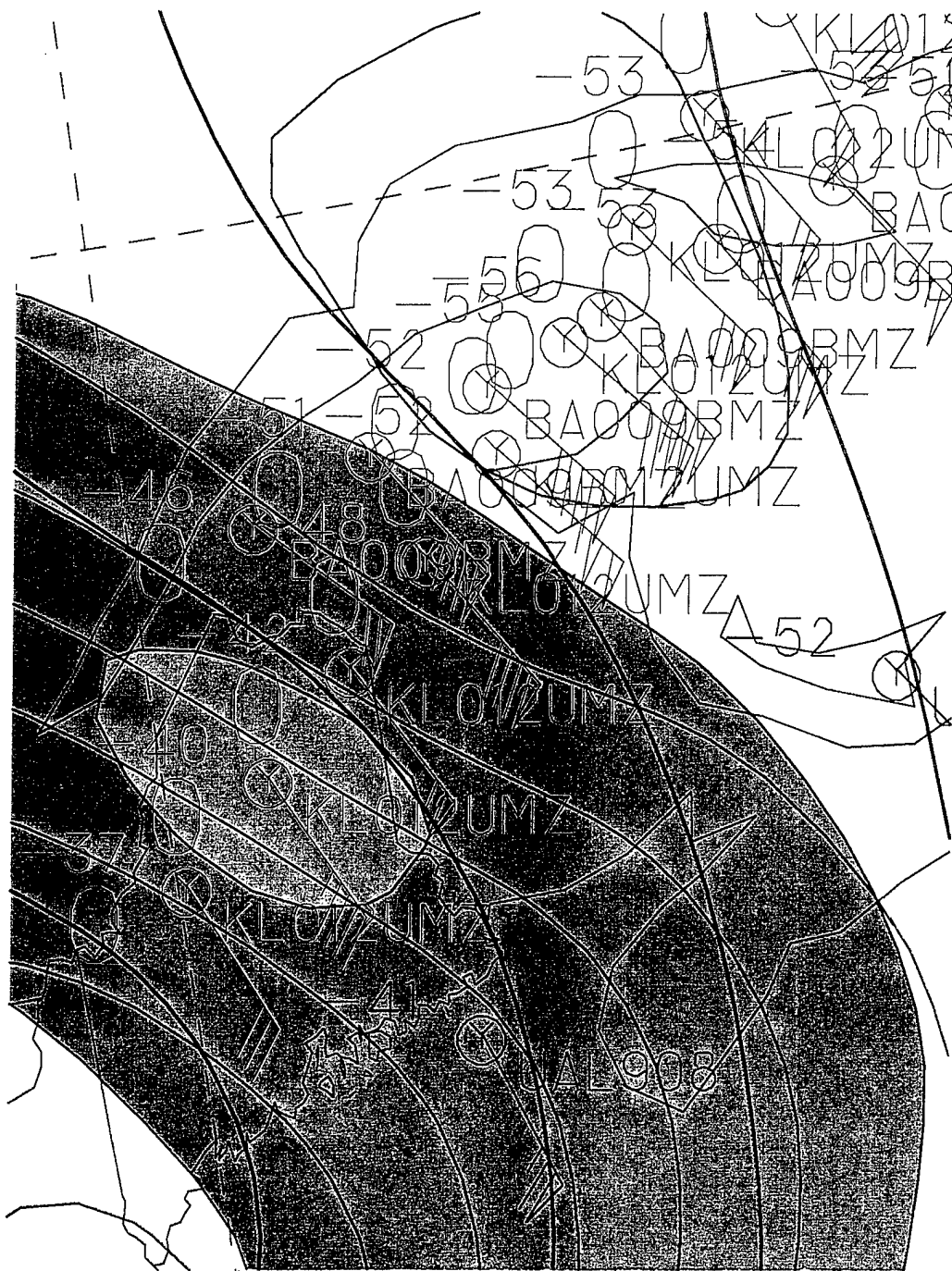
Figure 55. Close-up of the tracks of BA009BMZ and KL012UMZ over
Maine on the NORAPS 250 mb potential temperature analysis at 1200 UTC 17
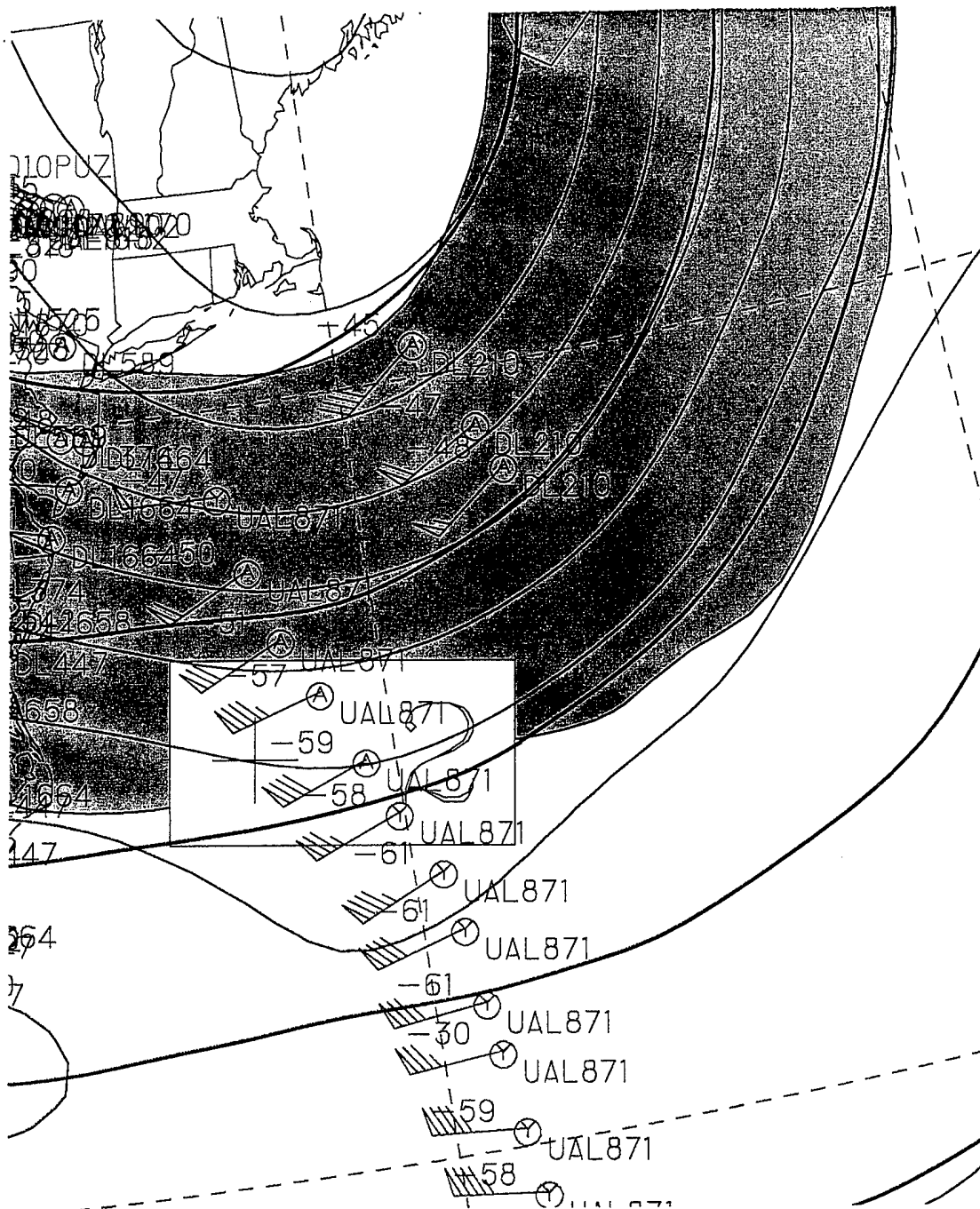April 1996.

Figure 56. Close-up of the tracks of UAL871 and DL210 over the Western Atlantic on the NORAPS 200 mb potential temperature analysis at 0000 UTC 18 April 1996.
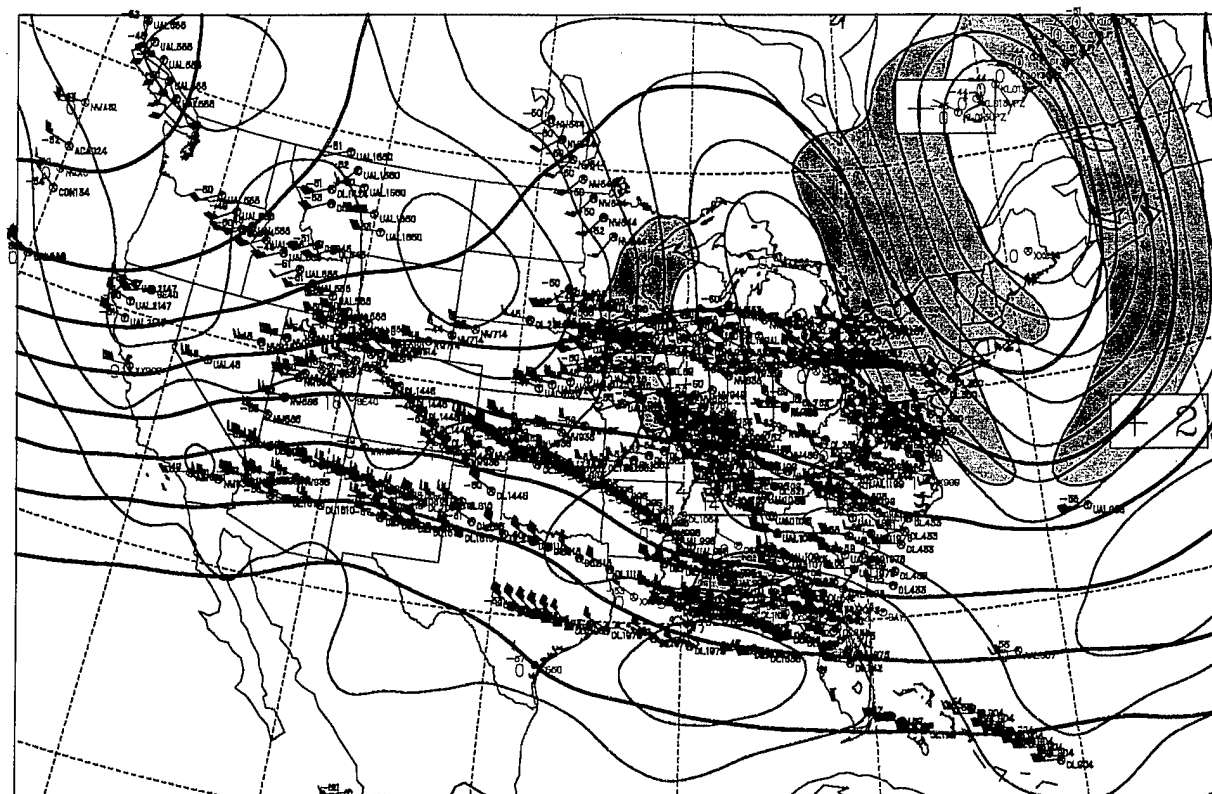
107

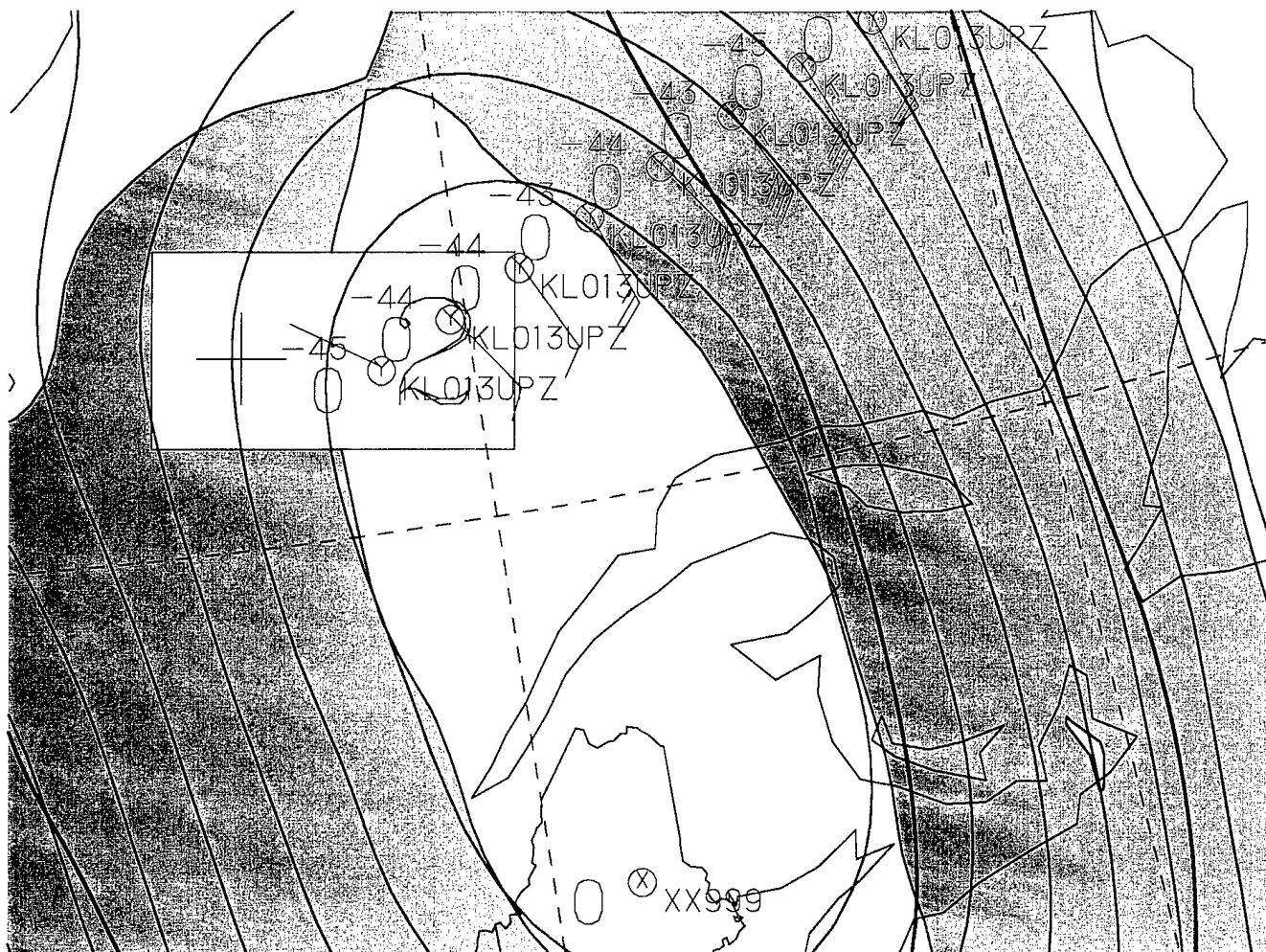**Figure 57.** Same as Fig. 24 at 1200 UTC 18 April 1996.

Figure 58. Close-up of the track of KL013UPZ over Quebec on the NORAPS 200 mb potential temperature analysis at 1200 UTC 18 April 1996.

109

LIST OF REFERENCES

Aviation Week and Space Technology, 1994: NOAA develops CAT index. **5,** 29.

Barwell, B. R. and A. C. Lorenc, 1985: A study of the impact of aircraft wind observations on a large-scale analysis and numerical weather predictions system. *Quarterly Journal of the Royal Meteorology Society*, **111,** 103-129.

Bayler, G., and H. Lewit, 1992: The Navy Operational and Regional Atmospheric Prediction Systems at the Fleet Numerical Oceanography Center. *Weather and Forecasting*, **7,** 273-279.

Bell, R. S., 1994: The beneficial impact of changes to observations usage in the U.K. Met. Office operational data assimilation system. *Tenth Conference on Numerical Weather Prediction*, Washington D.C., American Meteorological Society, 485-487.

Benjamin, S. G., K. A., Brewster, R., Brummer, B. F., Jewett, T. W., Schlatter, T. L., Smith, and P. A., Stamus, 1991: An isentropic three-hourly data assimilation system using ACARS aircraft observations. *Monthly Weather Review*, **119,** 888-906.

Brewster, K.A., S.G. Benjamin, and R. Crawford, 1989: Quality control of ACARS meteorological observations- A preliminary data survey. Preprints, *Third International Conference on the Aviation Weather System*, Anaheim, CA, American Meteorological Society, 124-129.

Briggs, J., and W. T. Roach, 1963: Aircraft observations near jet streams. *Quarterly Journal of the Royal Meteorological Society*, **89,** 225-247.

Danielsen, E. F., 1964: Project Springfield report. DASA 1517, Defense Atomic Support Agency, Washington DC 20301, 97 pp.

Ellrod, G. P., 1985: Detection of high level turbulence using satellite imagery and upper air data. *NOAA Technical Memo. NESDIS 10*, U.S. Department of Commerce, Washington D.C., 30 p.

Ellrod, G. P., 1993: A northern hemisphere clear air turbulence climatology. Preprints, *Fifth Conference on Aviation Weather Systems*. Washington D.C., American Meteorological Society, 444-448.

Ellrod G.P., and D.I. Knapp , 1991: An objective clear air turbulence forecasting technique- verification and operational use. *Weather and Forecasting,* 7, 150-164.

Fleming, R. J., 1996: The use of commercial aircraft as platforms for environmental measurements. *Bulletin of the American Meteorological Society.* 77, 2229-2242.

Gleim, I. N., 1993: Aviation weather and weather services. Gleim Publications Inc., Gainesville, FL, 442 p.

Jane's Avionics, 1996: C. Johnson, C., Ed., 15th Edition, Couldson, Surrey, U.K. 696.

Julian, P. R., 1989: Quality control of the aircraft file at the NMC. *Office Note* **358.** U.S. Department of Commerce, National Oceanic and Atmospheric Administration, National Weather Service, National Meteorological Center, 13 p.

Keyser, D., and M. A. Shapiro, 1986: A review of the structure and dynamics of upper-level frontal zones. *Monthly Weather Review.,* **114,** 452-499.

Kruus, J., 1986: The aircraft to satellite data relay- ASDAR. *International Conference on the Results of the Global Weather Experiment and their Implications for the World Weather Watch.,* **I,** No. 26, 145-155.

Lord, R.J., W.P. Menzel, and L.E. Pecht, 1984: ACARS wind measurements: an intercomparison with radiosonde, cloud motion, and VAS thermally derived winds. *Journal of Atmos. Oceanic Technol.,* 1, 131-137.

Martin, R. C., M. W. Wolfson, and R. G. Hallowell, 1993: MDCRS: Aircraft observations collection and uses. Preprints, *Fifth International Conference on Aviation Weather Systems,* American Meteorology Society, Vienna, VA, 317-321.

Moninger, W.R., 1995: Quality control of ACARS data. *FSL Forum,* Forecast Systems Laboratory, Boulder CO, December 1995, 38-41.

National Weather Service Modernization Committee, 1994: Toward a New National Weather Service-- Weather for those who fly. National Academy Press, Washington D.C., 100 p.

Pauley, P. M., N. L. Baker, and E. H. Barker, 1996: An observational study of the "Interstate-5" dust storm case. *Bulletin of the American Meteorological Society,* 77, 693-720.

Reap, R. M., 1996: Probability forecasts of Clear-Air-Turbulence for the contiguous U.S. *Technical Procedures Bulletin* **430.** National Weather Service Office of Meteorology, Department of Commerce, Washington D.C., 15 p.

Sanders, F., L. F. Bosart, and C. C. Lai, 1991: Initiation and evolution of an intense upper-level front. *Monthly Weather Review,* **119,** 1337-1367.

Schwartz, B., 1996: The quantitative use of PIREPS in developing aviation weather guidance products. *Weather and Forecasting,* **11,** 372-384.

Schwartz, B., and S.G. Benjamin, 1995: A comparison of temperature and wind measurements from ACARS-equipped aircraft and rawinsondes. *Weather and Forecasting,* **10,** 528-544.

Shapiro, M. A., 1974: A multiple structured frontal zone-jet stream system as revealed by meteorologically instrumented aircraft. *Monthly Weather Review,* **102,** 244-253.

Shapiro, M. A., 1976: The role of turbulent heat flux in the generation of potential vorticity in the vicinity of upper-level jet stream systems. *Monthly Weather Review,* **104,** 892-906.

Smith, T. L., and S. G. Benjamin, 1994: Relative Impact of Data Sources on a Data Assimilation System. *Tenth Conference on Numerical Weather Prediction,* Washington D.C., American Meteorological Society, 491-493.

Tenenbaum, J., 1991: Jet Stream Winds: Comparisons of Analyses with Independent Aircraft Data over Southwest Asia. *Weather and Forecasting.* **6,** 320-336.

Tenenbaum, J., 1996: Jet Stream Winds; Comparisons of Aircraft Observations with Analyses. *Weather and Forecasting.* **11,** 188-197.

INITIAL DISTRIBUTION LIST

		No. Copies
1.	Defense Technical Information Center 8725 John J. Kingman Rd., STE 0944 FT Belvoir, VA 22060-6218	2
2.	Library, Code 13 Naval Postgraduate School Monterey, CA 93943-5122	2
3.	Meteorology Department Code MR Naval Postgraduate School 589 Dyer Rd Rm 254 Monterey, CA 93943-5114	1
4.	Oceanography Department Code OC Naval Postgraduate School 883 Dyer Rd Rm 328 Monterey, CA 93943-5122	1
5.	Dr. Patricia M. Pauley Code MR/PA Naval Postgraduate School 589 Dyer Rd Rm 254 Monterey, CA 93943-5114	4
6.	Dr. Wendell A. Nuss Code MR/NU Naval Postgraduate School 589 Dyer Rd Rm 254 Monterey, CA 93943-5114	1
7.	LT Edward L. Stephens II, USNR 2562 Aly Sheba Dr. Burlington, KY 41005	1

8.   Commander   1
      Naval Meteorology and Oceanography Command
      Stennis Space Center
      MS 39529-5001

9.   Commanding Officer   1
      Naval Oceanographic Office
      Stennis Space Center
      MS 39529-5001

10.   Commanding Officer   1
      Fleet Numerical Meteorology and Oceanography Center
      7 Grace Hopper Ave Stop 1
      Monterey, CA 93943-5001

11.   Superintendent   1
      Naval Research Laboratory
      7 Grace Hopper Ave Stop 2
      Monterey, CA 93943-5502